MATHEMATICAL MODELLING AND COMPUTER SIMULATIONS OF INDUCED VOLTAGE CALCULATIONS IN AC ELECTRIC TRACTION

IMTITHAL M ABDULAZIZ

DOCTOR OF PHILOSOPHY

NAPIER UNIVERSITY, EDINBURGH

APRIL 2003

MATHEMATICAL MODELLING AND COMPUTER SIMULATIONS OF INDUCED VOLTAGE CALCULATIONS IN AC ELECTRIC TRACTION

Imtithal Mohammed Abdulaziz

A thesis submitted in partial fulfilment of the requirements of Napier University for the Degree of Doctor of Philosophy

April 2003

DEDICATED TO

Basma, Mohammed, and Hiba

NOMENCLATURE

Abbreviations used:

A	=	**A**erial earth wire
ABC	=	**A**bsorbing **B**oundary **C**ondition
AC	=	**A**lternating **C**urrent
AT	=	**A**uto**T**ransformers
B	=	**B**uried earth wire
BR	=	**B**ritish **R**ail
BT	=	**B**ooster **T**ransformer
CCITT	=	**I**nternational **T**elegraph and **T**elephone **C**onsultative **C**ommittee
CCM	=	**C**arson's **C**orrection **M**ethod
COS	=	**C**able on the **O**ther **S**ide
CNS	=	**C**able on the **N**ormal **S**ide
CW	=	**C**ontact **W**ire
DC	=	**D**irect **C**urrent
EMC	=	**E**lectro**M**agnetic **C**ompatibility
emf	=	**E**lectro**M**otive **F**orce
EMI	=	**E**lectro**M**agnetic **I**nterference
EW	=	**E**arth **W**ire
F	=	**F**eeder wire
FDTD	=	**F**inite **D**ifference **T**ime **D**omain
FDM	=	**F**requency **D**ivision **M**ultiplex
FEM	=	**F**inite **E**lement **M**ethod
FF	=	Self and mutual impedance of **F**eed system matrix
IV	=	**I**nduced **V**oltage

LM	=	**L**oco**M**otives
M	=	**M**essenger wire
mmf	=	**M**agneto **m**otive **f**orce
MTL	=	**M**ulti-conductor **T**ransmission **L**ine
OCS	=	**O**verhead **C**atenary **S**ystem
OHE	=	**O**ver**H**ead **E**lectrification
OHL	=	**O**ver**H**ead **L**ine
PEC	=	**P**erfect **E**lectric **C**onductor
PUL	=	**P**er-**U**nit **L**ength
RF	=	Mutual impedance of **R**eturn system against **F**eed system matrix
RR	=	Self and mutual impedances of **R**eturn system matrix
RT	=	**Re**turn conductor
TL	=	**T**ransmission **L**ine
TP	=	**T**ouch **P**otential
3D	=	Three **D**imension

Symbols used:

a	=	Cross-section area (m^2)
C	=	Capacitor (F)
c	=	Speed of light
E	=	Electric field (V/m)
e	=	Electromotive force (V)
f	=	Frequency (Hz)
G	=	Conductance (s)
H	=	Magnetic field (A/m)
I	=	Current (A)
J	=	Current density (A/m)
K	=	Screening factor
l	=	Length (m)
L	=	Inductor (H)
P	=	Power (W)
q	=	Charge (coulomb)
Rd	=	Rail conductor
R	=	Resistor (ohm)
Re	=	Earth resistor (ohm)
V	=	Voltage (V)
X	=	Inductance (ohm/m)
Y	=	Admittance (mho/m)
Z	=	Impedance (ohm/m)
Zm	=	Mutual impedance (ohm/m)
Zs	=	Self impedance (ohm/m)
Z0	=	Characteristic impedance (ohm/m)
σ	=	Conductivity of conductor (S/m)
ρ	=	Resistivity of conductor (ohm-m)
θ	=	Angle (rad)
μ	=	Permittivity of conductor

ε	=	Permeability of conductor
δ	=	Skin depth
α	=	Attenuation constant
γ	=	Propagation constant
ω	=	Angular frequency (rad/s)
ψ	=	Magnetic flux (weber)
π	=	pi (22/7)

List of Figures:

List of tables:

CONTENTS

APPENDICES

ABSTRACT

This thesis studies the foundation of a new method to calculate the induced voltage into line-side signalling circuits using numerical modelling technique.

The need for accurate calculations of induction due to the high power overhead line has prompted the development of such a new approach. Due to the complexity of the railway systems, measurements are not always possible. An alternative approach, either analytical or numerical analysis, is required. The analytical method has been developed and applied since the beginning of electrification. Although this method provided reasonable results, it has certain limitations with respect to frequency range, and hence accuracy. The development of computers provided us with a new and exciting analysis, that is, mathematical modelling techniques. This project devised a new method based on the finite difference time domain to calculate the impedances of the rail track and overhead line and the longitudinal induced voltage into nearby signalling systems. The method is simple and has been developed using known software (MATHCAD & APLAC) in order to reduce any additional cost that may arise.

Calculations have been carried out for uncompensated systems (no booster transformer) and compensated systems for various overhead catenary configurations relating to one-track and two-track layouts in open areas. Two different overhead ratings namely 1250 Amps and 760 Amps have been considered. The signalling cable can be placed at either side of the track(s). Both positions haven been considered as well as normal and fault conditions.
The position of the signalling cable has greater effect for one-track case than two-track or more. The level of induction is also greatly related to the number of the track used (i.e. worse induction for one track than for two, four or more). The design of the booster transformer is very important in order to reduce any induction, this becomes more evident at short circuit conditions when the magnetising current effect is more evident.

ACKNOWLEDGMENTS

My thanks first go to Dr Naren Gupta, my supervisor, whose continuous support and feedback on the work have been invaluable. I am grateful to him for his kind help throughout, including in the preparation of this thesis and ensuring timely completion of this project.

For one reason or the other, the author would also like to thank Prof. A Almaini, Mr J Sharp, Prof. S Gair, Dr W Buchanan and Dr T Grassie.

My research-student colleagues participated with discussions and useful criticism. I am grateful to all the staff in the school of Engineering, in particular Mr B Young and Mr B Campbell for providing technical support. Many thanks to Ms Linda Dunn who has willingly helped with my studentship arrangements.

I thank Professor Jorge Kubie, Head of department, and the whole of Napier University for giving me the opportunity to do this work.

I have always been grateful to my parents who have enriched my life with great values.

Finally, my special thanks go to Osman for his on-going support and encouragement throughout the project, without him I couldn't have done it.

DECLARATION

I declare that this thesis was composed and originated entirely by myself, other than those items acknowledged in the text. The work was completed under a full time supervised program at Napier University between March 2000 and March 2003.

Imtithal M Abdulaziz

CHAPTER (1)

Introduction

AC single-phase 25 kV, 50 Hz systems are commonly used for electrified railways world-wide. A major problem with this system is the interference it causes into nearby signalling systems. This interference can be very severe and endangers personnel and equipment. To constrain any interference caused, booster transformers have been employed. However, these transformers can add significantly to the cost of the railway systems. Hence to justify their use, it is essential to know the level of longitudinal induced voltage into the signalling systems. This thesis relates to work carried out by my supervisor Dr N K Gupta on models for induced voltage calculations into line-side signalling cables. Gupta's model uses Carson's method for impedance calculations, whereas in this thesis impedances have been calculated by FDTD (finite-different-time-domain method). It also provides a mathematical model, which can be modified and applied to different systems.

The main problems addressed in this thesis are:

1. Calculations of self and mutual impedance of return and feed conductors.
2. Calculations of the induced voltage for uncompensated systems both under normal and short circuit conditions.
3. Calculations of the induced voltage for compensated systems both under normal and short circuit conditions.

In this chapter, the general concept of interference will be discussed along with an overview of relevant previous work in this field.

1.1 Overview of electric railway systems and its problems

1.1.1 Electrification

Electrification means the removal of the prime mover from the train. This provides a technical strength because it removes items, which can fail and are costly to maintain and hence improve performance. Although economically, this can be considered as a weakness in the sense that it provides energy greatly in excess of that previously utilised and hence increases the initial cost, but the long-term benefits outweigh the initial disadvantages.

The complete electrification of all major lines was carried out in the then British railway (BR) by 1960, except between England and Scotland, which due to cost implications was completed in 1967. Since then electric trains have proved to be more reliable and environment friendly compared to the old fashioned steam or diesel trains.

A typical 25 kV a.c single-phase power supply system and an electric traction system are shown in Figures 1.1[48] and 1.2[78].

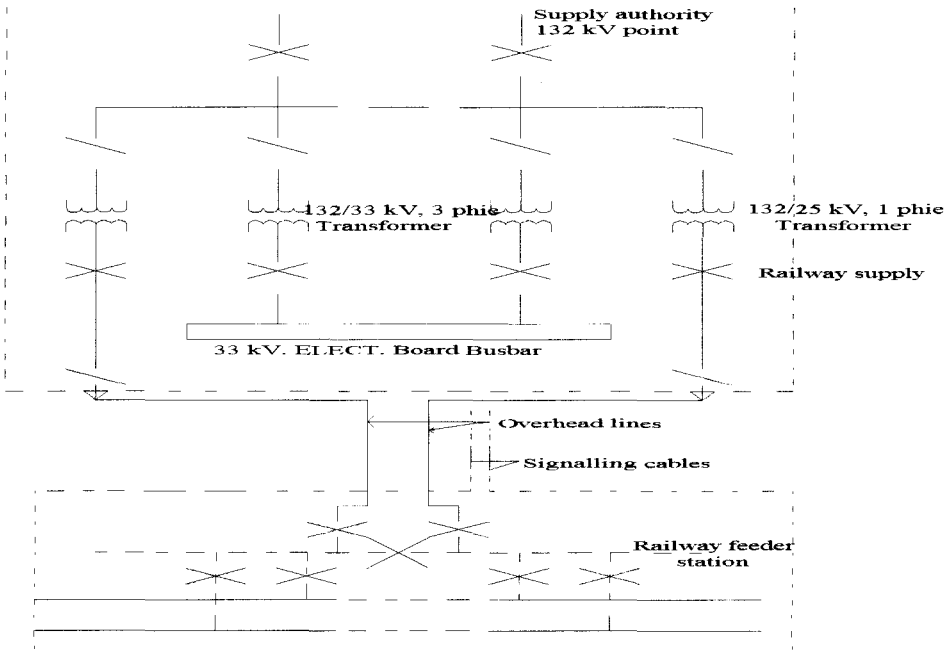

Figure 1.1: A typical 25 kV, a.c single-phase power supply system

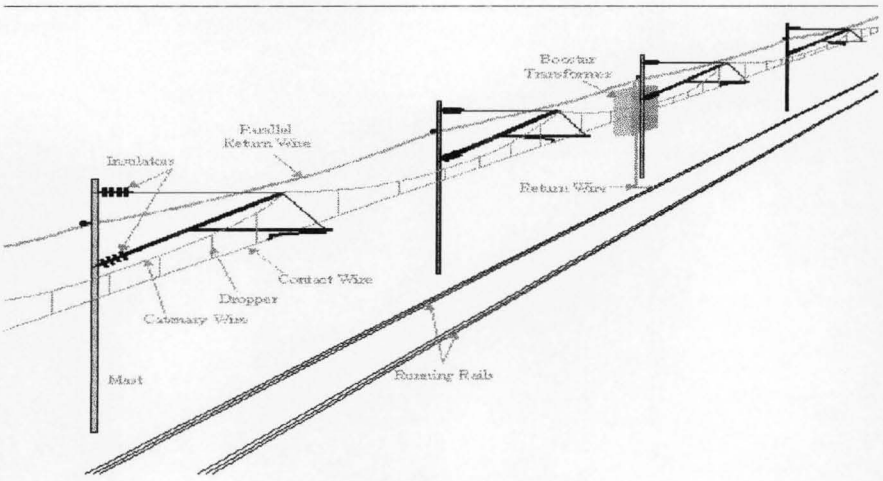

Figure 1.2: A typical a.c single-phase, electric railway systems (diagram obtained from www.trainweb.com[78])

For a train to keep moving, it has to collect electricity on the go, since it cannot possibly store enough electricity to last the whole journey. This can be achieved in two ways. The first method many current-collecting **shoes** fitted next to the wheels on the outside of the bogies. This is accomplished by using the third rail system (Figure 1.3), where by electricity is supplied through a thick conductor running along the track. The Locomotive (LM) has a shoe, which maintains sliding contact with it while the train is in motion to draw currents from it. The third-rail systems are usually d.c systems at much lower voltages (500 V-750 V rms). This arrangement is considered less satisfactory due to the technical limitation of the current collecting shoes and the speed limit of 100 mph. Furthermore, the live line is a hazard to personnel and animals which can be devastating.

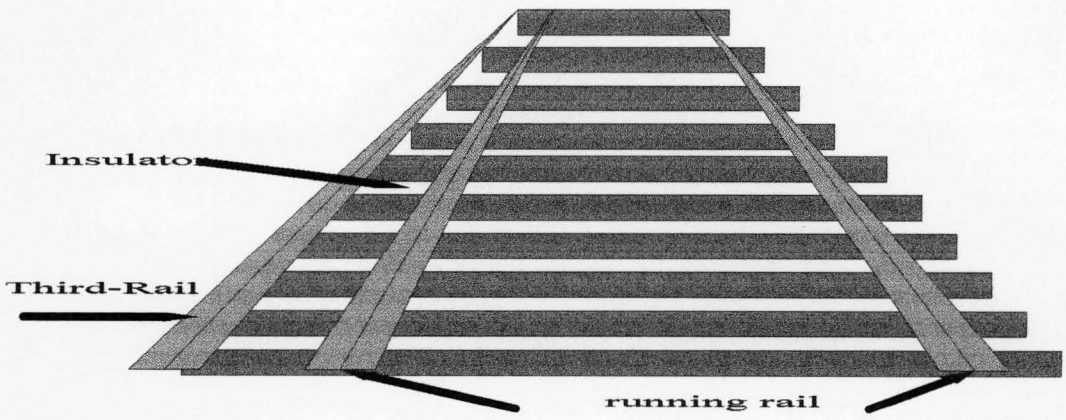

Figure 1.3: Third-rail concept

The second method uses a retractable **pantograph** (Figure 1.4) fitted to the top of one or more of the carriages, the following discussion concentrates mainly on this system.

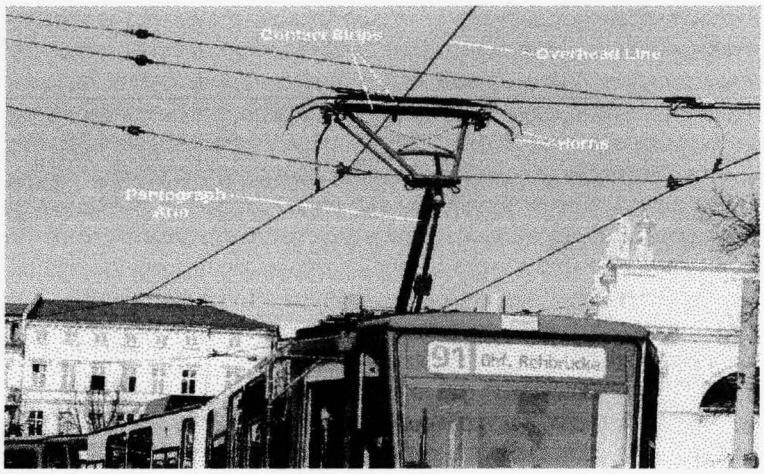

Figure 1.4: The pantograph (diagram obtained from trainweb.com[78])

1.1.2 Electric traction systems

An electric traction system is basically composed of three groups of equipment; (a) Fixed equipment required for bringing power from the supply point to the collecting devices on the train. (b) The motive power units, and (c) Other components which, although not directly part of the first and second groups, contribute to or are influenced by the conditions within these groups such as neighbouring telecommunication systems, the signalling systems and the rails on which the motive power units run[13].

A traction supply system is very complex compared to the normal power supply. Whereas in power supply transmission systems the places at which the load is imposed are known and definite, the load imposed on a traction supply system by individual motive power units' moves between one point of supply and another as the train moves between one point and another. Next follows a brief discussion of the components of electric railways.

1.1.3 Components of electric railway systems

An electric railway system is mainly composed of[13]:

1. Feeder stations, which supply power to the overhead wires.
2. Pantographs fitted to the electric trains, which collect the required traction current from the overhead lines.

3. Return conductors, which return the current back to the feeder stations.

The return current passes via the wheels of the vehicle to the running rails and hence to the supply point through the earthy bar connection. Aerial earth wires act as additional return conductors.

1.1.4 Electrified railway configurations

In overhead electrification (OHE) systems, the supply of electricity is through an overhead system of suspended cables known as the catenary. A contact wire or cable actually carries the electricity; it is suspended from or attached to other cables above it, which ensure that the contact cable is at a uniform height and in the right position.

The locomotive (LM) itself uses a pantograph, a metal structure that can be raised or lowered, to make contact with the overhead contact cable to draw electricity to power its motors. The electric current usually passes first through a transformer and not directly to the motors. The return path for the electricity is through the body of the LM and the wheels to the tracks, which are electrically grounded. Modern electric LM have some fairly sophisticated electronic circuitry to control the motors depending on the speed, load, etc., often after first converting the incoming 25kV AC supply to an internal AC supply with more precisely controlled frequency and phase characteristics to drive AC motors.

The two types of power supply for the electric traction systems discussed above are:
(a) *AC Single system:* The overhead catenary is fed electricity at 25kV a.c (single-phase) from electric sub-stations positioned at frequent intervals (35-50km) along the route. The sub-stations are spaced closer (10-20km) in areas where there is high load or traffic.

These sub-stations in turn are fed electricity at 750kV a.c or so from the regional grids operated by state electricity authorities. A Remote Control Centre, usually close to the divisional traffic control office, has facilities for controlling the power supply to different sections of the catenaries fed by several sub-stations in the area. Figure 1.5[78] below shows the electronic power of an a.c system.

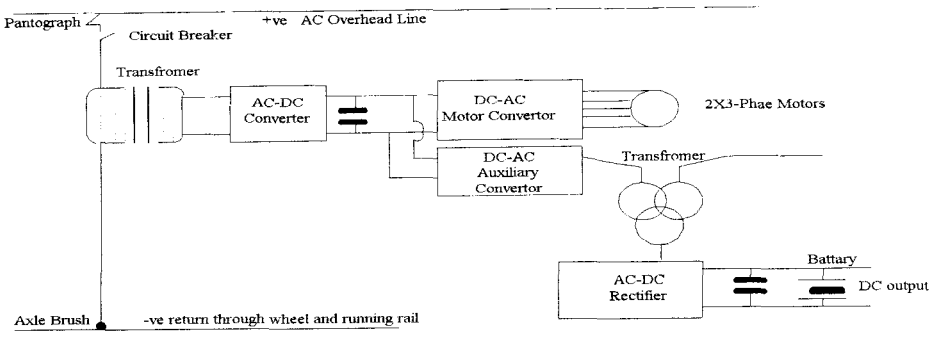

Figure 1.5: Circuit diagram for the electronic power for an a.c system

(b) DC System: In d.c systems with overhead catenary, the basic principle is the same, with the catenary being supplied electricity at 1.5kV d.c. Usually the current from the catenary goes directly to the motors. A d.c LM may however convert the d.c supply to a.c internally using inverters or a motor-generator combination, which then drives a.c motors.

The a.c system is more expensive as the traction motors aboard a train usually requires a d.c supply, hence a heavy and expensive transformer-rectifier has to be included in the multiple unit. If a.c traction motors were used instead, an expensive frequency-alternator would have to be included so that the traction speed of the motor can be controlled. The electronic power of the dc system is shown in Figure 1.6[78].

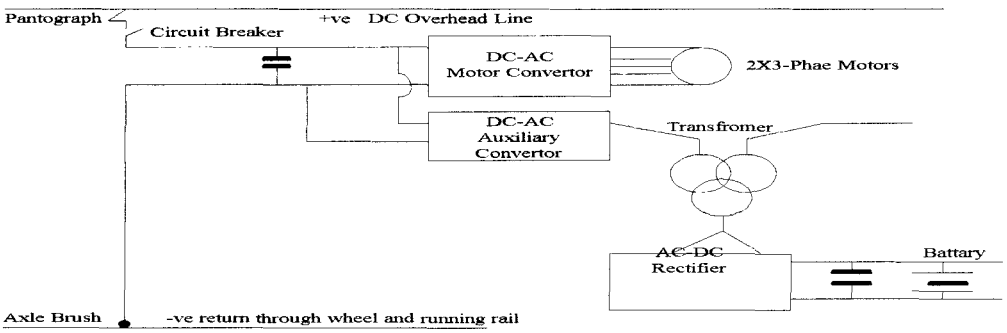

Figure 1.6: Electronic power circuit for d.c system

The reason AC is now the preferred option for electrification is because AC substations are much easier to build, as **25kV** AC supply is available directly from the national grid. However, the AC scheme causes some other troubles. For instance, with the basic system, the 25kV AC supply to the energised catenary can cause severe interference in telecommunication and other

circuits, which are in close vicinity. The induced voltage can be quite high; in the hundreds of volts.

To mitigate this problem, a return conductor is provided parallel to the catenary, usually a little above and to the side of the catenary. There are also booster transformers provided at intervals. This method usually reduces the induced voltages in telephone and other circuits to below 60V (although under fault conditions 400V-500V or more of induced voltage is not unusual). Sometimes the return conductor is also connected to the rails at some points, to ensure that more of the return current flowing through the rail stays in them rather than going through the surrounding ground. This can also cause interference and other problems, although not to the magnitude as that seen in a.c systems without booster transformers (Uncompensated systems).

1.1.5 Interference mitigation methods

There two main methods that can be used to control and reduce any interference caused into line-side signalling and telecommunication cables, these are:

(A) Dual system (a.c): In the dual a.c system (or 2 * 25kV a.c system), the supplied electricity from the substations is actually at 50kV a.c. An autotransformer connected across the 50kV supply has a centre tap connected to the rails, whereas connections from either end of the transformer winding go to the catenary and the return conductor, this is shown in Figure 1.7. Thus, there is a 25kV differential between the catenary and the rails as before, but now there is a 50kV difference between the catenary and the return conductor. (Note, however, that the centre tap of the autotransformer, and hence the rails, are grounded to avoid hazards to people or animals walking across the tracks). Also, at points further away from the substation, the centre tap of the autotransformer can be adjusted so that the voltage between catenary and rails is always 25kV, even as the total voltage across the catenary and the return conductor drops due to resistive or impedance losses. So this allows substations to be spaced further apart (30-50km). Thus far the dual system is only used in about 10% of British railways[16].

The dual system corresponds to what is called the 3-wire system (with transmission line) in other railways. This is a more recent approach compared with the well-known booster transformer.

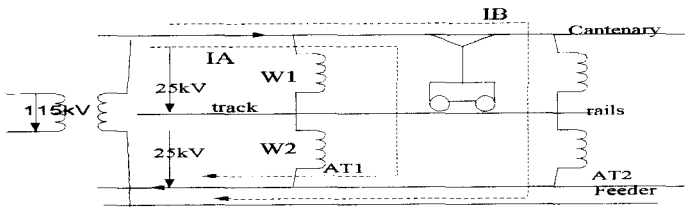

Figure 1.7: AutoTransformer (AT) systems

(B) Booster Transformers[15]*:* On lines equipped with a.c overhead wires, special precautions are taken to reduce interference in communication cables. If a communications cable is laid alongside rails carrying the return current of the overhead line supply, it can have unequal voltages induced in it. Over long distances the unequal voltages can represent a safety hazard. To overcome this problem, booster transformers are provided. These are positioned on masts at intervals along the route. They are connected to the feeder station by a return conductor cable hung from the masts so that it is roughly the same distance from the track as the overhead line. The return conductor is connected to the running rail at intervals parallel to the return cable and rails, as shown in Figure 1.8.

The effect of this arrangement is to reduce the noise levels in the communications cable and ensure the voltages remain at a safe level. Booster transformers are the common method used to reduce interference.

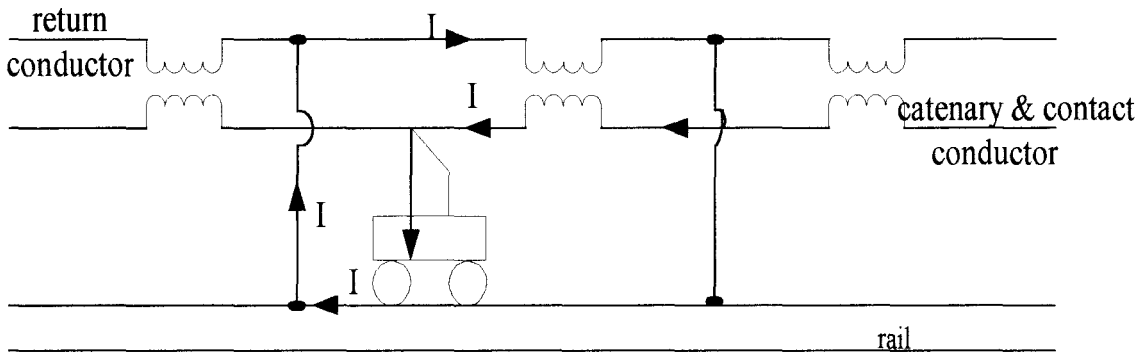

Figure 1.8: Booster Transformers (BTs) with a special return conductor

The normal arrangement of the conductors (overhead wires and running rails) for the a.c single-phase system of railway electrification forms an unbalanced circuit. The effect is that by magnetic induction the traction current causes induced voltages to appear in neighbouring parallel conductors such as telecommunication cables, the effect varying directly with the traction currents. The booster transformers are in effect power current transformers with unity ratio and are used with their primary windings connected in series with overhead line and with their secondary connected either directly to the running rails or to special return conductor.

The most important effect is the increase in impedance of the power circuit, which because of its influence on voltage drop on the distribution system requires special attention to ensure that the performance of the traction equipment is not adversely affected. There is also the effect on the action on the definite distance impedance protective system fitted to the track feeder equipment. Although the sensitivity of this equipment is increased to some extent by the increase in impedance per unit length the step in impedance at the booster transformer itself causes the location of the fault by the system to be less exact.

With the system with booster transformers connected directly to the running rails the potential of the rail when several trains are taking current becomes progressively higher in steps until the feeder station is reached.

It is important when designing the booster transformer insulation that the magnitude of induced voltages from normal service has to be differentiated from the load due to:

- Cables & accessories
- Auxiliary supplies
- Battery equipment
- Feeder station
- Main transformers.

Booster transformer connected to a special return conductor is the most commonly used method, and is discussed in detail later in the thesis.

1.1.6 Signalling and Telecommunications

For the railway to function, it is vital to have telecommunication and signalling equipment in the near vicinity. This has a particular effect of the inevitable transfer of energy by induction from one circuit to a neighbouring one. The extent of this transfer is dependent upon a number of factors; in the case of three phase power lines, for instance, the currents are normally balanced in all three phases and the resulting imbalance, which causes interference, is small. Interference derived from harmonic currents may occur with both ac and dc electrification, and this is an issue that needs special consideration to avoid undue noise in the light current circuits.

Magnetic induction is the main cause of interference and its extent clearly depends upon the magnitude of the currents in the power circuit. Some of the protective measures[1] that can be applied to control interference are:

(a) At the source

(b) In the low current circuits affected and,

(c) By screening.

- Screening by cable sheath
- Induction from power cables
- Screening by rails.

Conductive coupling is another source of interference that remains to be mentioned in connection with effects on railway signalling circuits. This occurs when two circuits have common branch and there are three choices of protective measures against this type of interference,

- Screening cables
- Compensation of supply
- Booster transformers.

Good grounding and shielding of cables also play a vital role in reducing electromagnetic interference.

Railway signalling system uses track circuits to detect the different positions of the train. A brief description about the different track circuits available are given in the section below (1.1.7)

1.1.7 Track circuit

Track circuits provide means for detecting trains in various section of a track and, hence form the basis for railway signalling. Although there are several types of track, the basic principle underlying their application is the same. The entire length of the track is divided into a number of track sections. For each section, current is fed in at one end and a relay is energised at the other end when the section is clear (i.e. not occupied by a train). The presence of a train in the track section causes the track relay to de-energise, because the supply current is diverted through the axles of the train[44,45]. As mentioned there many different type of track circuits, these are d.c, Reed, TI 21, and HVI covering different range of frequencies. In this thesis only d.c track circuit as applied in a.c railway are discussed.

Track circuits for one-rail traction return systems are called single-track. Both d.c and a.c single track circuits can be used for one-rail ac traction return systems.
The simplest track circuit, utilising a battery feed as shown in Figure 1.9[47] below, is not owing to the false operation, which can be caused by ac potentials across the track.

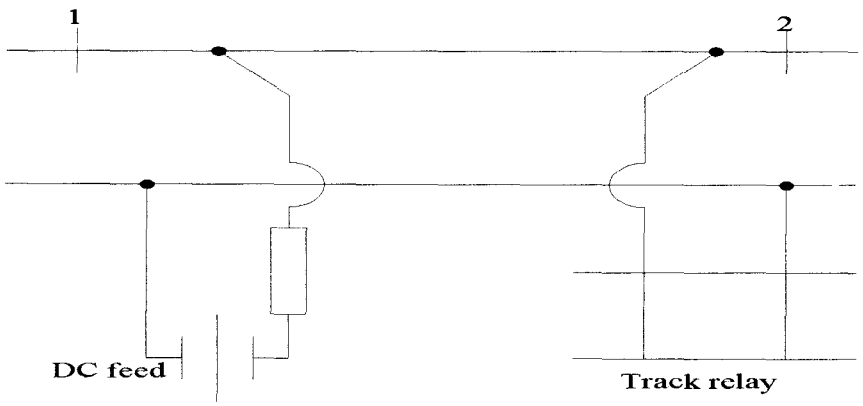

1,2 = Insulated block joints

Figure 1.9: DC single rail track circuit

In other words, the relay, which is energised in the absence of a train, might not de-energise when a train enters into the section. One remedy of this wrong-side failure would be to fit a choke in series with the relay. Nevertheless, it would still be unsafe, because if the choke

became short circuited, the relay would no longer be immune to ac voltages and would readily pick up due to the effects of ac current, when a train is standing on the track circuit. Almost all dc track circuits therefore employ track relays, which are especially designed to be immune to ac voltages. Additionally a choke may however be fitted at the feed-end of this track circuit in order to reduce the ac current flowing through the track feed battery[46,62,63]. From above it follows that a suitable dc track circuit would be as shown in Figure 1.10 below.

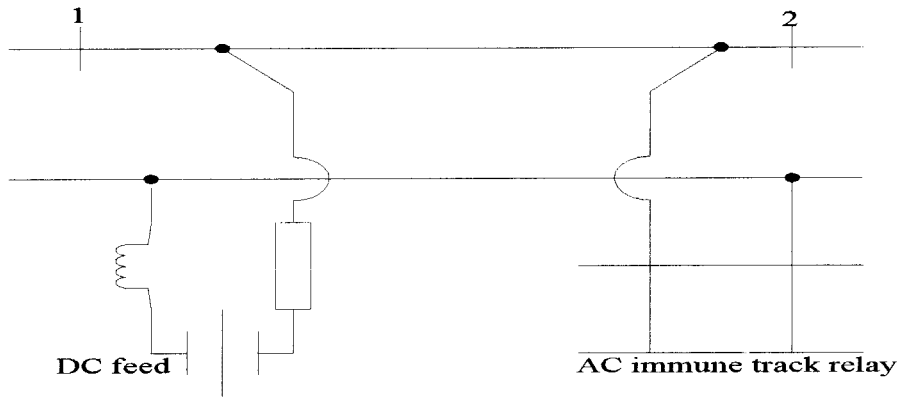

Figure 1.10: AC immune DC single rail track circuit

In a two-rail return traction system, the traction current returning to the sub-station is shared between the two rails; also the track circuit uses both rails. Ac track circuits are used in such systems, which by virtue of their use in two-rail traction return systems are called double-rail ac track circuits.

The frequency for single or double rail ac track circuits must be clear of 50 Hz and its harmonics. 831/3 Hz track circuits have been employed; this frequency may be obtained by using a motor alternator set in which a synchronous motor having 3 pole pairs is coupled to an alternator having 5 pole pairs. The motor speed would be 1000 rpm and the output from the alternator is thus 505/3=831/3 Hz[46,47,48].

In 831/3 Hz track circuits, a central power supply is employed which provides two phases of 831/3 Hz over a signalling area. Figure 1.11[47] below shows one arrangement of the 831/3 Hz single rail track circuits.

For optimum operation the local and control voltages on the relay should be in quadrature; thus if the two 831/3 Hz supply phases are in quadrature, the track circuit equipment should be

designed to produce a minimum phase shift. The feed-end equipment consists of a step-down transformer and track-feed resistor.

At the relay end there is a filter tined to 831/3 Hz and a saturable transformer. The filter will reject all normal levels of 50Hz. Whilst under fault conditions the saturable transformer will prevent the relay from operating. This happens even if at the same time there were to be some infiltrated 50Hz voltage of the correct phase relationship on the local winding of the track relay, provided this does not exceed the level at which the detection equipment is set to operate[49].

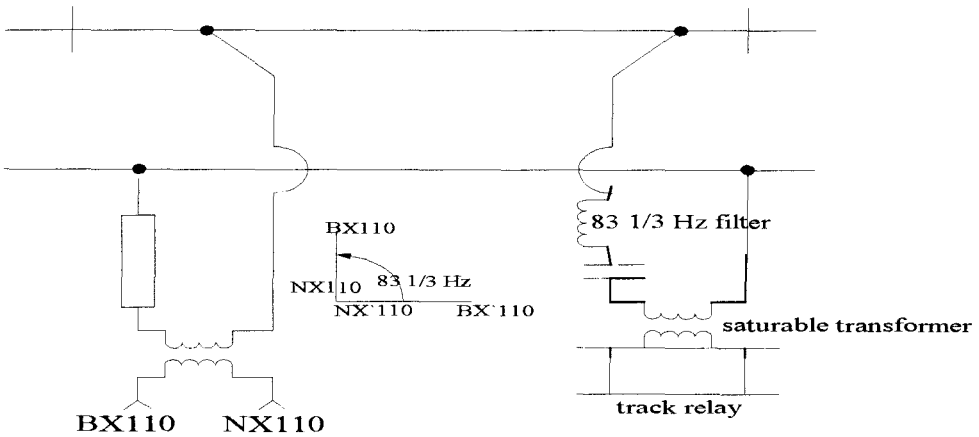

Figure 1.11: 831/3 Hz single-track circuits

The 831/3 double rail track circuits are similar to single track one and are shown in Figure 1.12[47].

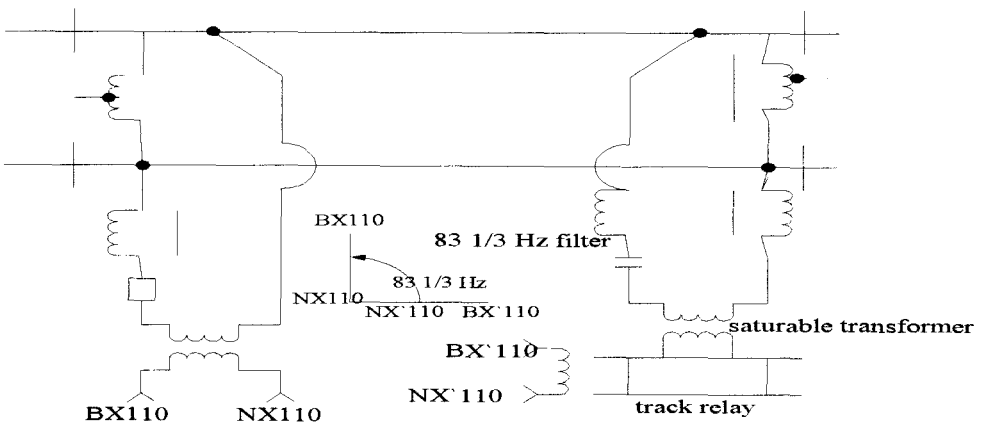

Figure 1.12: 831/3 Hz double track circuit

The track-feed resistor may be of a lower voltage type due to reduced out-of-balance 50 Hz voltages across the track. As the track circuit rail voltages are less for the double rail track circuit an ac type auto impedance bond is used, designed to saturate at a low rail voltage in order to prevent high voltages being fed to the track circuit equipment under fault conditions. Signalling cables unlike telecommunication cables are unscreened, this is due to the fact that only trained personnel are allowed in those area. However some sort of screening can be still be achieved from the nearby earthed conductor. This is explained briefly in section 1.1.8 below.

1.1.8 Screening factor of return system

The earthed conductors in the near vicinity such as cable sheaths, metal pipes, earth wire and rails provide screening effect, which helps in reducing the induction caused. This effect is known as the screening factor and is defined as:

The voltage induced in the presence of the conductor to which the screening factor refers to, divided by the voltage that would be induced if the conductor to which the screening factor refers were absent[52,53,54].

This effect is better understood from the Figure (1.13) below.

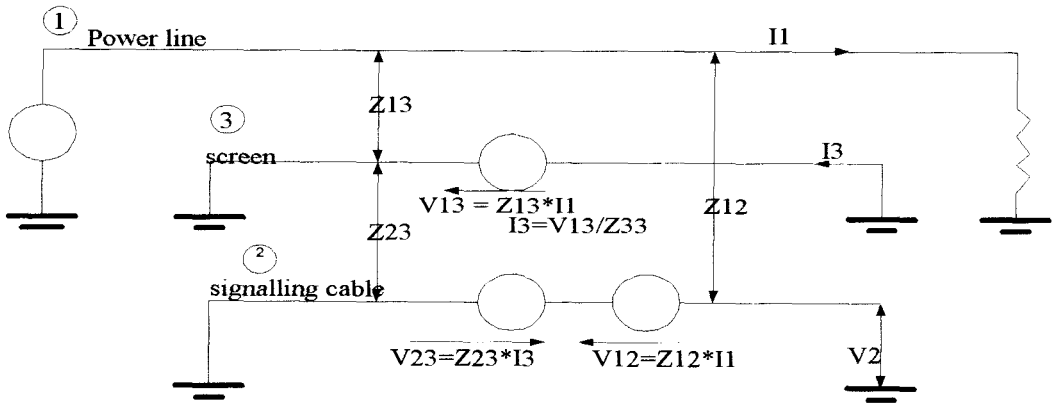

Figure 1.13: Screening factor effect

The current I in the overhead line induces a longitudinal voltage V_{12} in the neighbouring signalling line. The railway and signalling lines can be considered as loop circuits each having earth return. These two loops have mutual impedance and the induced voltage is directly proportional to this mutual impedance and to the current following in the railway circuit.

1.1.9 Quantifying interference

One of the most controversial issues is the magnitude of electric disturbance caused to signalling and telecommunication circuits along or near the electrified lines. When electrification was carried out, cables replaced existing open wire routes on poles whose sheaths could form an adequate screen against induction. However, it was important to remove them for locating the overhead contact system supports.

The use of unbalanced circuits for dialling and ringing was a common practice. Due to the huge cost of altering such work, it was decided to restrict the interference at the source. One way of doing so is to introduce a return conductor with booster transformers at intervals of about 2 miles. It is now common practice to use BTs and return conductors to reduce the level of induced voltage. With the introduction of the EMC directive in 1996, further analysis and quantification of the problem was required.

1.2 Reasons for Calculations

As BTs can add significantly to the cost of railway systems, their use should be justified. This can only be accomplished if the level of the induced voltage is known. The methods used to calculate this induction are not new and have been investigated for many years. However, the work in this thesis is about a new approach which uses finite different time domain method for mathematical and computer simulation.

The following section provides a brief account of some of the main contributions in this field.

1.3 Literature review

This section contains a brief review of literature helpful for understanding the material presented in this thesis. The references in this section are relevant to the thesis as a whole and to the material presented in Chapters (2),(3), and (4) in particular.

Several textbooks outside the field of railway and power engineering were particularly useful for this project. The derivations and computational methods presented in Chapters (2) require an understanding of differential form of Maxwell's equations. The first two chapters of [Taflove, 2000][1] and the first chapter of [Sullivan, 2000][2] are recommended. [Roters, 1992][3] is an excellent reference for electromagnetic and transmission line computations and [Grivet, 1990][4] for transmission of the high power line. [Perry, 1992][5] is an accessible and clear reference for C programming. [Karmel, 1998][6] is a popular reference for electromagnetic. [Magid, 1968][7] is a valuable reference concerning electromagnetic computations and is most frequently cited in transmission systems papers concerning voltage and current computations. [Yee, 1966][8] presents an explanation of the basic and the application of FDTD method, which forms the backbone of the methods in this report.

The fundamentals of transmission line and its parameters are covered in [Wodelifi, 1978][9], and [Galloway, 1964][10]. Electric traction is discussed in [Dover, 1963][11], and [Partab, 1973][12]. [Electrification, 60][13] by IEE is a most comprehensive reference that contains different papers on the basic of ac single-phase electrification. [Klewe, 1958][14] describes interference problem with respect to telecommunication cables. [Rosen, 1956][15] has the clearest explanation of the interference problem. Supplemental to these, [Gupta, 1985][47] and [Millet, 1987, 1990][16,17,18] provide good explanation of induced voltage calculations.

Gupta and Millet have forwarded an approach of the induced voltage analysis using computational method, influential to this thesis. Gupta has applied his method to signalling cables, while Millet's work is related to telecommunication cables. Millet also provided the useful comparison between booster transformers and autotransformers. [CCITT, 1980][19] directive, suggesting the use of computers in these calculations, was also useful source. [Tierney, 1983][20] contains a broad range of ideas and experiences concerning booster transformers. Further references are given throughout the thesis.

1.4 Summary

This thesis demonstrates that the longitudinal voltage induced into signalling systems can be computed with respect to any system parameter using mathematical modelling.

In this chapter, the use of booster transformers in reducing the interference and the voltage level induced was discussed. Also considered was the usefulness of accurate computing of the parameters involved. The layout of the remainder of the thesis is as follow:

Chapter (2) provides the methodology for calculating the impedances of rail-track and overhead conductors and the general framework and assumption used for voltages and current calculations.
Chapter (3) provides calculations and results of induced voltage for uncompensated systems under normal operation conditions for one and two track layouts, for 1250 A and 760 A overhead ratings.
Chapter (4) describes calculations and results for uncompensated systems under fault conditions for the one and two track layouts
Chapter (5) gives the calculations and results of induced voltage for compensated systems under normal operation for one and two track layouts and the two overhead ratings, as well as analysis of the booster transformer itself.
Chapter (6) provides calculations and results of induced voltage under short circuit conditions for compensated systems of one and two track layouts.
Chapter (7) discusses the results obtained, comparison with existing methods, limitation of the project, suggestions for future work and draws conclusions.
Chapter (8) provides references
Appendix A gives data used in the thesis and sample of program developed.
Appendix B contains some formula derivation that is not included in the text.
Appendix C gives list of publications based on this thesis.

CHAPTER (2)

Methodology: The self and Mutual Impedance of Rail and Overhead Conductors

Introduction

In order to calculate the voltage induced into signalling cables, the self and mutual impedances of all conductors used, are required. It is important that the calculations are as accurate as possible.

The most commonly used method for the calculation of rail impedance and overhead parameters with respect to railways is Carson's correction method.
This standard analytical method was first introduced by J. R. Carson[21] in the US and almost simultaneously by F. Pollaczek[22] in Germany. Known as Carson's correction method today, it provided the first analytical approach that included the earth return effect. Carson's method is effectively used today and can produce reliable results for the lower range of frequency (load flow studies). At higher frequencies however, the results converge very quickly and errors are produced resulting in inaccurate calculations. This is due to the assumption made that the earth is a semi-infinite series and the correction terms can be tedious and time consuming. With the improvement in computer systems, it is now possible to use as many correction terms as needed and hence improve the results. Moreover, developments in computer speed have made the use of mathematical modelling possible. However the need for higher frequency analysis has prompted engineers to find alternative approaches.

Hill and carpenter[23] provided a complete investigation for the calculation of the rail tack impedance using Finite Element Method (FEM), which requires the solution of Maxwell's

equations. The FEM requires that an appropriate boundary be defined first, and all bodies (including the air and the ground) included in the boundary are modelled as areas. Each area has its own geometric shape and physical properties, such as conductivity, permeability, non-linearly of magnetisation etc. All areas are subdivided into first order triangular finite elements. The boundary conditions must then be given to allow Maxwell's equations to be solved correctly according to the nature of the problem. The electromagnetic energy of the system is then solved and, using energy relation, the impedance of the track is obtained. The FEM is a powerful tool that is able to consider the skin and proximity effects simultaneously and give accurate results. The disadvantages of the FEM include the high cost of software and hardware, long computation times and the need for experience in using the software (training cost).

This prompted the search for a more simple approach that can give the same as or close reliability to the FEM. This has been accomplished by the use of Finite Difference Time Domain method (FDTD). The FDTD method has been growing rapidly in the electromagnetic calculations, its main advantage is that it is a direct solution of Maxwell's equation. The method is simple to develop and implement.

In this section the impedance of rail track and overhead line conductors are calculated using the FDTD approach. Existing software (MATHCAD & APLAC) are used for these calculations and hence any added cost is reduced. First a brief explanation of the FDTD method is given in the following section.

2.1 FDTD Method

The Finite-Difference Time-Domain (FDTD) method is becoming one of the most popular numerical methods for electromagnetic solutions. The method was first introduced by Yee[8]in 1966 and is also known as the Yee algorithm. The popularity of FDTD has continued to grow as computing costs declined. Furthermore, much research has gone into improving the method and more work is still continuing in this field. The method is very useful for engineering research since it is a direct solution of Maxwell's equations which is simply and elegantly discretized. The method employs leapfrog scheme to solve the electric and magnetic field over a wide range of frequencies. Although the method is very simple and easy to implement, it

received little attention when first introduced due to the high computational cost and speed required at that time. With the progress in computers achieved, the interest in the FDTD began to soar. An estimate of the progress in publications is shown in Figure 2.1[9]. The FDTD method can be applied in many areas where numerical and accurate calculations are required, such as power and telecommunications engineering. This is particularly useful for complex systems where practical measurements are not always possible.

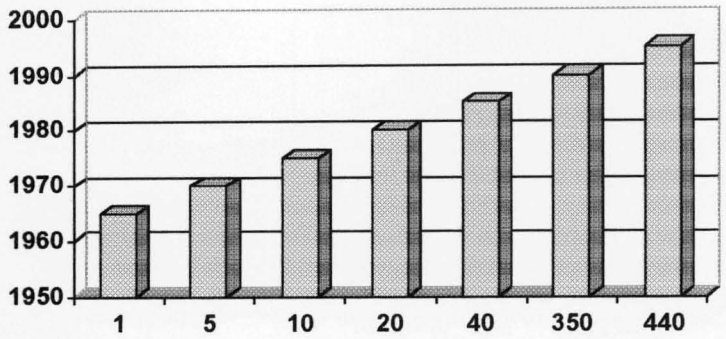

Figure 2.1: FDTD publications (showing years between 1950-1995)

Maxwell's differential equations;

$$\varepsilon \frac{\delta E}{\delta t} + J = \nabla \times H$$

$$\mu \frac{\delta H}{\delta t} = -\nabla \times E \qquad \text{----------(2.1)}$$

$$\nabla \cdot E = \frac{\rho}{\varepsilon}$$

$$\nabla \cdot H = 0$$

These four equations express the basic laws of electricity and magnetism. From the above it can be seen that any change in the electric field (E) with respect to time causes a change in the magnetic field (H) relative to distance.

In formulation, Maxwell's continuous equations convert to a discrete form, which is then solved by a computer. The FDTD has the advantage over other methods in that it can take into account all fields (electric & magnetic) in a three-dimensional (3D) model if required[24]. A 3D Yee cell is shown in Figure 2.2.

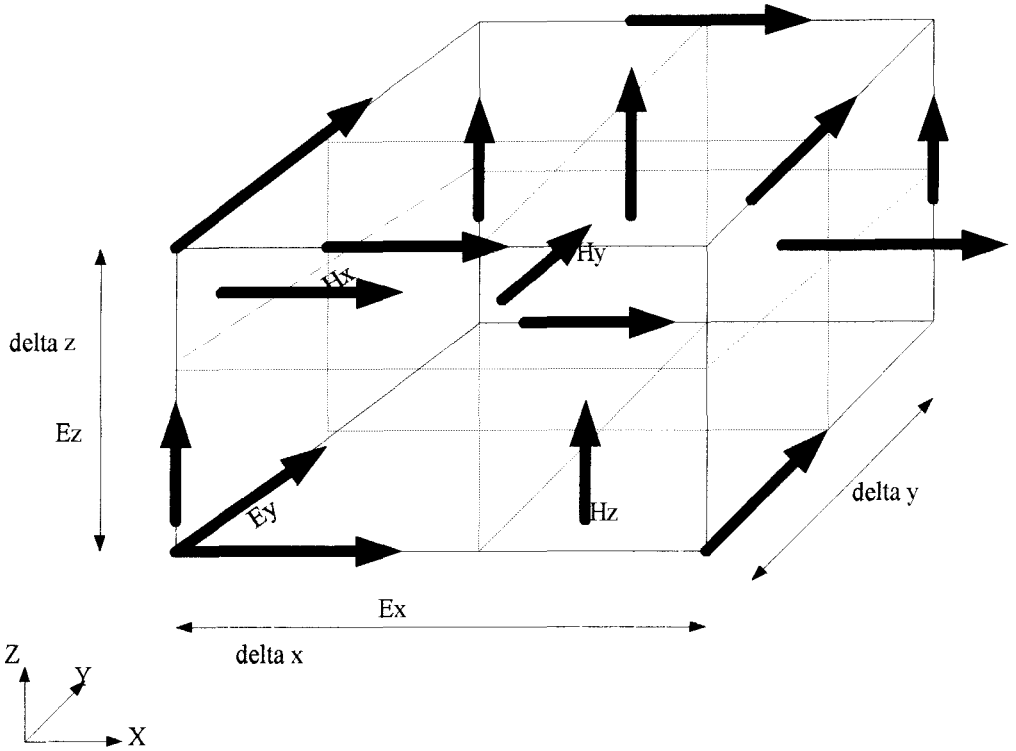

Figure 2.2: Typical Yee cell

Another benefit of the FDTD method is that, since it is a time-domain technique, it can cover a wide frequency range with a single simulation run. Electromagnetic simulation involves representing the system required by a mathematical model. The type of model usually depends on the required accuracy, simulation time and type of results required

The FDTD method belongs to the general class of differential time domain numerical modelling methods. Maxwell's (differential form) equations are simply modified to central-difference equations, discretized and implemented in software. The equations are solved in a leap-frog manner (see Figure 2.3); that is, the electric field is solved at a given instant in time then the magnetic fields are solved at the next instant in time, and the process is repeated over and over again[25,26].

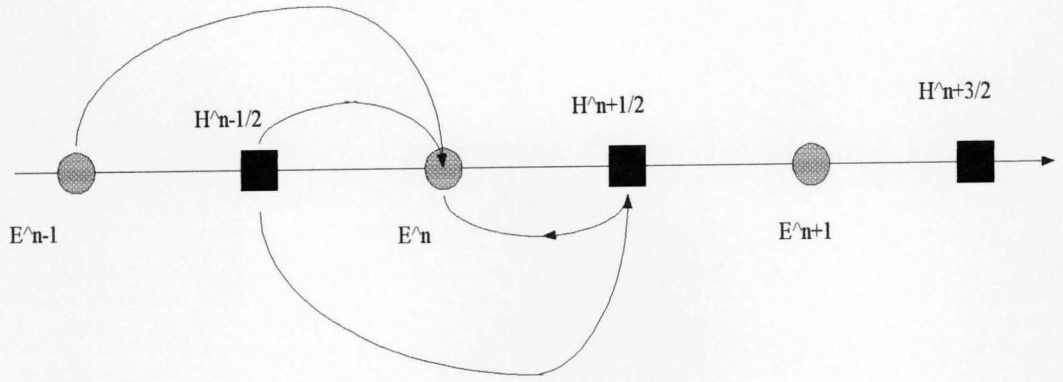

Figure 2.3: Leapfrog scheme

When Maxwell's differential equations are examined, it can be seen that the time derivative of the E field is dependent on the Curl of the H field. This can be simplified to state that the change in the E field (time derivative) is dependent on the change in the H field across space (the Curl). This results in the basic FDTD equation in that the new value of the E field is dependent on the old value of the H field on either side of the E field point in space. Naturally this is a simplified description, which has omitted some details, such as constants, etc. showing only the overall effect.

The H field is found in the same manner. The new value of the H field is dependent on the old value of the H field (hence the difference in time), and also depends on the difference in the E field on either side of the H field point. In order to use FDTD a computational domain must be established. The computational domain is simply the 'space' where the simulation will be performed. The E and H fields will be determined at every point within the computational domain. The material of each cell within the computational domain must be specified. Typically, the material will be free-space (air), metal (perfect electrical conductors (PEC)), or dielectric. Any material can be used as long as the permeability, permitivity and conductivity can be specified[27].

Once the computational domain and the grid material are established, a source is specified. The source can be an impinging plane wave, a current on a wire, or an electric field between metal plates (basically a voltage between the two plates) depending on the type of the situation to be modelled.

Since the E and H fields are determined directly, the output of the simulation is usually either the E or H field at a point or a series of points within the computational domain. The sequence of the FDTD method is better understood from Figure 2.4 below;

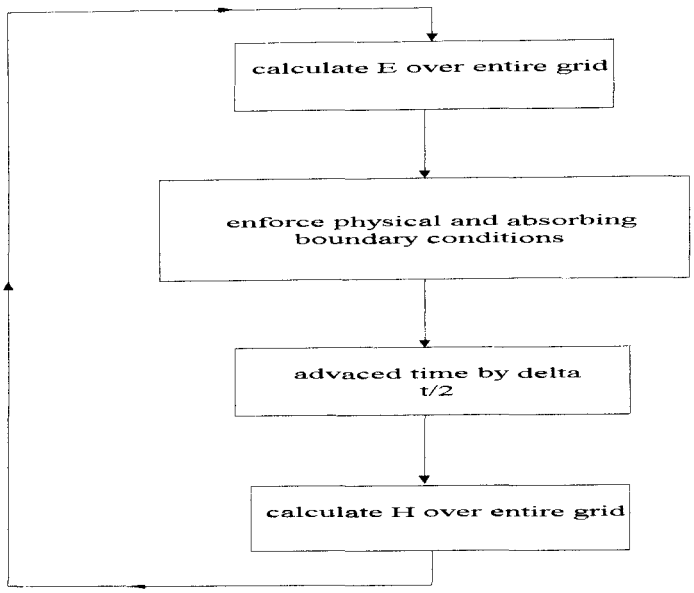

Figure 2.4: Typical sequence of field calculations in FDTD method

For a uniform perfect electric conductor, Maxwell's equations become:

$$\mu \frac{\delta H}{\delta t} = -\nabla \times E \quad \text{----------(2.2)}$$
$$\varepsilon \delta E / \delta t = \nabla \times H$$

Consider the equation in the i (x) direction:

$$\mu \frac{\Delta H_x}{\Delta t} = \frac{\Delta E_y}{\Delta t} - \frac{\Delta E_z}{\Delta y} \text{----------(2.3)}$$

Using the central difference approximation on both time and space to provide discrete approximations:

$$(Hxi, j, k)^{n+\frac{1}{2}} = (Hxi, j, k)^{n-\frac{1}{2}} + \frac{\Delta t}{\mu \Delta z}[(Eyi, j, k)^{n-} - (Eyi, j, k-1)^n] - \frac{\Delta t}{\mu \Delta y}[(Ezi, j, k)^n - (Ezi-1, j, k)^n] \quad \text{---------(2.4)}$$

The half time-steps indicate that E & H are calculated alternately to obtain central differences for the time derivatives.

There are six equations similar to (2.4) in total. These define the E & H fields in the x, y, and z directions and are shown below.

The permittivity (ε) and permeability (μ) values in these cases are set to approximate values depending on the location of each of the field component.

$$(Hxi,j,k)^{n+\frac{1}{2}} = (Hxi,j,k)^{n-\frac{1}{2}} + \frac{\Delta t}{\mu\Delta z}[(Eyi,j,k)^n - (Eyi,j,k-1)^n] - \frac{\Delta t}{\mu\Delta y}[(Ezi,j,k)^n - (Ezi-1,j,k)^n]$$

$$(Hyi,j,k)^{n+\frac{1}{2}} = (Hyi,j,k)^{n-\frac{1}{2}} + \frac{\Delta t}{\mu\Delta x}[(Ezi,j,k)^n - (Ezi,j,k-1)^n] - \frac{\Delta t}{\mu\Delta z}[(Exi,j,k)^n - (Exi-1,j,k)^n] \quad \text{---------(2.5)}$$

$$(Hzi,j,k)^{n+\frac{1}{2}} = (Hzi,j,k)^{n-\frac{1}{2}} + \frac{\Delta t}{\mu\Delta y}[(Exi,j,k)^n - (Exi,j,k-1)^n] - \frac{\Delta t}{\mu\Delta x}[(Eyi,j,k)^n - (Eyi-1,j,k)^n]$$

$$(Exi,j,k)^{n=1} = (Exi,j,k)^{n} + \frac{\Delta t}{\mu \Delta y}[(Hzi,j+1,k)^{n+\frac{1}{2}} -$$

$$(Hzi,j,k)^{n+\frac{1}{2}}] - \frac{\Delta t}{\mu \Delta z}[(Hyi,j,k)^{n+\frac{1}{2}} - (Hyi-1,j,k)^{n+\frac{1}{2}}]$$

$$(Eyi,j,k)^{n+1} = (Eyi,j,k)^{n} + \frac{\Delta t}{\mu \Delta z}[(Hxi,j,k+1)^{n+\frac{1}{2}} -$$

$$(Hxi,j,k-1)^{n+\frac{1}{2}}] - \frac{\Delta t}{\mu \Delta z}[(Hzi,j,k+1)^{n+\frac{1}{2}} - (Hzi-1,j,k)^{n+\frac{1}{2}}]$$

$$(Ezi,j,k)^{n+1} = (Ezi,j,k)^{n} + \frac{\Delta t}{\mu \Delta x}[(Hyi+1,j,k)^{n+\frac{1}{2}} -$$

$$(Hyi,j,k-1)^{n+\frac{1}{2}}] - \frac{\Delta t}{\mu \Delta y}[(Hxi,j+1,k)^{n+\frac{1}{2}} - (Hxi,j,k)^{n+\frac{1}{2}}] \quad \text{------(2.6)}$$

It is important that the time step is set to a certain limit for the stability criteria requirement, this given as;

$$\Delta t \leq \frac{1}{c\sqrt{(1/\Delta x)^2 + (1/\Delta y)^2 + (1/\Delta z)^2}} \quad \text{---(2.7)}$$

where c is the speed of light.

Now that the model and the equations are set, the boundary conditions on the sources and the conductor model are required to obtain reliable results. It is important that the right boundary condition should be applied for meaningful results.

2.1.1 Absorbing boundary condition (ABC)

The main solution using FDTD method is within the computation region set at the beginning of the simulation. For open structure such as overhead and rail conductors and antennas, it is important that analysis should extent beyond the computation region to infinity in order to obtain meaningful results for these calculations. Now an obvious problem is how to extend the simulating structure to infinity rather than the computation region.

The solution is, instead, to terminate the computing region with absorbing boundary conditions that "eat" the incoming wave or pulse in a way that does not give rise to any reflections. In the realm of FDTD simulations no perfect absorbing boundaries exist - they all reflect some part of the incoming wave or pulse. However, these boundaries absorb most of the wave and therefore open structures can be modelled with sufficient accuracy. Quite often an absorbing boundary condition is abbreviated to ABC in the FDTD literature[1,28,29,30,31].

From the definition of the FDTD method we proceed to the system considered and calculation steps.

The steps taken to calculate the induced voltage into signalling systems are as follows;
Step 1: Calculation of rail track impedance
Step 2: Calculation of overhead transmission line parameters (inductance, resistance & capacitance).
Step 3: development of the voltage and current equations.

2.2 Step1: Rail-track impedance calculations

In this thesis the rail-track conductor above ground is solved simply by dividing it up into appropriately sized unit cells, each with a certain value, setting initial values for all of the field components, then calculating the field equations iteratively for as long as the response is of interest.

The behaviour of the field components over the problem space gives an essentially complete characterisation of the behaviour of the structure. It can then be post-processed and information over a broad frequency range can be obtained in a single run. This algorithm, as well as giving an understanding of the operations implied by Maxwell's equations, is a powerful and practical solution method.

Note: certain assumptions have been made in order to simplify the model, these are:
1) All track materials are assumed to be anisotropic,
2) The rails, ballast and sleepers are assumed to be homogeneous,

3) The ground is stratified into homogenous horizontal layers that can be assigned different material properties,
4) The rail fastenings to the sleepers are not modelled.

The impedance of the rail track is solved first and, using the same approach, the overhead parameters are obtained. The rail track impedance model is shown in Figure 2.5 below;

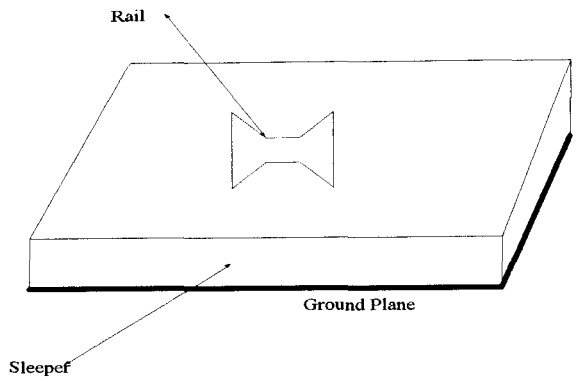

Figure 2.5: Representation of the rail track

The equivalent electric circuit for two rail conductor is as shown in Figure 2.6.

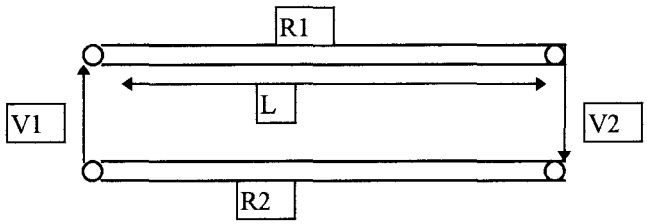

Figure 2.6: Two rail conductor circuit

The above rail structure is analysed using APLAC (see Appendix B, for program description); an electromagnetic software which has built-in components and FDTD analysis facilities. The required components are set and the program is written in a code similar to C, an example is shown in Appendix A.

The voltage response and the currents are obtained for the rail-track and hence the impedance is calculated. The results in Figures 2.7-2.10 are for 50Hz system frequency. The frequency can be changed according to requirements.

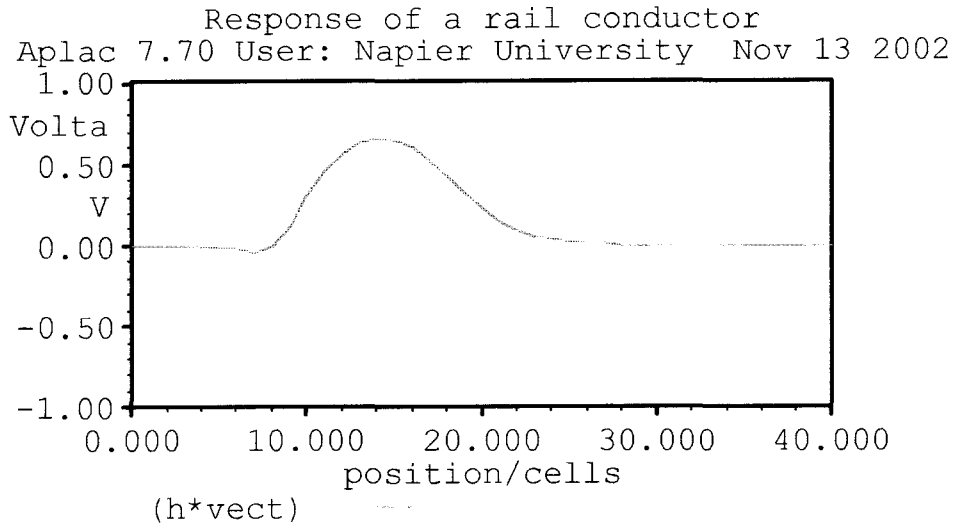

Figure 2.7: The voltage response at a certain time

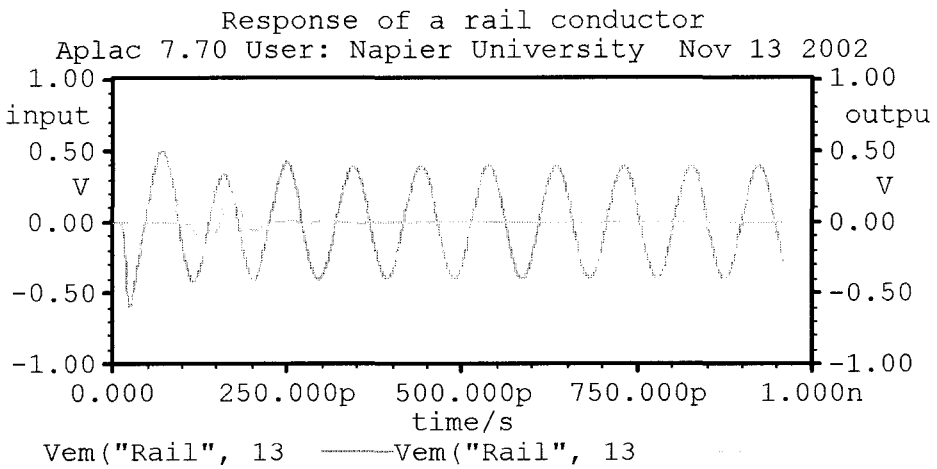

Figure 2.8: The input and output voltage results

Once the computational domain and the grid material are established, a source is specified. The source can be an impinging plane wave, a current on a wire, or an electric field between metal plates (basically a voltage between the two plates) depending on the type of the situation to be modelled.

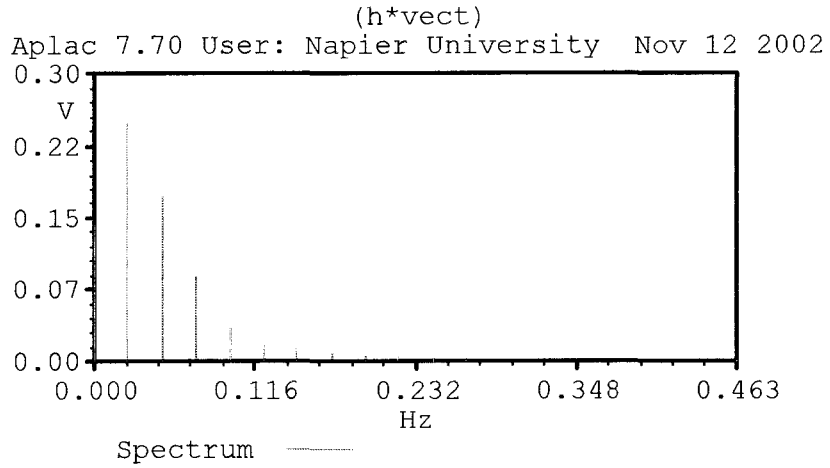

Figure 2.9: Fourier transform for the rail

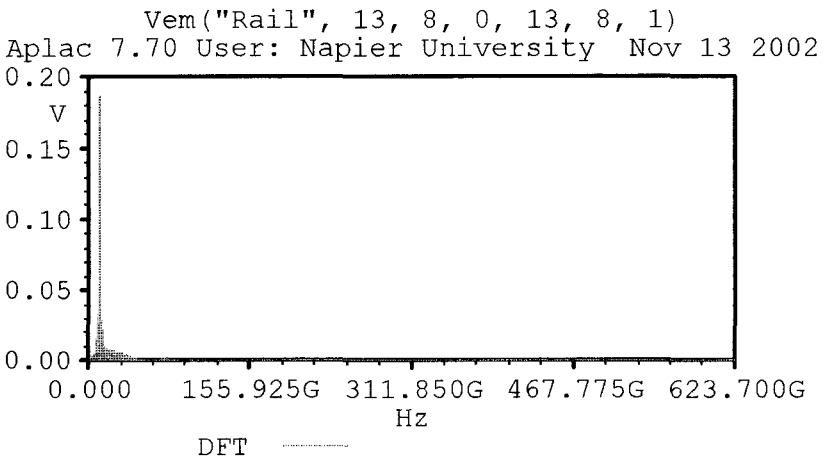

Figure 2.10: Fourier transform for the output.

2.2.1 Comparison of rail track impedance methods

In order to establish the credibility of the method mentioned above, comparison with an existing method is required.

The rail impedance results over the frequency range of 50Hz-1MHz are given for three different methods; Carson's correction term, FEM and FDTD. The results are shown in Table 2.1.

Frequency (Hz)	Carson (ohm/km)	FE (ohm/km)	FDTD (ohm/km)
50	0.402	0.400	0.401
100	0.475	0.456	0.457
1k	1.59	1.230	1.301
5k	1.672	1.251	1.312
8k	1.691	1.273	1.324
10k	2.258	2.451	2.431
30k	2.432	2.458	2.441
60k	2.545	2.537	2.489
80k	2.621	2.562	2.576
100k	4.102	3.572	3.631
200k	9.746	3.924	4.113
400k	12.589	4.127	4.213
600k	14.972	4.365	4.387
800k	15.134	4.392	4.401
1M	15.785	4.689	4.712

Table 2.1: Rail impedance using analytical and numerical methods

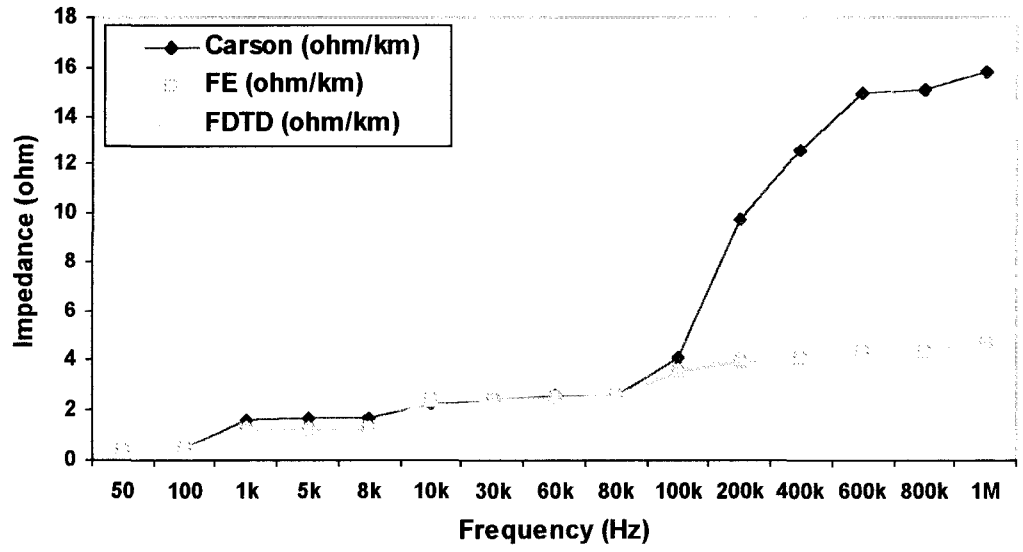

Figure 2.11: Rail-track impedance using Carson's, FE & FDTD methods

Figure 2.11 shows the results of the rail-track impedance using three different methods. From the figure we can see that the FE and FDTD methods provide better results for the calculations of conductor above ground impedance. Although all three methods provide almost exactly the same results for frequency up to 80K Hz, it is clearly obvious that Carson's method overestimates the value of the impedance, this is due to the assumption used (earth is semi-infinite series). The FDTD provides reliable results and is in agreement with the FE method, this is due to the fact these methods take into account the material properties of the conductors and the ground in the from of the conductivity, permeability and permittivity.

2.3 Step 2: Overhead lines (OHL) and their parameters

Overhead transmission lines are used to carry electrical power for large-scale electricity supply. The lines form a network joining generating stations and load centres. Transformers are used to connect lines operating at different voltage levels. For the control of the voltage and power factor and to protect against lightening and other disturbances, electrical calculations for the transmission lines are required.

For a short power line only the series impedance has an effect on its behaviour, the capacitance effect can be considered as negligible. The line impedance consists of two parameters; resistance of the conductor and the reactance which is caused by magnetic flux surrounding the conductors and passing between them. Those two parameters can be measured or calculated using the line dimensions and certain other factors as will be described[33].

For the line shunt admittance, only the line capacitive susceptance can be considered since conductance currents to ground and between conductors are negligible for overhead lines. The capacitive shunt reactance can also be calculated from line dimensions.

The types of conductors used in overhead power transmission lines are stranded hollow conductors of different constructions. Solid conductors are also used to a certain extent. Some typical overhead line support structures with the conductors are shown in Figure 2.12.

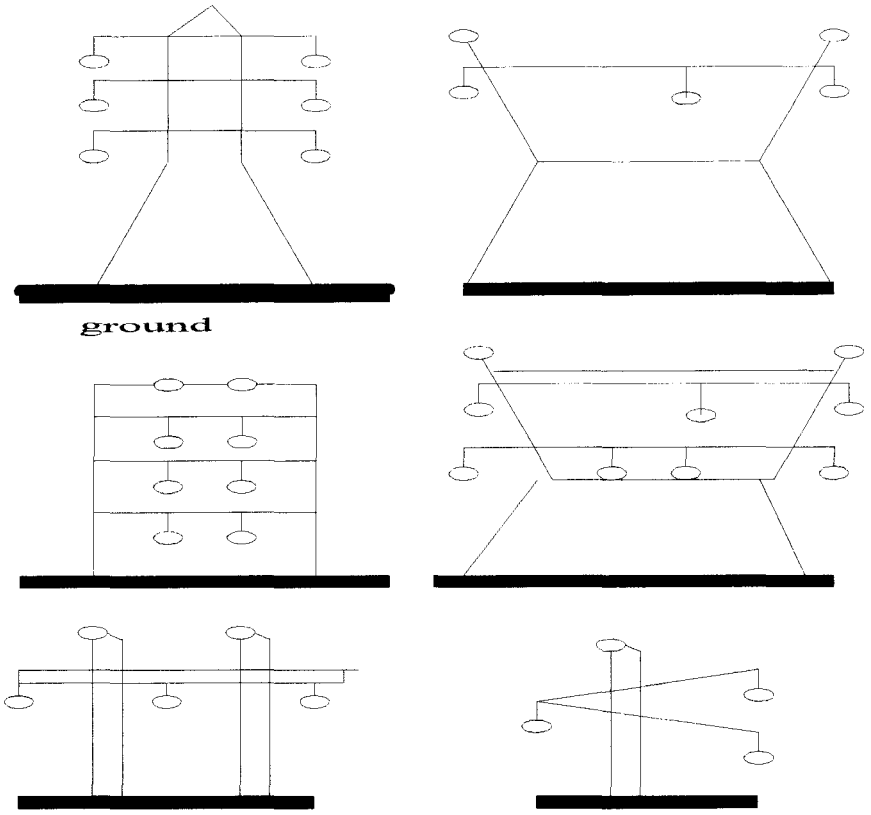

Figure 2.12: Some typical overhead transmission structure

The conductor materials which are in general use for OHL are; hard-drawn-high conductivity copper, hard-drawn aluminium, aluminium alloy and steel-cored aluminium. Data relating to these materials and to stranded conductors made from these materials are given in Table (2.2)[34].

+Application	Material	Composition No. of Strands/DIA. (MM)	Overall DIA. (MM)	Resistance (ohms/km)
Contact Wire	H.D.Copper	Solid	12.3	0.1695
Messenger	AWAC	Alumoweld 6/2.42 Aluminium 31/2.42	16.9	0.1903
Earth Wire	ACSR	Steel 7/2.89 Aluminium 16/2.57	16.3	0.2143
Feeder	ACSR	Steel 7/2.89 Aluminium 26/3.72	23.5	0.1027
Buried Earth wire	Bare Copper	7/3.5	13.0 (67.4 mm^2)	0.280
Continuity	Steel	19/3.81	20.0	0.670
Rail	Steel		(146.0)*	0.024

Table 2.2: **+ Data given for new contact wire-for impedance and current rating calculations, 25% reduction in area due to wear is allowed**

* Diameter of equivalent conductor, having circular cross-section.

The most important property of an OHL conductor material is high tensile strength (high breaking load), so that longer spans can be achieved with the smallest possible sag. This provides a reduction in the number and height of the towers (or poles) and the number of insulators required. It is also important that the conductors have low resistance to reduce power loss and voltage drop[35,36].

For the development of overhead line parameter calculations, many simplifying assumptions have been made and calculations were carried out for single track and double track at system frequency (50 Hz). Generally the parameter calculations are based on conductor configuration for every system. The bonding of the rails are neglected throughout the study.

2.3.1 Transmission line parameters (TL)

The parameters of multi-conductor transmission line (MTL) can generally be divided into two groups; those at power frequency and those at higher frequencies. The first are required for load flow studies, system stability, and fault levels. The second are needed for re-striking voltages, radio interference, propagation characteristics of power line and switching over-voltages.

In steady state (SS) the resistance of an overhead TL determines the energy loss and therefore the current carrying capacity of the line. The series reactance controls directly the maximum power flow capability of the line and to some extent the system fault level. The shunt susceptance determines the VAR generation and affects the system voltage profile.

2.3.1.1 Overhead transmission line (OHTL) resistance

The effective resistance (= power loss (w/rms)/ I^2 (amp)), is equal to dc resistance of the conductor only if the current distribution over the cross area of the conductor is uniform. The dc resistance is given by;

$R_{dc} = \rho L / A$ (ohm)-----(2.8)

where;

ρ= resistivity of conductor material

L = length

A = cross-section area.

Or

$R_{dc} = 2.5\rho / \pi a^2$ ohm/mile----(2.9)

a = conductor radius

The dc resistance of stranded conductors is greater than that computed above due to spiralling of the strands which makes them longer than conductor length. The increased resistance due to spiralling was estimated as 2%[37] for concentrically stranded conductors.

2.3.1.2 The skin effect and OHTL inductance

When an alternating current flows in a conductor, the alternating magnetic flux within the conductor induces an e.m.f., which causes the current density to decrease in the interior of the conductor and increase on the surface. This phenomenon is known as the skin effect which results in changes of the resistance and internal inductance of the conductor. Skin effect becomes more pronounced as the frequency increases and for large diameters of the conductor.

Analytical and approximated methods have been developed to estimate the resistance ratio (R_{ac} / R_{dc}) and the internal inductance ratio ($L_{i\,ac} / L_{i\,dc}$). These approximated methods are based on Bessel[38] and Butterworth[39]. Bessel function provides better results for higher frequency (> 12kHz) while Butterworth can be used effectively for frequencies up to 12 kHz, both formulas can be found in Appendix B.

The inductance of an overhead line on the other hand is a combination of internal (due to internal flux linkages) and external (due to external flux linkages) inductance (derivations are given in Appendix B) and is given as;

$$L = L_{\text{int}} + L_{ext} \text{ --------(2.10)}$$

where, $L_{\text{int}} = \frac{\mu}{8\pi}$ and $L_{ext} = \frac{\mu}{2\pi} \cdot \ln(\frac{D}{r})$ --------(2.11)

giving the total inductance reactance of:

$$L = \frac{\mu}{2\pi}(\frac{1}{4} + \ln(\frac{D}{r}) \text{ ------(2.12)}$$

where D = distance between conductors.

2.3.1.3 OHTL capacitive reactance

In order to calculate the capacitance, the following assumptions are made:

1. OHTL conductors are on straight lines at average heights above the ground and parallel to it.
2. Each conductor is at the same potential throughout its length and the charge on it is uniformly distributed.

3. The existence of the line impedance is neglected.
4. Effect of surrounding structure is neglected.
5. Earth surface is an equi-potential plane of zero potential.

For a multi-conductor line, the inductance and capacitance matrices are shown below;

For L matrix, the inductance is obtained from the relationship of the total magnetic flux in the i-th circuit, to all the line currents producing it as;

$$[\psi]=[L][I]$$

exp*anding*; --------(2.13)

$$\begin{bmatrix}\psi_1\\ \psi_2\\ \vdots\\ \psi_n\end{bmatrix}=\begin{bmatrix}l_{11} & l_{12} & \cdots & l_{1n}\\ l_{12} & l_{22} & l\ldots & l_{2n}\\ \vdots & \vdots & \ddots & \vdots\\ l_{1n} & l_{2n} & \cdots & l_{nn}\end{bmatrix}\begin{bmatrix}I_1\\ I_2\\ \vdots\\ I_n\end{bmatrix}$$

If we interpret the above relations in a manner similar to the n-port parameters, we obtain the following relations for the entries in L:

$$l_{ii}=\frac{\psi_i}{I_i}\Big|_{I_1=\ldots=I_{i-1}=I_{i+1}=\ldots=I_n=0}$$

--------(2.14)

$$l_{ij}=\frac{\psi_i}{I_j}\Big|_{I_1=\ldots=I_{j-1}=I_{j+1}=\ldots=I_n=0}$$

Thus the inductance can be computed by placing a current on one conductor and setting the current on all other conductors to zero. The definition of the i-th circuit is critically important in obtaining the correct value and sign of these elements.

Now the capacitance matrix entries are considered. C relates the total charge on the i-th conductor PUL to all of the line voltages producing it as;

[Q]=[C][V]-----(2.15)

Expanding the above;

$$\begin{bmatrix} q_1 \\ q_2 \\ \vdots \\ q_n \end{bmatrix} = \begin{bmatrix} \sum_{k=1}^{n} c_{1k} & -c_{12} & \cdots & -c_{1n} \\ -c_{12} & \sum_{k=1}^{n} c_{2k} & \cdots & -c_{2n} \\ \vdots & \vdots & \ddots & \vdots \\ -_{1n} & -c_{2n} & \cdots & \sum_{k=1}^{n} c_{nk} \end{bmatrix} \begin{bmatrix} V_1 \\ V_2 \\ \vdots \\ V_n \end{bmatrix} \text{------(2.16)}$$

Applying the same approach above, the c matrices can be obtained as;

$$c_{ii} = \frac{q_i}{V_i}\Big|_{V_1=\ldots=V_{i-1}=V_{i+1}=\ldots=V_n=0}$$

--------(2.17)

$$c_{ij} = \frac{q_j}{V_j}\Big|_{V_1=\ldots=V_{j-1}=V_{j+1}=\ldots=V_n=0}$$

The C matrix can also be obtained from the relation:

[V]=[P][Q]-----(2.18)

And [C]=[P]^-1.-----(2.19)

Using the method of images as described below, the inductance and capacitance of an "n" wire above ground can be obtained form the Figure 2.13.

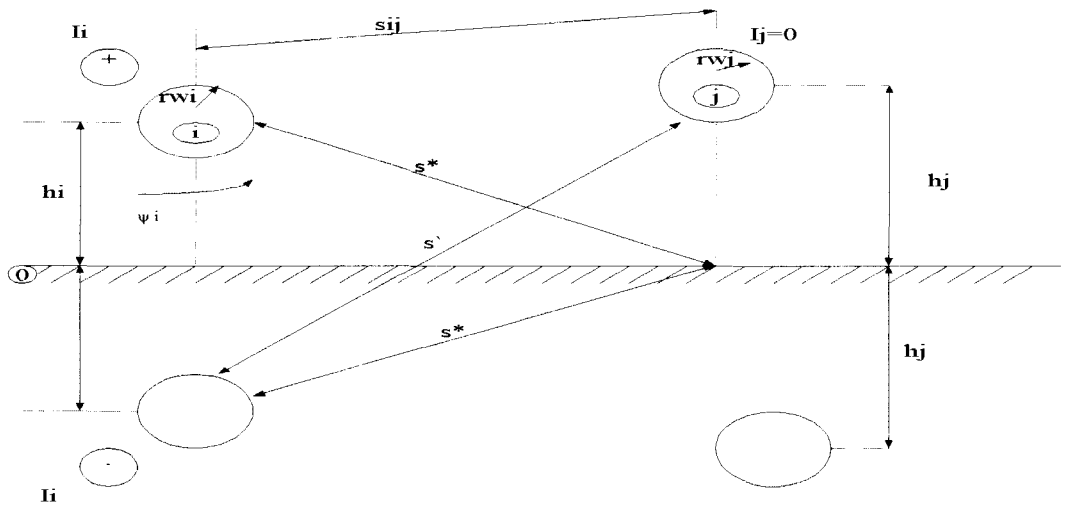

Figure 2.13: Images method for an "n" wires above ground

In the above figure, the infinite plane for conductors "i" and "j" above ground is replaced with an equal but negative conductor below ground. This is known as the method of images. The same can be applied by replacing the plane with the image currents and using the fundamental result derived above;

$$l_{ii} = \frac{\psi_i}{I_i}\Big|_{I_1=\ldots=I_{i-1}=I_{i+1}=\ldots=I_n=0} = \frac{\mu}{2\pi}\ln(\frac{h_i}{r_{wi}}) + \frac{\mu}{2\pi}\ln(\frac{2h_i}{h_i}) = \frac{\mu}{2\pi}\ln(\frac{2h_i}{r_{wi}})$$

$$l_{ij} = \frac{\psi_i}{I_j}\Big|_{I_1=\ldots=I_{j-1}=I_{j+1}=\ldots=I_n=0} = \frac{\mu}{2\pi}\ln(\frac{s^*}{s_{ij}}) + \frac{\mu}{2\pi}\ln(\frac{\hat{s}}{s^*}) = \frac{\mu}{2\pi}\ln(\frac{\sqrt{s_{ij}^2 + 4h_i h_j}}{s_{ij}}) \text{----(2.20)}$$

$$l_{ij} = \frac{\mu}{4\pi}\ln(1 + \frac{4h_i h_j}{s_{ij}^2})$$

2.3.1.4 Consideration of losses: (R, Li)

It has been mentioned that for comprehensive analysis, the above method will provide incomplete analysis unless the losses accounted for. These losses are considered in the form of resistance matrix. Also, the current of imperfect conductors does not flow solely on the conductor surfaces as with perfect conductors but are distributed over the conductor cross sections. This gives rise to a portion of the PUL inductance matrix, the internal inductance Li, due to magnetic flux internal to the conductors. This can be included in the total PUL inductance matrix as:

$L = L_i + L_e$ -------(2.21)

For perfect conductor L = Le

2.3.1.5 Representation of conductor losses

In contrast to losses in the surrounding medium, losses due to imperfect line conductors may be significant even for frequencies below the low giga-hertz range. These losses are determined by the entries in the PUL resistance matrix R. At low frequencies the entries in R are constant whereas at higher frequencies they typically vary as the square root of frequency, as a result of skin effect. Also the imperfect conductors give rise to internal inductance which contribute to Li. These elements typically are constant at low frequencies and decrease as $\sqrt{f}$ at higher frequencies. Thus their inductive reactance Li increases with $\sqrt{f}$, and external reactance Le increases as f.

The current density and the electric and magnetic fields in good conductors are governed by the diffusion equation. Ampere's law relates the magnetic field to the sum of conduction current and displacement current as:

$$\nabla \times \vec{H} = \sigma\vec{E} + j\omega\varepsilon\vec{E} \text{ --------(2.22)}$$

In a good conductor, the conduction current greatly exceeds the displacement current which is satisfied for most metallic conductors and frequencies of reasonable interest.
Thus the above equation can be approximated as:

$$\nabla \times \vec{H} = j\sigma\vec{E} \text{ -----(2.23)}$$

Similarly Faraday's law:

$$\nabla \times \vec{E} = -j\omega\mu\vec{H} \text{ -----(2.24)}$$

Taking the curl of Faraday's law gives

$$\nabla \times (\nabla \times \vec{E}) = \nabla \cdot (\nabla \cdot \vec{E} - \nabla^2 \cdot \vec{E}) = -j\omega\mu\nabla \times H \text{ ------(2.25)}$$

Substituting Gusses's law:

$$\nabla \cdot \varepsilon_0\vec{E} = 0 \text{ -------(2.26)}$$

Gives;

$$\nabla^2 \cdot \vec{E} = j\omega\mu\sigma\vec{E} \text{ ----(2.27)} \qquad \text{(since j = σE)}$$

$$\nabla^2 \cdot j = j\omega\mu\sigma j \text{ -----(2.28)}$$

Now the resistance of a wire and internal inductance may be considered:
For circular cylindrical conductors (wires), two identical wires in homogeneous medium with radius r_w and separated by s;

$$r = \frac{2R_s}{2\pi r_w}\left(\frac{s}{2r_w}\Big/\sqrt{\left(\frac{s}{2r_w}\right)^2 - 1}\right) \text{------(2.29)} \quad \text{ohm/m}$$

where

$$R_s = \frac{1}{\sigma\delta} = \sqrt{\frac{\pi f \mu}{\sigma}} \text{-----(2.30)}$$

2.3.1.6 Surface impedance of plane conductors

Consider a semi-infinite conductor half-space with parameters σ, ε, μ, whose surface lie in x-y plane as shown in Figure 2.14.

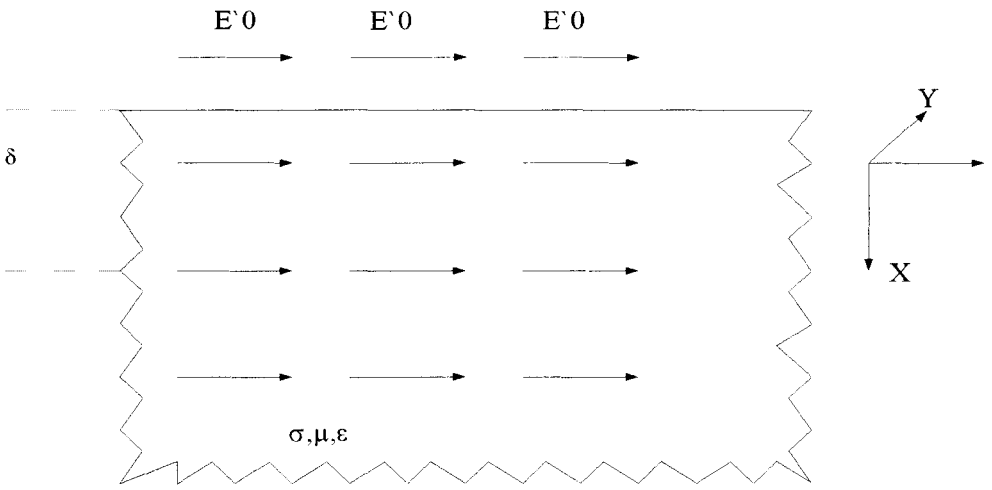

Figure 2.14: Diffusion of current and fields into semi-infinite conductor half-space

Assuming that electric field (E) and associated conductor current density are directed in the z direction, diffusion equation term of z directed E field becomes:

$$\frac{d^2\hat{E}_z}{dx^2} = j\omega\mu\sigma\overline{E}_z \text{--------(2.31)}$$

Similarly for magnetic field, Hy, and jz;

$$E_z = E_0 e^{-x/\delta} e^{-j_0 x/\delta}$$

$$H_y = H_0 e^{-x/\delta} e^{-j_0 x/\delta}$$

where --------(2.32)

$$\delta = \frac{1}{\sqrt{\pi f \mu \sigma}} (skin - depth)$$

H_0, E_0, j_0, are surface quantities.

The surface impedance can be defined as the ratio of the z-directed E field to surface and total current density;

$$Z_s = \frac{E_0}{j_t} \text{------(2.33)}$$

$$j_t = \int_0^\infty j_z dx = \frac{j\delta}{1+j} \text{-----(2.34)}$$

$$Z_s = R_s + j\omega L_i \text{------(2.35)}$$

$$R_s = \frac{1}{\sigma\delta} = \sqrt{\frac{\pi f \mu}{\sigma}} \text{-----(2.36)}$$

If $\omega L_i = R_s$, then

$$Z_s = \sqrt{\frac{\pi f \mu}{\sigma}} \text{-----(2.37)}$$

2.3.1.7 Resistance (R) and internal inductance (L_i) of wires

For a circular cylindrical conductor (wire) and perfect conducting, the current flows on the surface of the conductor. R and L_i result from the current and magnetic flux internal to the imperfect conductors in a fashion similar to that of the surface impedance of a plane conductor. L_i results from magnetic flux internal to the conductor that links the current.

For a wire, assuming current is symmetric about the axis of the wire, the radius is r_w;

$$r = \frac{2R_s}{2\pi r_w}\left[\frac{s/2r_w}{\sqrt{(s/2r_w)^2 - 1}}\right] \text{-----(2.38)}$$

Using the above information the inductance and resistance can be obtained from the FDTD analysis. From the FDTD figure for transmission line the flux integral would be performed on the surface S with the direction of the surface vector DS as shown in Figure 2.15. The current integral would be performed along the contour C.

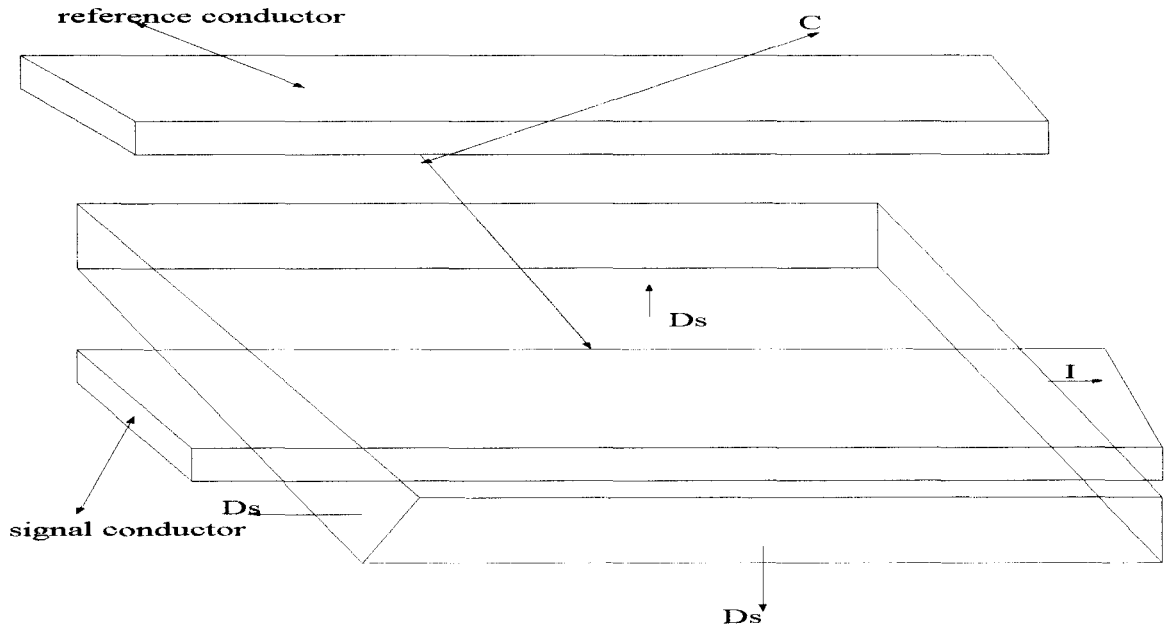

Figure 2.15: Inductance calculated from flux through S and current on the transmission line

$$L = \frac{\phi}{I} = \frac{\int B.ds}{\oint H.dl} = \frac{\int \mu H.ds}{\oint H.dl} \text{ ------(2.39)}$$

In the FDTD grid these integral translate into sums as given by;

$$L = \frac{\mu \sum H.\Delta.\Delta}{\sum H.\Delta} \text{ -------(2.40)}$$

Thus, an inductance per unit length can be calculated by taking the ratio of the sum of the H field values over the surface S, and the sum of the H fields in the direction of dL divided by the length along the transmission line that the surface extends over.

The capacitance is defined as the ratio of the charge in an enclosed surface to the electromagnetic potential of the surface region.

$$C = \frac{Q}{V} = \frac{\oint D.ds}{\int E.dl} = \frac{\oint \varepsilon E.ds}{\int E.dl} \text{-----(2.41)}$$

In the FDTD grid, these integrals translate into sums as given by:

$$C = \frac{\varepsilon \sum E.\Delta.\Delta}{\sum E.\Delta} \text{-----(2.42)}$$

For the calculations of the self and mutual impedances of the conductor i and j at system frequency (50Hz), the equations are as follow;

$$\begin{aligned} Z_{ii} &= R_{ii} + jL_{ii} \\ Z_{ij} &= R_{ij} + jL_{ij} \end{aligned} \text{------(2.43)}$$

2.4 System considered for self and mutual impedances calculations

The data for the system considered are shown below, the self and mutual impedance for single track and double track railway systems with two different overhead rating (1250 and 760 Amps) were calculated and the results are given below:

Note: self and mutual impedances were calculated at system frequency, hence the impedance consists of resistance and inductance only as the capacitance effect is considered to be negligible

2.4.1 Data for uncompensated systems

Tables 2.3-2.6 show the position (x & y) of the conductors for uncompensated systems with two different overhead ratings and cable (signalling) position. Their positions are shown in Figures 2.16-2.18 and 2.19 respectively[47].

Conductor	X (m)	Y (m)
R1	-.08	0.1524
R2	0.8	0.1524
B1	-4.5	-1.66
EW1	-2.988	6.875
EW2	-3.463	6.093
M	0	6.6
CW	0	5.7
F	-4.18	6.543

Table 2.3: Open track 1250 amps cable on normal side (Figure 2.16)

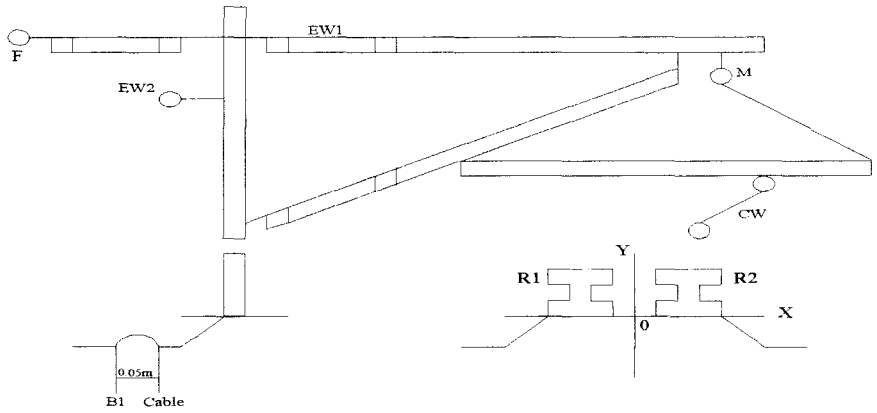

Figure 2.16: One-track case with 1250 Amps OCS configuration, cable on normal side

Conductor	X (m)	Y (m)
R1	-.08	0.1524
R2	0.8	0.1524
B2	4.5	-1.66
EW1	-2.988	6.875
EW2	-3.463	6.093
M	0	6.6
CW	0	5.7
F	-4.18	6.543

Table 2.4: open track 1250 amps cable on the other side (Figure 2.17)

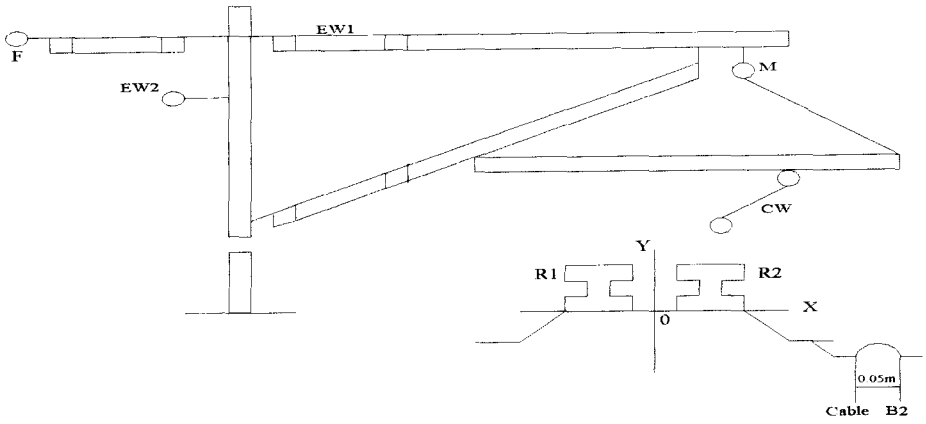

Figure 2.17: One-track case with 1250 Amps OCS configuration, cable on the other side

Conductor	X (m)	Y (m)
R1	-.08	0.1524
R2	0.8	0.1524
B1	-4.5	-1.66
EW1	-2.988	6.875
M	0	6.6
CW	0	5.7

Table 2.5: Open track 760 amps cable on normal side (Figure 2.18)

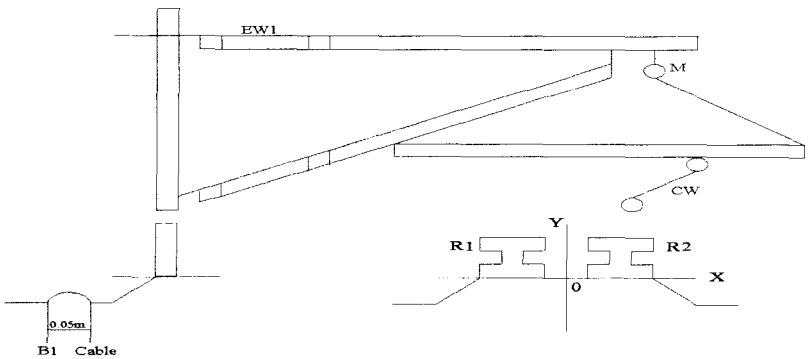

Figure 2.18: One-track case with 760 Amps OCS configuration, cable on normal side

Conductor	X (m)	Y (m)
R1	-.08	0.1524
R2	0.8	0.1524
B2	4.5	-1.66
EW1	-2.988	6.875
M	0	6.6
CW	0	5.7

Table 2.6: Open track 760 amps cable on the other side (Figure 2.19)

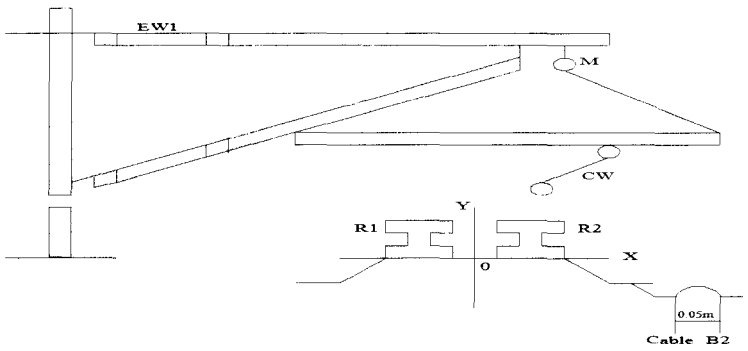

Figure 2.19: One-track case with 760 Amps OCS configuration, cable on the other side

2.4.2 Data for compensated systems

Here we have the data (Tables 2.7 and 2.8) and diagrams (2.20 and 2.21) for compensated system conductors[47].

Conductor	X (m)	Y (m)
R1	0.73152	0.1524
R2	-0.73152	0.1524
RT	3.048	5.7912
CW	0	4.7244
F	0	-4.732

Table 2.7: One track configurations in an open area (Figure 2.20)

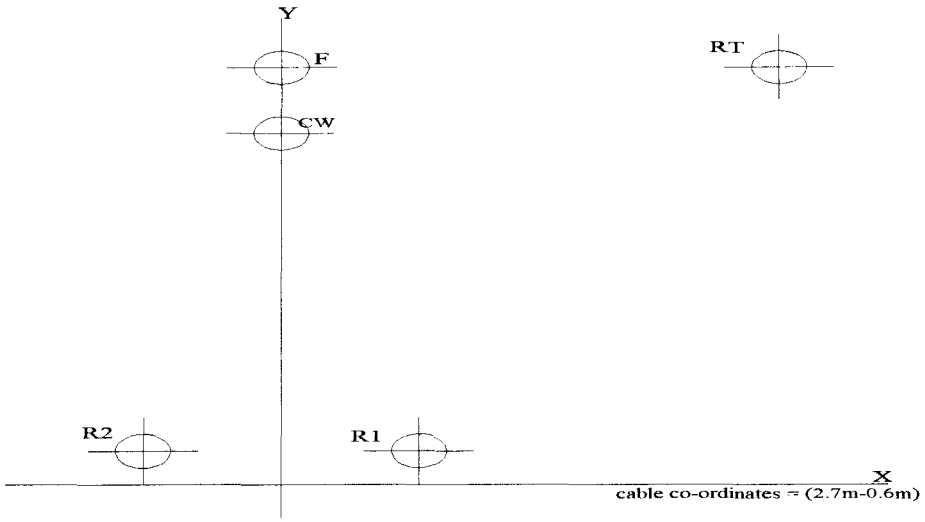

Figure 2.20: One-track configuration for a compensated system

Conductor	X (m)	Y (m)
R1	-2.40792	0.1524
R2	-0.97536	0.1524
R3	2.40792	0.1524
R4	0.97536	0.1524
RT1	-4.45008	5.7912
RT2	4.45008	5.7912
CW1	-1.69164	4.7244
CW2	1.69164	4.7244
F1	-1.69164	5.6388
F2	1.69164	5.6388

Table 2.8: Two track configurations in an open area(Figure 2.21)

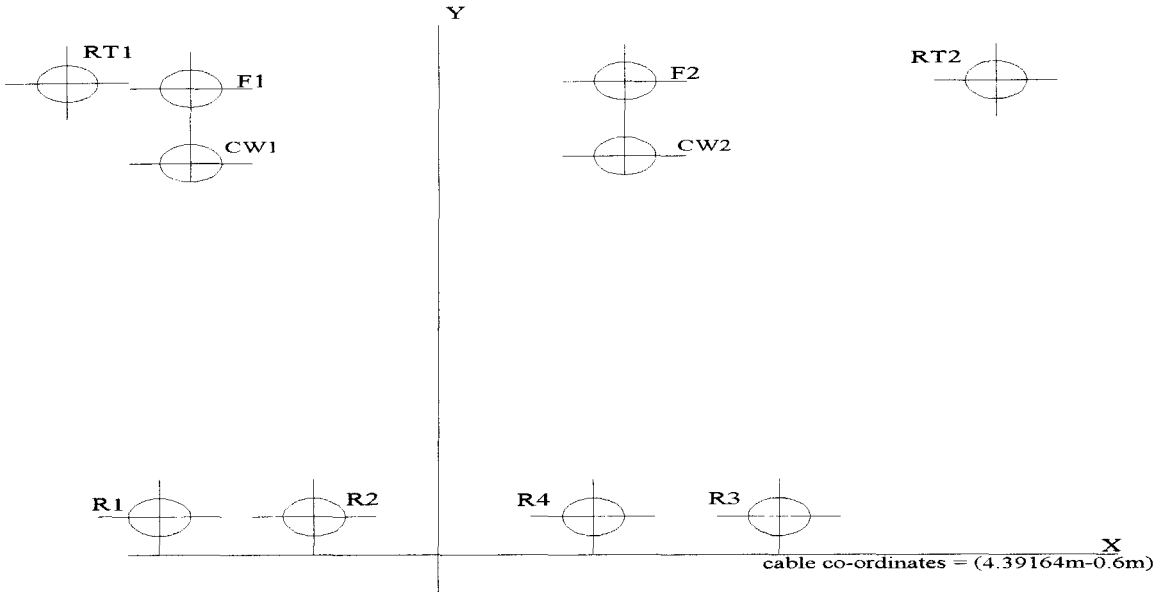

Figure 2.21: Two-track configuration for a compensated system

The other data used for the above calculations are shown in Table 2.9[47].

Conductor	Height (m)	Radius (mm)	Dc resistance (ohm/mile)	Internal reactance (mho/mile)
Buried earth wire	0.1	6.5	0.4508	0.06484
Aerial earth wire	6.875	8.15	0.34502	0.04778
Messenger wire	6.6	8.45	0.30638	0.03260
Contact wire	5.7	6.15	0.27290	0.03033
Feeder wire	6.543	11.75	0.16535	0.07807

Table 2.9: Data for other Conductors

The self and mutual impedance were calculated using the above information for uncompensated systems (no booster transformer), using Mathcad and Aplac the results obtained, at 50Hz frequency, were as follow:

2.4.3 Single-track uncompensated results, 1250 Amps ratings

Here we have the self and mutual impedances of return conductors (rail & earth) (RR) and feed conductors (overhead) (FF) and return against feed conductors (RF).

$$RR := \begin{bmatrix} Z12 & Z13 & Z14 & Z15 \\ Z21 & Z22 & Z23 & Z24 & Z25 \\ Z31 & Z32 & Z33 & Z34 & Z35 \\ Z41 & Z42 & Z43 & Z44 & Z45 \\ Z51 & Z52 & Z53 & Z54 & Z55 \end{bmatrix} \qquad RR = \begin{bmatrix} 0.134+2.208i & 0.095+0.877i & 0.095+0.718i & 0.095+0.554i & 0.095+0.627i \\ 0.095+0.877i & 134+2.208i & 0.095+0.718i & 0.095+0.599i & 0.095+0.627i \\ 0.095+0.718i & 0.095+0.718i & 0.546+1.341i & -0.098-0.047i & 0.095+0.439i \\ 0.095+0.554i & 0.095+0.599i & -0.098-0.047i & 0.44+1.783i & 0.095+0.865i \\ 0.095+0.627i & 0.095+0.627i & 0.095+0.439i & 0.095+0.865i & 0.44+1.783i \end{bmatrix}$$

$$RF := \begin{bmatrix} Z17 & Z18 \\ Z26 & Z27 & Z28 \\ Z36 & Z37 & Z38 \\ Z46 & Z47 & Z48 \\ Z56 & Z57 & Z58 \end{bmatrix} \qquad RF = \begin{bmatrix} 0.095+0.453i & 0.095+0.488i & 0.095+0.601i \\ 0.095+0.453i & 0.095+0.488i & 0.095+0.621i \\ 0.095+0.572i & 0.095+0.593i & 0.095+0.285i \\ 0.095+0.8i & 0.095+0.784i & 0.095+0.903i \\ 0.095+0.78i & 0.095+0.782i & 0.095+0.934i \end{bmatrix}$$

$$FF := \begin{bmatrix} Z67 & Z68 \\ Z76 & Z77 & Z78 \\ Z86 & Z87 & Z88 \end{bmatrix} \qquad FF = \begin{bmatrix} 0.402+1.77i & 0.095+0.368i & 0.095+0.76i \\ 0.095+0.368i & 0.368+1.784i & 0.095+0.755i \\ 0.095+0.76i & 0.095+0.755i & 0.261+1.798i \end{bmatrix}$$

Results at higher frequencies can be obtained by changing the frequency accordingly in the program.

2.4.4 Single-track uncompensated results, 760 Amps ratings

$$RR = \begin{bmatrix} 0.133+2.212i & 0.095+0.881i & 0.095+0.723i & 0.095+0.603i & 0.095+0.645i \\ 0.095+0.881i & 0.0133+2.212i & 0.095+0.723i & 0.095+0.603i & 0.095+0.645i \\ 0.095+0.881i & 0.095+0.723i & 0.623+1.431i & 0.095+0.052i & 0.095+0.523i \\ 0.095+0.603i & 0.095+0.678i & 0.095+0.052i & 0.439+1.792i & 0.095+0.901i \\ 0.095+0.645i & 0.095+0.645i & 0.095+0.456i & 0.095+0.901i & 0.439+1.792i \end{bmatrix}$$

$$RF = \begin{bmatrix} 0.095+0.473i & 0.095+0.489i & 0.095+0.611i \\ 0.095+0.473i & 0.095+0.489i & 0.095+0.631i \\ 0.095+0.611i & 0.095+0.61i & 0.095+0.31i \\ 0.095+0.801i & 0.095+0.789i & 0.095+0.91i \\ 0.095+0.79i & 0.095+0.791i & 0.095+0.923i \end{bmatrix}$$

$$FF = \begin{bmatrix} 0.421i+1.77i & 0.095+0.376i & 0.095+0.762i \\ 0.095+0.376i & 0.366+1.771i & 0.095+0.762i \\ 0.095+0.763i & 0.095+0.763i & 0.263+1.78i \end{bmatrix}$$

2.4.5 Double-track uncompensated, 1250 Amps ratings

$$RR=\begin{bmatrix} 0.133+2.202i & 0.095+0.873i & 0.095+0.669i & 0.095+0.543i & 0.095+0.623i \\ 0.095+0.872i & 0.133+2.202i & 0.095+0.669i & 0.095+0.598i & 0.095+0.623i \\ 0.095+0.8721i & 0.095+0.669i & 0.523+1.311i & 0.095+0.042i & 0.095+0.423i \\ 0.095+0.598i & 0.095+0.678i & 0.095+0.042i & 0.439+1.782i & 0.095+0.841i \\ 0.095+0.623i & 0.095+0.623i & 0.095+0.439i & 0.095+0.841i & 0.439+1.782i \end{bmatrix}$$

$$RF=\begin{bmatrix} 0.095+0.443i & 0.095+0.488i & 0.095+0.6i \\ 0.095+0.443i & 0.095+0.488i & 0.095+0.621i \\ 0.095+0.621i & 0.095+0.591i & 0.095+0.278i \\ 0.095+0.787i & 0.095+0.783i & 0.095+0.891i \\ 0.095+0.69i & 0.095+0.711i & 0.095+0.892i \end{bmatrix}$$

$$FF=\begin{bmatrix} 0.401i+1.77i & 0.095+0.366i & 0.095+0.76i \\ 0.095+0.366i & 0.366+1.77i & 0.095+0.76i \\ 0.095+0.76i & 0.095+0.76i & 0.263+1.77i \end{bmatrix}$$

2.4.6 Double-track uncompensated , 760 Amps ratings

$$RR=\begin{bmatrix} 0.133+2.205i & 0.095+0.877i & 0.095+0.711i & 0.095+0.543i & 0.095+0.623i \\ 0.095+0.872i & 0.133+2.202i & 0.095+0.711i & 0.095+0.598i & 0.095+0.623i \\ 0.095+0.8771i & 0.095+0.771i & 0.523+1.311i & 0.095+0.042i & 0.095+0.423i \\ 0.095+0.598i & 0.095+0.678i & 0.095+0.042i & 0.439+1.782i & 0.095+0.841i \\ 0.095+0.623i & 0.095+0.623i & 0.095+0.439i & 0.095+0.841i & 0.439+1.782i \end{bmatrix}$$

$$RF=\begin{bmatrix} 0.095+0.447i & 0.095+0.489i & 0.095+0.601i \\ 0.095+0.447i & 0.095+0.489i & 0.095+0.611i \\ 0.095+0.611i & 0.095+0.591i & 0.095+0.278i \\ 0.095+0.787i & 0.095+0.783i & 0.095+0.891i \\ 0.095+0.69i & 0.095+0.711i & 0.095+0.891i \end{bmatrix}$$

$$FF=\begin{bmatrix} 0.401i+1.77i & 0.095+0.369i & 0.095+0.763i \\ 0.095+0.369i & 0.366+1.77i & 0.095+0.763i \\ 0.095+0.763i & 0.095+0.762i & 0.263+1.77i \end{bmatrix}$$

Now the compensated (system with booster transformers) are considered, using the same approach as above. The same overhead ratings and track as above are analysed.

2.4.7 Single-track compensated results, 1250 Amps ratings

$$RR := \begin{array}{c} \\ R1 \\ R2 \\ Rt \end{array} \begin{array}{c} \begin{array}{ccc} R1 & R2 & Rt \end{array} \\ \begin{bmatrix} Zr1 & Zr1r2 & Zrtr \\ Zr1r2 & Zr1 & Zrtr \\ Zrtr & Zrtr & Zrt \end{bmatrix} \end{array} \qquad RR = \begin{bmatrix} Z11 & Z12 & Z13 \\ Z21 & Z22 & Z23 \\ Z31 & Z32 & Z33 \end{bmatrix}$$

$$RF := \begin{array}{c} \\ Rt \\ CW \\ F \end{array} \begin{array}{c} \begin{array}{ccc} Rt & CW & F \end{array} \\ \begin{bmatrix} Zrt & Zrtcw & Zrtf \\ Zrtcw & Zcw & Zcwf \\ Zrtf & Zcwf & Zfw \end{bmatrix} \end{array} \qquad RF = \begin{bmatrix} Z44 & Z45 & Z46 \\ Z54 & Z55 & Z56 \\ Z64 & Z65 & Z66 \end{bmatrix}$$

$$FF := \begin{array}{c} \\ CW \\ F \end{array} \begin{array}{c} \begin{array}{cc} CW & F \end{array} \\ \begin{bmatrix} Zcw & Zcwf \\ Zcwf & Zfw \end{bmatrix} \end{array} \qquad FF = \begin{bmatrix} Z55 & Z56 \\ Z65 & Z66 \end{bmatrix}$$

2.4.8 Single-track compensated, 760 Amps ratings

$$RR = \begin{bmatrix} 0.132 + 0.908i & 0.079 + 0.366i & 0.079 + 0.306i \\ 0.079 + 0.366i & 0.132 + 0.908i & 0.079 + 0.306i \\ 0.079 + 0.306i & 0.079 + 0.306i & 0.262 + 0.615i \end{bmatrix}$$

$$RF = \begin{bmatrix} 0.264 + 0.62i & 0.079 + 0.467i & 0.079 + 0.478i \\ 0.079 + 0.467i & 0.37 + 0.621i & 0.079 + 0.63i \\ 0.079 + 0.478i & 0.079 + 0.63i & 0.762 + 0.651i \end{bmatrix}$$

$$FF = \begin{bmatrix} 0.37 + 0.621i & 0.079 + 0.63i \\ 0.079 + 0.63i & 0.762 + 0.65i \end{bmatrix}$$

2.4.9 Double-track compensated, 1250 Amps ratings

$$RR = \begin{bmatrix} 0.133 + 0.907i & 0.079 + 0.368i & 0.079 + 0.289i \\ 0.079 + 0.368i & 0.133 + 0.908i & 0.079 + 0.289i \\ 0.079 + 0.289i & 0.079 + 0.289i & 0.264 + 0.61i \end{bmatrix}$$

$$RF = \begin{bmatrix} 0.264 + 0.62i & 0.079 + 0.447i & 0.079 + 0.468i \\ 0.079 + 0.447i & 0.37 + 0.621i & 0.079 + 0.63i \\ 0.079 + 0.468i & 0.079 + 0.63i & 0.762 + 0.631i \end{bmatrix}$$

$$FF=\begin{bmatrix} 0.37+0.621i & 0.079+0.63i \\ 0.079+0.63i & 0.762+0.631i \end{bmatrix}$$

2.4.10 Double-track compensated, 760 Amps ratings

$$RR=\begin{bmatrix} 0.131+0.9i & 0.079+0.358i & 0.079+0.287i \\ 0.079+0.358i & 0.133+0.901i & 0.079+0.287i \\ 0.079+0.287i & 0.079+0.288i & 0.264+0.617i \end{bmatrix}$$

$$RF=\begin{bmatrix} 0.254+0.62i & 0.079+0.437i & 0.079+0.448i \\ 0.079+0.437i & 0.37+0.621i & 0.079+0.63i \\ 0.079+0.448i & 0.079+0.63i & 0.762+0.621i \end{bmatrix}$$

$$FF=\begin{bmatrix} 0.37+0.621i & 0.079+0.63i \\ 0.079+0.63i & 0.762+0.621i \end{bmatrix}$$

2.5: Step 3: Overhead transmission line equations

Knowing the impedances of the conductors, the OHTL equations can be derived.

Note: In all the calculations carried out, the line is considered as immersed in a homogeneous medium (free space). The derivation of the transmission line equations can be determined in three different ways:

1. From the integral form of Maxwell's equations,
2. From the differential form of Maxwell's equations,
3. From the per-unit-length equivalent circuit.

The last approach is used in this thesis for its simplicity. A derivation form Maxwell's equations are also shown in Appendix B.

For an n line above ground shown in Figure 2.22:

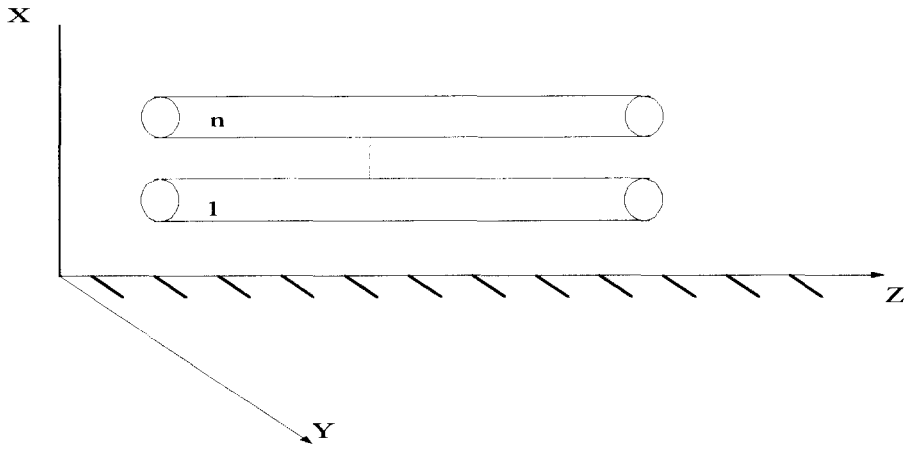

Figure 2.22: n wires above ground

TL Per-unit-length equivalent circuit derivation:

Consider the circuit shown in Figure 2.23.

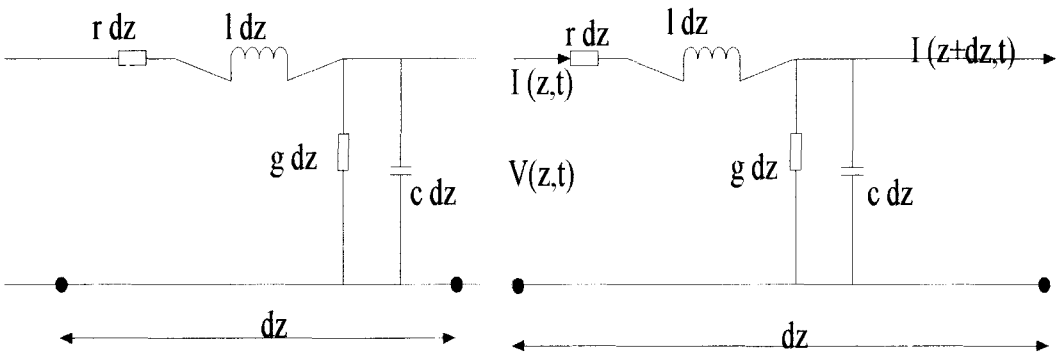

Figure 2.23: Per-unit-length equivalent circuit

The current is broken into small dz length sub-sections. "l" represents the magnetic flux passing between the conductors due to current in them. "c" is the displacement current between the two conductors, and "g" represents the transverse conduction current flowing between two conductors.
To account for loss, the resistance "r" is included.

From the circuit following Kirchoff's voltage and current law;

$$V(z+dz,t)-V(z,t)=-rdzI(z,t)-ldz\frac{\partial I(z,t)}{\partial t}$$
$$I(z+dz,t)-I(z,t)=-gdzV(z+dz,t)-cdz\frac{\partial V(z,t)}{\partial t} \quad \text{--------(2.44)}$$

Dividing the above equations by dz and taking the limit dz = 0, we obtain the voltage and current TL equations;

$$\frac{\partial V(z,t)}{\partial z}=-rI(z,t)-l\frac{\partial I(z,t)}{\partial t}$$
$$\frac{\partial I(z,t)}{\partial z}=-gV(z,t)-c\frac{\partial I(z,t)}{\partial t} \quad \text{------(2.45)}$$

For homogeneous surroundings the following identity is valid;

lc = με

gl = σμ

For the second order of the TL equations above, we differentiate with respect to z and t respectively;

$$\frac{\partial^2 V(z,t)}{\partial z^2}=gl\frac{\partial V(z,t)}{\partial t}+lc\frac{\partial^2 V(z,t)}{\partial t^2}$$
$$\frac{\partial^2 I(z,t)}{\partial z^2}=gl\frac{\partial I(z,t)}{\partial t}+lc\frac{\partial^2 I(z,t)}{\partial t^2} \quad \text{------(2.46)}$$

For MTL equations, consider the circuit shown in Figure 2.24 below;

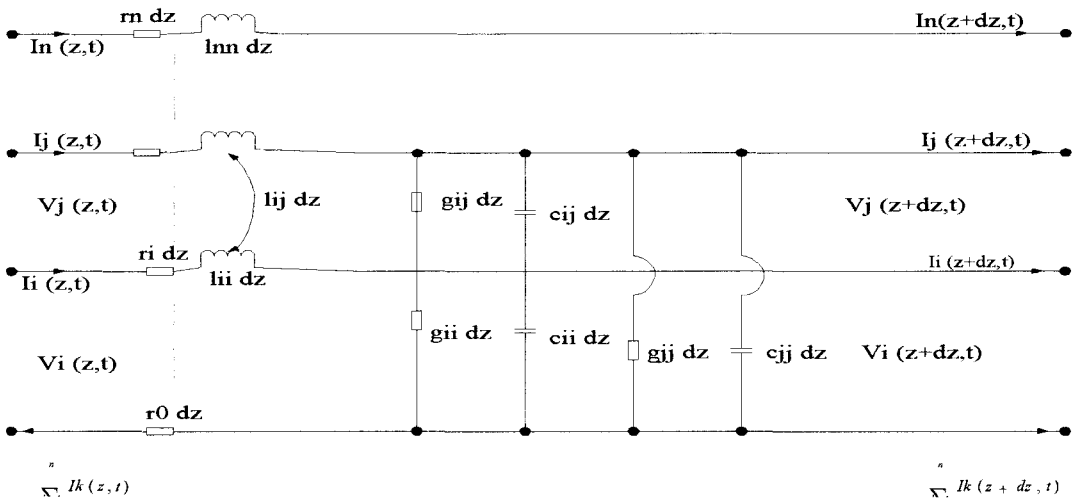

Figure 2.24: Per-unit length MTL model

From the circuit using Kirchhoff's voltage law around the i-th circuit consisting of the i-th conductor and the reference conductor yields;

$$-V_i(z,t)+r_i\Delta z I_i(z,t)+V_i(z+\Delta z,t)+r_0\Delta z\sum_{k=1}^{n}I_k(z,t)=-l_{i1}\Delta z\frac{\partial I_1(z,t)}{\partial t}- l_{i2}\Delta z\frac{\partial I_2(z,t)}{\partial t}-\ldots-l_{ii}\Delta z\frac{\partial I_i(z,t)}{\partial t}-..l_{in}\Delta z\frac{\partial I_n(z,t)}{\partial t} \quad \text{-----(2.47)}$$

Dividing both sides by delta.z and taking the limit as deltaz=0, once again yields the first TL equation given above, with the collection for all "I" given in matrix form. Similarly the second transmission line equation can be obtained by applying K- current law from the above circuit;

$$-I_i(z+\Delta z,t)+I_i(z,t)=-g_{i1}\Delta z(V_i-V_1)-\ldots-g_{ij}\Delta z(V_i-V_j)-\ldots-g_{ii}\Delta z(V_i-V_n)-\ldots -c_{i1}\Delta z\frac{\partial(V_i-V_1)}{\partial t}-\ldots-c_{ii}\Delta z\frac{\partial V_i}{\partial t}-\ldots-c_{in}\Delta z\frac{\partial(V_i-V_n)}{\partial t} \quad \text{-----(2.48)}$$

Dividing both sides by delta z and taking the limit =0 and collecting terms once again yields the second MTL equation.

$$\frac{\partial[V](z,t)}{\partial z}=-[R][I](z,t)-L\frac{\partial I(z,t)}{\partial t}$$
$$\frac{\partial[I](z,t)}{\partial z}=-[G][V](z,t)-[C]\frac{\partial[V](z,t)}{\partial t} \quad \text{------(2.49)}$$

The above equation are a set of 2n, coupled, first order differential equations. They can be put in a more compact form as;

$$\frac{\partial}{\partial z}\begin{bmatrix}(V)(z,t)\\(I)(z,t)\end{bmatrix}=-\begin{bmatrix}0 & (R)\\(G) & 0\end{bmatrix}\begin{bmatrix}(V)(z,t)\\(I)(z,t)\end{bmatrix}-\begin{bmatrix}0 & (L)\\(C) & 0\end{bmatrix}\frac{\partial}{t}\begin{bmatrix}(V)(z,t)\\(I)(z,t)\end{bmatrix} \quad \text{-----(2.50)}$$

For perfect conductors; R=0 and if the surrounding medium is loss-less (segma=0), G=0, the above equation reduces to;

$$\frac{\partial}{\partial z}\begin{bmatrix}(V)(z,t)\\(I)(z,t)\end{bmatrix} = -\begin{bmatrix}0 & (L)\\(C) & 0\end{bmatrix}\frac{\partial}{t}\begin{bmatrix}(V)(z,t)\\(I)(z,t)\end{bmatrix} \text{-----(2.51)}$$

The analysis is carried out at system frequency where the capacitance and conductance effect can be neglected. Hence the parameters of the overhead line are based on the resistance (power loss) and inductance, which can be written as Z.

For self impedance;

$$Z_{ii} = R_{ii} + j\omega l_{ii} \text{-----(2.52)}$$

And for mutual impedance;

$$Z_{ij} = R_{ij} + j\omega l_{ij} \text{------(2.53)}$$

From the parameters of the conductors above, the voltage and current of the TL can be obtained using FDTD method as described below.

In order to illustrate the method, consider a two-conductor, loss-less transmission line of length L and distance of separation between the conductors equal to d ,as depicted in Figure 2.25.

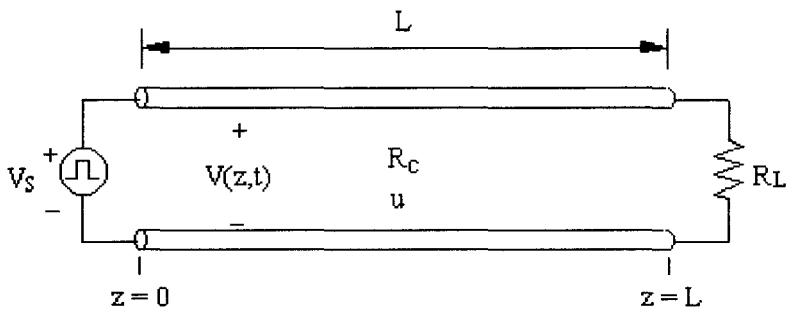

Figure 2.25: Two conductor transmission lines

For the above, the source generates a voltage pulse Vs at z = 0, that changes from zero volts to some value for a specified length of time and then switches back to zero.

When the source voltage transitions to the "on" state at time t =0, a voltage propagates down the TL.

The propagation speed of this voltage disturbance and the reflection from the load and some ends of the TL are determined at any time.

In this work, the voltage on the TL is solved in a different fashion. Here a numerical method is used to compute the voltage at a discrete set of points along the TL and at a discrete set of times. This is accomplished by using the FDTD method.

As mentioned earlier, in the FDTD method, the TL is divided into nz segments as shown below (Figure 2.26)[1,2,3,4].

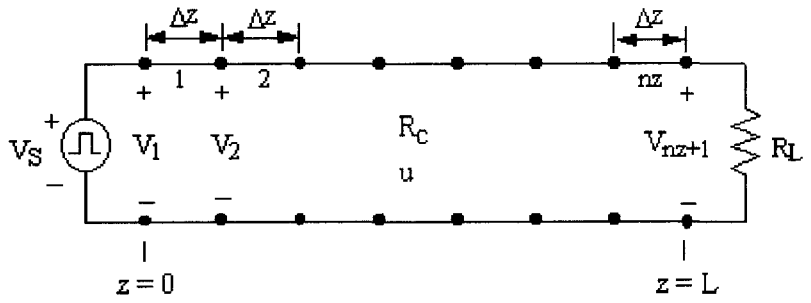

Figure 2.26: FDTD Method for the above Circuits

The voltage will be computed at the nz+1 "nodes" and at a discrete number of "nt" time instances. Each of these times is separated by an equal amount dt that is computed later. The FDTD solution is accomplished by applying the central difference approximation for the derivatives in space and time that appear in the equations for the voltages and current below.

$$\frac{\partial V(z,t)}{\partial z} + l\frac{\partial I(z,t)}{\partial t} + rI(z,t) = V_F(z,t)$$
$$\frac{\partial I(z,t)}{\partial z} + c\frac{\partial V(z,t)}{\partial t} + gV(z,t) = I_F(z,t) \qquad \text{----------(2.54)}$$

Where "I" and c are the per-unit-length inductance and capacitance of the TL respectively, and V (z,t), I (z,t) are the line voltage and current along the TL respectively.

The FDTD technique seeks to approximate the derivatives in (2.49) with regard to the discrete solution points defined by spatial and temporal cells.

According to this notation, the finite difference representation of the spatial and temporal derivative of a function f (z,t) is written as:

$$\frac{\partial f(x,t)}{\partial x} = \frac{f_{k+1}^{n+1} - f_k^{n+1}}{\Delta x}$$
$$\frac{\partial f(x,t)}{\partial t} = \frac{f_k^{n+1} - f_k^{n}}{\Delta t} \quad \text{--------(2.55)}$$

Substituting (2.50) into (2.49), the finite difference approximation yields:

$$\frac{V_{n+1}^{k+1} - V_k^{n+1}}{\Delta z} + l\frac{I_k^{n+3/2} - I_k^{n+1/2}}{\Delta t} = 0$$
$$\frac{I_k^{n+1/2} - I_{k-1}^{n-1/2}}{\Delta z} + l\frac{V_k^{n+1} - V_k^{n}}{\Delta t} = 0 \quad \text{---------(2.56)}$$

Where Vk^n, Ik^n are defined as;

$$V_k^n = V((k-1)\cdot\Delta z, n\cdot\Delta t)$$
$$I_k^n = I((k-1/2)\cdot\Delta z, n\cdot\Delta t) \quad \text{---------(2.57)}$$

Equation (2.61) is solved by extracting $V_k^{n+1}, I_k^{n+3/2}$;

$$V_k^{n+1} = V_k^n - \frac{\Delta t}{c\cdot\Delta x}(I_k^{n+1/2} - I_{k-1}^{n+1/2})$$
$$I_k^{n+3/2} = I_k^{n+1/2} - \frac{\Delta t}{l\cdot\Delta x}(V_{k+1}^{n+1} - V_k^{n+1)} \quad \text{---------(2.58)}$$

The above equations can be solved in a "bootstrapping "fashion[1].

At each time step "n" the voltages along the line are computed in terms of the previous voltage and current values (starting with an initially relaxed line at t =0). Afterwards, the currents along the line are evaluated for the next temporal cell. The final step for the determination of the FDTD code is the incorporation of terminal constraints of the TL.

Under the assumption of TEM propagation along the TL mentioned above, the lumped resistive loads at the two ends of the TL could be characterised as:

$$V(0,t) = V_s - R_s * I(0,t)$$
$$V(L,t) = V_L + R_L * I(L,t) \quad \text{----------(2.59)}$$

Where VS, VL are the lumped voltage sources at the near-and far-end of the TL. Incorporating the latter equations in (2.53), the final FDTD code is obtained. For each time step "n" the voltage at the near-and far-end of the TL are evaluated byTaflove[1]:

$$V_1^{n+1} = \frac{1}{(R_s \cdot \frac{c}{2} \cdot \frac{\Delta z}{\Delta t} + \frac{1}{2})} \cdot \{(R_s \cdot \frac{c}{2} \cdot \frac{\Delta z}{\Delta t} - \frac{1}{2}) \cdot V_1^n - R_s \cdot I_1^{n+1/2} + \frac{V_s^{n+1} + V_s^n}{2}\}$$

$$V_{KTot+1}^{n+1} = \frac{1}{(R_L \cdot \frac{c}{2} \cdot \frac{\Delta z}{\Delta t} + \frac{1}{2})} \cdot \{(R_L \cdot \frac{c}{2} \cdot \frac{\Delta z}{\Delta t} - \frac{1}{2}) \cdot V_{KTot+1}^n - R_L \cdot I_{KTot}^{n+1/2} + \frac{V_L^{n+1} + V_L^n}{2}\} \quad \text{---(2.60)}$$

Also, the voltage and current at each intermediate spatial segment is evaluated by equations (2.58). This procedure goes on for each time cell until final solution time is reached.

2.5.1 Voltage result at different time step

Figure 2.27 and 2.28 shows the voltage at a different time step as calculated by the FDTD for non-homogeneous medium and homogeneous medium.

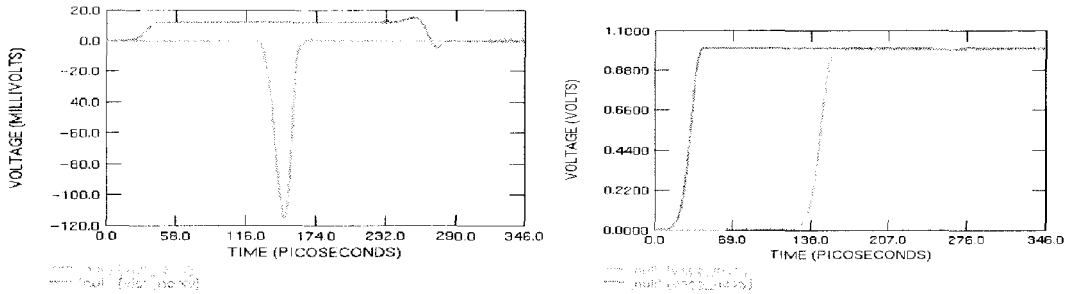

Figure 2.27: Typical non-homogeneous medium voltage result

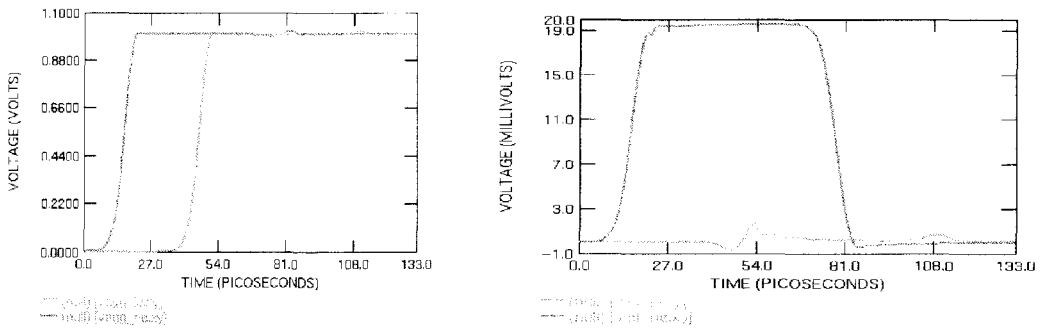

Figure 2.28: Typical homogeneous medium voltage result

2.6 Summary

The method used for the calculations of the self and mutual impedances of rail track and overhead line conductors have been developed as well as the calculations of the voltage and currents in the overhead lines (feed systems) and the return systems. The results obtained have also been presented. The self and mutual impedance have been calculated using finite difference time domain (FDTD) method which is a mathematical modelling technique based on solving Maxwell's equations. The results obtained have been compared with existing standard approach. The method provides better and more accurate results for these calculations. Using the impedance results obtained here, further analysis and calculations of the induced voltage for the uncompensated and compensated systems under normal and short circuits conditions are given in chapters (3), (4), (5), & (6).

CHAPTER (3)

Induced Voltage In Uncompensated Systems under Normal Operation Conditions

Introduction

In the previous chapter the self and mutual impedances of feed and return conductors have been calculated and generalised formulae for the line voltage and current have been developed. Using this information we now proceed to calculate the induced voltage into line-side signalling cables. In this section uncompensated (no booster transformers) systems of one and two track layouts in an open area have been considered. Calculations and results given in this section are for normal operation condition.

3.1 Uncompensated system configuration

In order to establish the induction effects caused into line-side signalling cables, consider the uncompensated system shown in Figure 3.1.

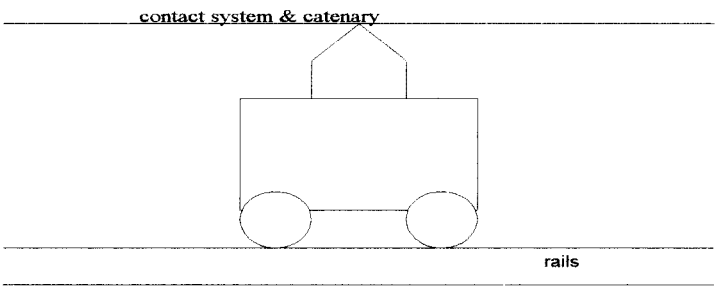

Figure 3.1: Uncompensated system (no BT)

The equivalent electric circuit for Figure (3.1) is shown in Figure 3.2.

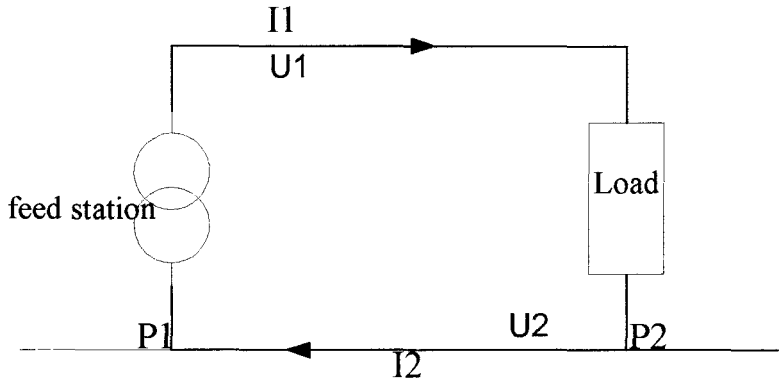

Figure 3.2: Current, potential and impedance for a railway section with feeding station & load

Where, P1 = node 1 is the feeding station

P2 = node 2 is the load

It is important to consider not just the induction effects from the railway system on signalling circuits in the neighbourhood of the track, but also the voltages between the rails and the earth especially from the point of view of danger.

From Figure 3.2, the current at P2 that is fed into the rail system is divided in two current components, one has the direction to the feeding station and thus flows in the opposite direction to the current in the contact conductor ($-I_1$), while the other one is directed from the feeding station. The currents in the rail system outside the feeding section (to the left of P1 and right of P2) are attenuated in a manner that is determined by the longitudinal impedance of the rail system and the leakance. Usually it can be assumed that the sections outside P1 & P2 are so long that their properties can be represented by the characteristic impedance of the circuit established by the rails and the earth[48,49].

For the assumption that the properties of the system conductors do not vary along the line, the following differential equations are valid.

$$-\frac{dU_1}{dx} = z_2 \cdot I_2 + z_{12} \cdot I_1$$
$$-\frac{dI_2}{dx} = y_2 \cdot U_2 \quad \text{------(3.1)}$$

where, x is measured from P1

The solution of the equation system is:

$$I_2 = A \cdot e^{\gamma_2 \cdot x} + B \cdot e^{-\gamma_2 \cdot x} - \frac{z_{12}}{z_2} \cdot I_1 \text{------(3.2)}$$

where;

$\gamma_2 = \sqrt{z_2 \cdot y_2} = \alpha_2 + \beta_2$ (Propagation coefficient)

The potential of the rail system is;

$U_2 = -Z_2(A \cdot e^{\gamma_2 \cdot x} + B \cdot e^{-\gamma_2 \cdot x})$ ------(3.3)

where;

$Z_2 = \frac{\gamma}{y_2} = \sqrt{\frac{z_2}{y_2}}$ (Characteristic impedance)

For the system considered in this thesis, the overhead conductor system (or feed system) consists of contact wire (CW), feed wire (F), and messenger wire (M) and the return conductor system consists of two rails (R1 and R2), earth wire (EW) and buried earth wire (B1), Figure 3.3[47]. The self and mutual impedances of these return and feed conductors have been determined as shown chapter (2).

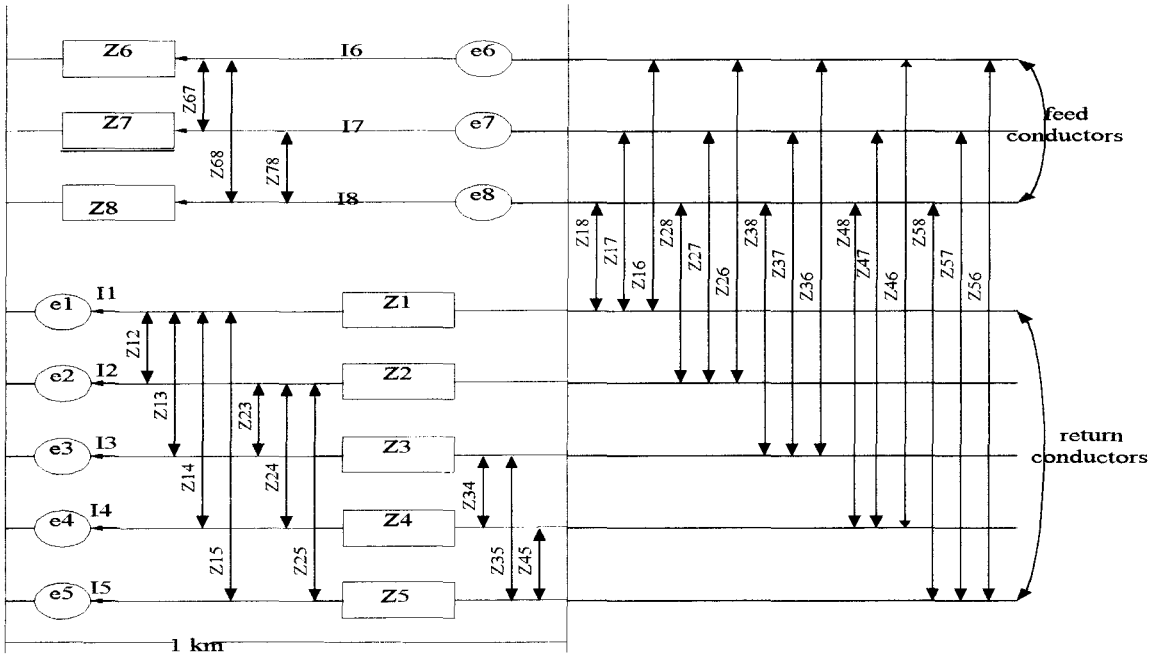

Figure 3.3: Mutual interaction among conductors (return & feed systems) for 1 km long mesh

Assume that the overhead catenary system (OCS) has a current of I Amps. First the current is considered as equally divided among feed conductors. Hence from the Figure 3.3, I_6, I_7 and I_8 (messenger, contact wire and feeder wire currents respectively) will be 1/3 I Amps.

Induced voltage calculation were carried out using the method described below[47]:
The current in the feed conductors will induce voltages e_1, e_2, e_3, e_4, and e_5 in the return conductors, such that;

$$e_1 = e_{61} + e_{71} + e_{81}$$
$$e_2 = e_{62} + e_{72} + e_{82}$$
$$e_3 = e_{63} + e_{73} + e_{83} \text{ -------(3.4)}$$
$$e_4 = e_{64} + e_{74} + e_{84}$$
$$e_5 = e_{65} + e_{75} + e_{85}$$

where,

$$e_{61} = Z_{16} * I_6 \text{ ----(3.5)}$$

hence,

$e_1 = Z_{16} * I_6 + Z_{17} * I_7 + Z_{18} * I_8$ -----(3.6)

For the current I = 1 Amps, then $I_6 = I_7 = I_8 = 1/3$ Amps

Hence,

$$e_1 = \frac{1}{3}(Z_{16} + Z_{17} + Z_{18})$$

or -------(3.7)

$$e_1 = \frac{1}{n} \cdot Z_{1T}$$

where;

n = Number of feed conductors in the system

Z_{1T} = Sum of element in the 1st row of RF-matrix

Similarly the formulae are developed for all the voltages

Now that the voltages induced in the return system are known, the return currents can be calculated as:

$$\begin{bmatrix} e_1 \\ e_2 \\ e_3 \\ e_4 \\ e_5 \end{bmatrix} = \begin{bmatrix} Z_{11} & Z_{12} & Z_{13} & Z_{14} & Z_{15} \\ Z_{21} & Z_{22} & Z_{23} & Z_{24} & Z_{25} \\ Z_{31} & Z_{32} & Z_{33} & Z_{34} & Z_{35} \\ Z_{41} & Z_{42} & Z_{43} & Z_{44} & Z_{45} \\ Z_{51} & Z_{52} & Z_{53} & Z_{54} & Z_{55} \end{bmatrix} \begin{bmatrix} I_1 \\ I_2 \\ I_3 \\ I_4 \\ I_5 \end{bmatrix}$$

and -------(3.8)

$$\begin{bmatrix} I_1 \\ I_2 \\ I_3 \\ I_4 \\ I_5 \end{bmatrix} = \begin{bmatrix} Z_{11} & Z_{12} & Z_{13} & Z_{14} & Z_{15} \\ Z_{21} & Z_{22} & Z_{23} & Z_{24} & Z_{25} \\ Z_{31} & Z_{32} & Z_{33} & Z_{34} & Z_{35} \\ Z_{41} & Z_{42} & Z_{43} & Z_{44} & Z_{45} \\ Z_{51} & Z_{52} & Z_{53} & Z_{54} & Z_{55} \end{bmatrix}^{-1} \begin{bmatrix} e_1 \\ e_2 \\ e_3 \\ e_4 \\ e_5 \end{bmatrix}$$

Following the same approach used for return current calculations, the current in the feed conductors can be calculated;

The currents in the return conductors induce voltages e_6, e_7, and e_8 in the feed conductors, such the;

$$e_6 = Z_{16} \cdot I_1 + Z_{26} \cdot I_2 + Z_{36} \cdot I_3 + Z_{46} \cdot I_4 + Z_{56} \cdot I_5 \text{-----(3.9)}$$

Similar approach is applied for e_7 and e_8, and the total equation can be written in a matrix from as;

$$\begin{bmatrix} e_6 \\ e_7 \\ e_8 \end{bmatrix} = \begin{bmatrix} Z_{16} & Z_{26} & Z_{36} & Z_{46} & Z_{56} \\ Z_{17} & Z_{27} & Z_{37} & Z_{47} & Z_{57} \\ Z_{18} & Z_{28} & Z_{38} & Z_{48} & Z_{58} \end{bmatrix} \cdot \begin{bmatrix} I_1 \\ I_2 \\ I_3 \\ I_4 \\ I_5 \end{bmatrix} \text{---------(3.10)}$$

Where, the above impedance matrix is the transposed of RF matrix.
Knowing the feed voltages e_6, e_7, e_8, the currents I_6, I_7, I_8 can be determined from the following relationship;

$$\begin{bmatrix} e_6 \\ e_7 \\ e_8 \end{bmatrix} = \begin{bmatrix} Z_{66} & Z_{67} & Z_{68} \\ Z_{76} & Z_{77} & Z_{78} \\ Z_{86} & Z_{87} & Z_{88} \end{bmatrix} \cdot \begin{bmatrix} I_6 \\ I_7 \\ I_8 \end{bmatrix}$$

or ----------(3.11)

$$\begin{bmatrix} I_6 \\ I_7 \\ I_8 \end{bmatrix} = \begin{bmatrix} Z_{66} & Z_{67} & Z_{68} \\ Z_{76} & Z_{77} & Z_{78} \\ Z_{86} & Z_{87} & Z_{88} \end{bmatrix}^{-1} \cdot \begin{bmatrix} e_6 \\ e_7 \\ e_8 \end{bmatrix}$$

The above method was developed based on the assumption that the OCS is divided equally between the feed systems. However this may not be true in real life, therefore consideration for inequality is required. This is achieved by applying simple correction method as shown below.

Consider the incorrect currents I_{6i}, I_{7i}, I_{8i} (not add up to 1 Amps), and $I_{Ti} = I_{6i} + I_{7i} + I_{8i}$ is the total incorrect current, then the corresponding corrected currents I_{6c}, I_{7c}, I_{8c} are;

$$I_{6c} = \frac{I_{6i}}{I_{Ti}}$$

$$I_{7c} = \frac{I_{7i}}{I_{Ti}} \quad \text{---------(3.12)}$$

$$I_{8c} = \frac{I_{8i}}{I_{Ti}}$$

Using the above method the return and feed currents were recalculated as;

$$\begin{bmatrix} e_{1c} \\ e_{2c} \\ e_{3c} \\ e_{4c} \\ e_{5c} \end{bmatrix} = \begin{bmatrix} Z_{16} & Z_{17} & Z_{18} \\ Z_{26} & Z_{27} & Z_{28} \\ Z_{36} & Z_{37} & Z_{38} \\ Z_{46} & Z_{47} & Z_{48} \\ Z_{56} & Z_{57} & Z_{58} \end{bmatrix} \cdot \begin{bmatrix} I_{6c} \\ I_{7c} \\ I_{8c} \end{bmatrix} \text{-------(3.13)}$$

and hence the return current can be determined as;

$$\begin{bmatrix} e_{1c} \\ e_{2c} \\ e_{3c} \\ e_{4c} \\ e_{5c} \end{bmatrix} = \begin{bmatrix} Z_{11} & Z_{12} & Z_{13} & Z_{14} & Z_{15} \\ Z_{21} & Z_{22} & Z_{23} & Z_{24} & Z_{25} \\ Z_{31} & Z_{32} & Z_{33} & Z_{34} & Z_{35} \\ Z_{41} & Z_{42} & Z_{43} & Z_{44} & Z_{45} \\ Z_{51} & Z_{52} & Z_{53} & Z_{54} & Z_{55} \end{bmatrix} \begin{bmatrix} I_{1c} \\ I_{2c} \\ I_{3c} \\ I_{4c} \\ I_{5c} \end{bmatrix}$$

and ---------(3.14)

$$\begin{bmatrix} I_{1c} \\ I_{2c} \\ I_{3c} \\ I_{4c} \\ I_{5c} \end{bmatrix} = \begin{bmatrix} Z_{11} & Z_{12} & Z_{13} & Z_{14} & Z_{15} \\ Z_{21} & Z_{22} & Z_{23} & Z_{24} & Z_{25} \\ Z_{31} & Z_{32} & Z_{33} & Z_{34} & Z_{35} \\ Z_{41} & Z_{42} & Z_{43} & Z_{44} & Z_{45} \\ Z_{51} & Z_{52} & Z_{53} & Z_{54} & Z_{55} \end{bmatrix}^{-1} \begin{bmatrix} e_{1c} \\ e_{2c} \\ e_{3c} \\ e_{4c} \\ e_{5c} \end{bmatrix}$$

Next the characteristic impedance and propagation coefficient of the return system can be determined as;

From the corrected return current and voltages the impedance of each conductor can be obtained using ohm's law;

$$Z_{1c} = \frac{e_{1c}}{I_{1c}} \text{-----(3.15)}$$

The admittance is the reverse of the impedance

$$Y_c = Y_{1c} + Y_{2c} + Y_{3c} + Y_{4c} + Y_{5c}$$

or -------(3.16)

$$Z_{cT} = \frac{1}{Y_{cT}}$$

The propagation coefficient is obtained from transmission line relation as;

$$\gamma = \sqrt{\frac{Z_c}{R_e}} \text{ -----(3.17)}$$

where, R_e = resistance to earth

and

$$Z_0 = \sqrt{Z_c \cdot R_e} \text{ ------(3.17)}$$

Z_0 = Characteristic impedance

3.1.1 Determination of conduction and induction currents

The rail as a conductor has a very small resistance. The inductance on the other hand is very large and varies with the level of traction current in the rails[49,50,51]. The attenuation is so large that the alternating current is diverted completely to earth after a few kilometres, or even sooner with higher frequencies. If the distance between the load and the sub-station is large and if the track is homogeneous, the rail currents divide equally in both directions at load or sub-station without any preference for inside direction. With a shorter distance, the impedance inside is much lower and as a result more current flows inside than outside.

With very small distance, the total current will flow back directly from the loading to the feeding end.

Consider a length of exposure as d (distance between load and sub-station) as shown in Figure 3.4[47].

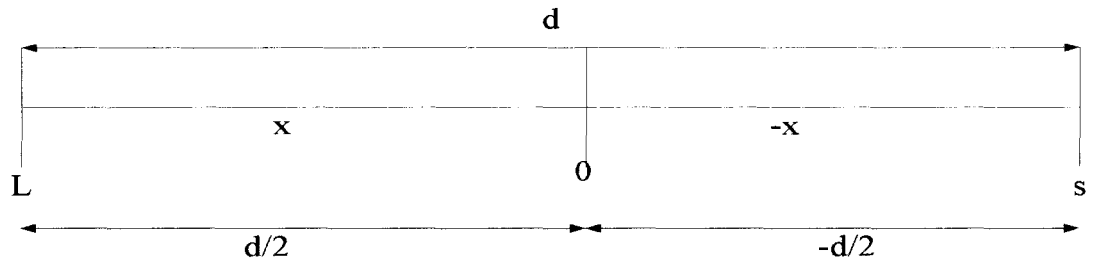

Figure 3.4: Distance between load (L) and substation (s) for a length of exposure d

Where, 0 is the centre of exposure, such that x is the distance measured from the centre towards the load and -x towards the sub-station;

0L = +d/2

0S=-d/2

If inductive coupling between the primary (inducing) and the secondary (induced) circuits is not considered, then the conduction current is given by;

$-x \leq -\frac{d}{2}$ (outside sub-station)

$$I_c = I \cdot e^{-\gamma(x)} \cdot \sinh(\gamma(\frac{d}{2}))\text{--------(3.19)}$$

$-x \geq -\frac{d}{2}$

or (between load and sub-station)

$x \leq \frac{d}{2}$

$$I_{cd} = I \cdot e^{-\gamma(\frac{d}{2})} \cdot \cosh(\gamma(x))\text{------(3.20)}$$

$x \geq \frac{d}{2}$ (outside the load)

$$I_{cd} = I \cdot e^{-\gamma(x)} \cdot \sinh(\gamma(\frac{d}{2}))\text{------(3.21)}$$

where, I = primary current (OCS current)

The above equations express the complete dc effect. For an ac effect a further current induced in the rails is superposed on the return current flowing in the rails and the earth. If the rails are perfectly earthed, then induced current I_{id} is;

$$I_{id} = -\frac{I \cdot j\omega M_{ps}}{R_s + j\omega L_s} \text{-------(3.22)}$$

M_{ps} = Mutual inductance between primary and secondary circuit PUL

This induced current can be re-written as;

$$I_{id} = -\frac{E_{id}}{Z_s} \text{-------(3.23)}$$

The current outside exposure in this case is negligible. However, if the rails are not perfectly earthed, the value of $-E_{id}/Z_s$ will be attained only in the middle of a long section. Near the ends, the induced current I_{id} decreases, but now flows outside the exposure.

The induction current can be given by;

$-x \le -d/2$ (outside sub-station)

$$I_{id} = -\frac{E_{id}}{Z_s} \cdot (e^{-\gamma(x)} \cdot \sinh(\gamma(\frac{d}{2})) \text{-------(3.24)}$$

$-x \ge -d/2$

or $x \le d/2$ (between load and sub-station)

$$I_{id} = -\frac{E_{id}}{Z_s} \cdot (e^{-\gamma(\frac{d}{2})} \cdot \cosh(\gamma(x)) \text{-------(3.25)}$$

$x \ge d/2$ (outside the load)

$$I_{id} = -\frac{E_{id}}{Z_s} \cdot (e^{-\gamma(x)} \cdot \sinh(\gamma(\frac{d}{2})) \text{---------(3.26)}$$

From the above it can be noted that, induction current has two expression for outside the exposure; one for outside load and the other for outside the sub-satiation, as in conduction current.

3.1.2 Determination of voltage induced due to return system

The total current (induction & conduction) at any arbitrary point c (to coincide with the centre of the cable) from the centre of the exposure 0, such that 0C = ± x may now be calculated, using equation (3.25), if the point is inside the exposure, or (3.26) if outside.

The total current now divided among the conductors in the return system is proportion to their admittances;

Such that,

$$I_t = I_{1n} + I_{2n} + I_{3n} + I_{4n} + I_{5n}$$

where -------(3.27)

$$I_{1n} = \frac{Y_{1c}}{Y_c} \cdot I_T$$

To determine the voltage induced into the cable the voltage induced in B1 may be determined, to which should then be added the voltage induced from the BEW (B1).This can be done since the cable is very close to B1 (about 0.05 m apart), hence the total voltage induced into the cable from the return conductors will be given by;

$$e_r = Z_{31} \cdot I_{1n} + Z_{32} \cdot I_{2n} + Z_{cb} \cdot I_{3n} + Z_{34} \cdot I_{4n} + Z_{35} \cdot I_{5n} \text{--------(3.28)}$$

where, Z_{cb} = mutual impedance between the cable and BEW B1.

3.1.3 Determination of voltage induced due to feed system

Since BEW B1 and the cable are very close, the distance of the cable from the feed conductors may be considered to be same as the distance of the BEW from the feed conductors.

Hence the total voltage induced in the cable is;

$$e_f = Z_{36} \cdot I_6 + Z_{37} \cdot I_7 + Z_{38} \cdot I_8 \text{-----(3.29)} \qquad \text{(e3 in section)}$$

The total voltage induced will be the vector resultant of the return induced voltage e_r plus the feed induced voltage e_f;

$$\hat{e} = \hat{e}_r + \hat{e}_f \text{------(3.30)}$$

e_f is fixed in magnitude and direction for a given OCS configuration and does not vary with exposure, while e_r is a function of exposure.

If there is a third parallel conductor in the vicinity connected to earth at both ends, it will carry a current I_3 due to the induced voltage from the railway line. It should be noted that the current I_3 due to the induced voltage V_{13} tends to flow in the direction opposite to the traction current I_1. I_3 therefore induces a voltage V_{23} in the signalling line, which is in the opposite direction of V_{12}. This opposing action gives rise to screening and this additional third conductor, which provides screening is called screen.

Hence, from the above;

$$V_2 = V_{12} - V_{23} = Z_{12} \cdot I_1 - (Z_{13} \cdot \frac{Z_{23}}{Z_{33}}) \cdot I_1 \text{--------(3.31)}$$

and the screening factor is;

$$K = \frac{1}{I_1} \cdot \frac{V_2}{Z_{12}} = 1 - \frac{Z_{13} \cdot Z_{23}}{Z_{12} \cdot Z_{33}} \text{--------(3.32)}$$

since;

e_r is the induced return voltage, e_f is the induced feed voltage and e is the total induction obtained from above;

$$e = e_r + e_f \text{-----(3.33)}$$

Hence screening factor for the return system is;

$$K = \frac{e_f}{e} = \frac{e_f}{e_r + e_f} \text{-------(3.34)}$$

In the case that there are more than one train, considerations for these effects have to be taken into account for worst-case scenarios. Hence a concentrated load of two trains should be taken.

For example if a train A is assumed to be situated at a distance 30 km from the sub-station, then for a given headway of 8 km, another train B may be regarded as present at 22 km from the sub-station.

Using the above steps, the total voltage induced e_1 and e_2 (30 km & 22 km exposure), into a cable, situated inside or outside the two exposures or inside one exposure (outside the other), may be determined for 1A of OCS current and 1 km length of cable.

e_1 and e_2 may be written as;

$$\begin{aligned} e_1 &= a_1 + jb_1 \\ e_2 &= a_2 + jb_2 \end{aligned} \text{-------(3.35)}$$

If the load currents at 30 km and 22km are Ix_1 and Ix_2, and if the length of the cable is L, then the total induced voltage will be;

$$[(a_1 + jb_1) \cdot Ix_1 + (a_2 + jb_2) \cdot Ix_2] \cdot L \text{-----(3.36)}$$

3.1.4 Systems considered

There are two different line-side cable conductors utilised for signalling control and indication function[47];

1. Direct wire, dc circuits or
2. Frequency division multiplex FDM system of transmission lines.

In the case of dc relay circuit, line sectionlisation will necessitate the use of a repeater relay for each circuit at each isolation point, together with an isolated power supply. The use of screened cable would increase the permitted distance between isolation points. But the relatively higher cost of screened cable to eliminate any consequential risk to maintenance technicians is a matter to be weighted against the respective economic/ technical consideration[54,55,56].

For FDM system, the case to be considered is much simpler. In such a system, a single pair of wires may be used to carry analogue commands by a number of channels of different frequencies. Line sectionlisation for each FDM system may be achieved by means of either an active line amplifier or a line isolation transformer. The standard configuration adopted for cables in ac electrified areas is one of interposing transformer and amplifier from section to section, at suitable separation distance in accordance with the signalling and traction conditions[57,58,59].

Using the same system configurations in chapter 2 and the method described in the above sections (3.1.1-3.1.4) the induced voltage can now be calculated.
The data used in the calculations for induced voltage (e.g. resistance to earth, length of cable etc) are given in Appendix A.

Note: Load and fault current values depend on the distance of the load or fault from the sub-station, this is because the impedance of the system changes with distance.

3.2 Two-track rail return systems

The self and mutual impedances for this system configuration are obtained from chapter 2, the induced voltages into signalling system have been calculated using the above formula in MATHCAD and the results obtained were as follow.

3.2.1 Two-track results

Results have been obtained using the load current values from Tables 3.1 and 3.2 for 1250 Amps, Tables 3.33 and 3.34 for 760 Amps OCS ratings[47]. For fault current results, substituted fault currents (also given in the above tables) for the corresponding load current values, have been used.

Distance from SS (km) (x)	Load current (A)	OCS fault current
30	1230	2545
29	1250	2686
28	1300	2743
27	1350	2857
26	1400	2900
25	1400	2910
24	1450	3143
23	1500	3257
22	1540	3371
21	1600	3450
20	1640	3455
19	1700	3700
18	1735	3714
17	1800	4057
16	1900	4150
15	1920	4182
14	2000	4364

Table 3.1: Load and fault currents for 1250 A OCS configuration

Distance from SS (km) (x)	Load current (A)	OCS fault current
13	2100	4546
12*	2200	4818
11*	2300	5000
10*	2400	5273
9*	2500	5646
8*	2650	5910
7*	2800	6270
6*	2950	6546
5*	3150	7091
4*	3350	7728
3*	3360	8182
2*	3950	8910
1*	4350	9819

Table 3.2: Load and fault currents for 1250 A OCS configuration

Distance from SS (km) (x)	Load current (A)	OCS fault current
30	780	1635
29	800	1637
28	830	1706
27	860	1775
26	890	1845
25	910	1914
24	940	2000
23	970	2091
22	1000	2182
21	1050	2273
20	1080	2364
19	1130	2455
18	1180	2546

Table 3.3: Load and fault currents for 760 A OCS configuration

Distance from SS (km) (x)	Load current (A)	OCS fault current
17	1200	2637
16	1280	2728
15	1320	2910
14	1400	3014
13	1450	3188
12*	1550	3364
11*	1650	3546
10*	1750	3819
9*	1850	4029
8*	2000	4429
7*	2150	4728
6*	2350	5182
5*	2550	5643
4*	2800	6171
3*	3150	6928
2*	3500	8000
1*	4050	9159

* Note: at each of these distances a maximum load current of 1500A for two concentrated loads has been assumed. Therefore, load currents for up to 12 km from the sub-station have been taken as 1500A in the calculations.

Table 3.4: Load and fault currents for 760 A OCS configurations

The induced voltage and screening factor results for one-track case are shown in Table 3.5 below;

OCS rating (A)	Track-layout	Cable position	Induced voltage (V)	Screening factor
1250	One-track open area	Normal	63	0.057
1250	One-track open area	Other side	60	0.053
760	One-track open area	Normal	54	0.076
760	One-track open area	Other side	57	0.079

Table 3.5: Induced voltage and screening factor for two different OCS ratings and cable position

The induced voltage was also determined at the centre of 30km exposure and at 12 km and 2 km exposures for two-track return systems, 1250 and 760 A OCS and for two different positions of the cable, the results are shown in Figures 3.5-3.16 below;

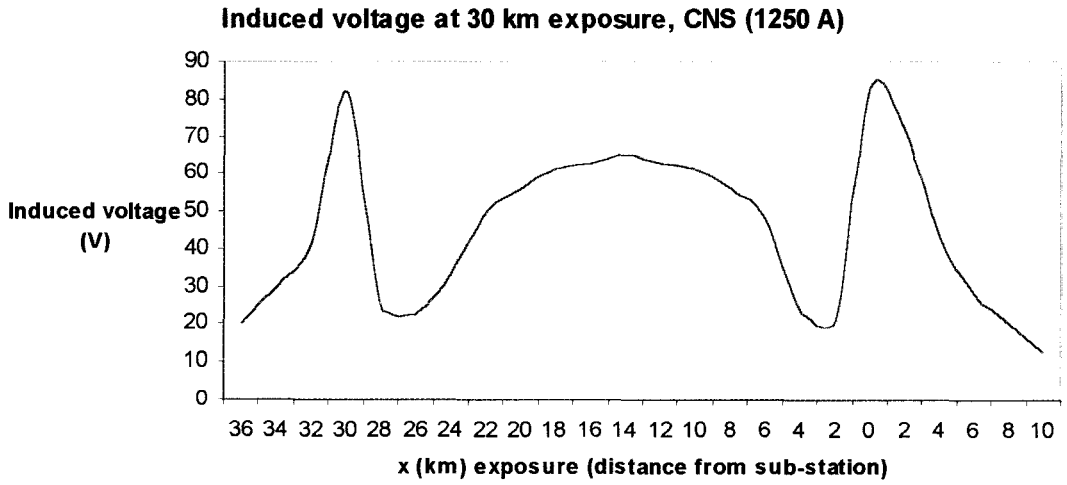

Figure 3.5: Induced voltage at 30 km exposure (1250 A) open track, normal cable position

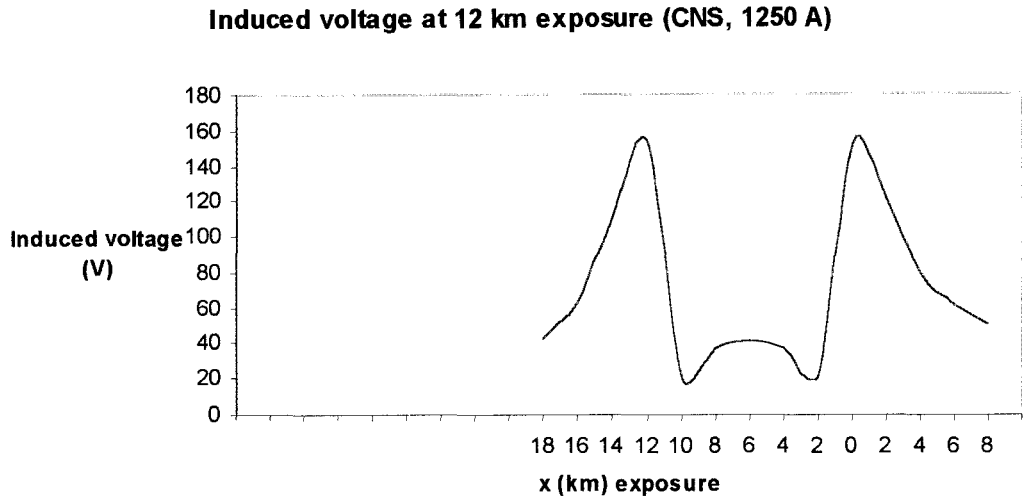

Figure 3.6: induced voltage at 12 km exposure (1250 A) normal cable position

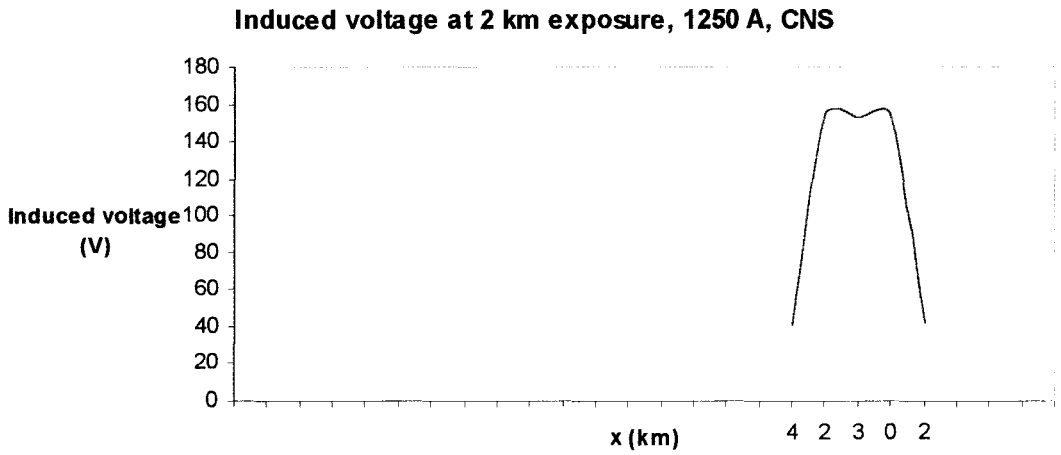

Figure 3.7: induced voltage for 2k exposure (1250 A) normal cable position

The Figures (3.8-3.10) below gives the highest voltage induced for the same exposures as above, but different position of the cable.

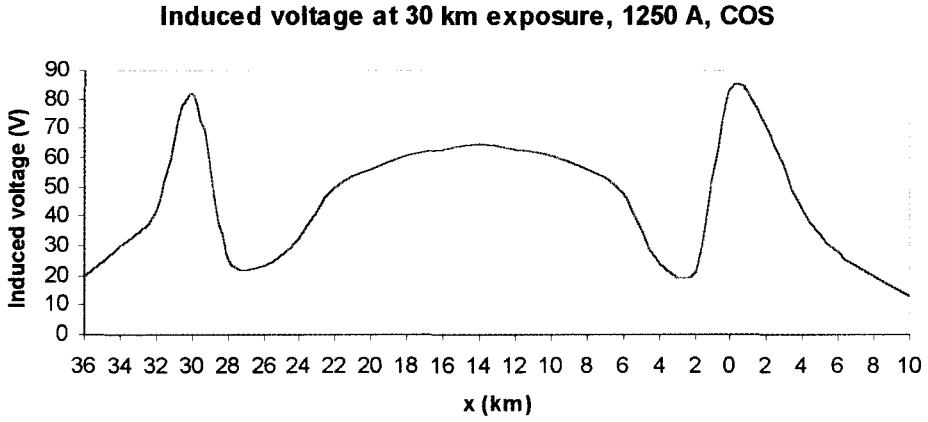

Figure 3.8: Induced voltage at 30 km exposure (1250 A) other side cable position

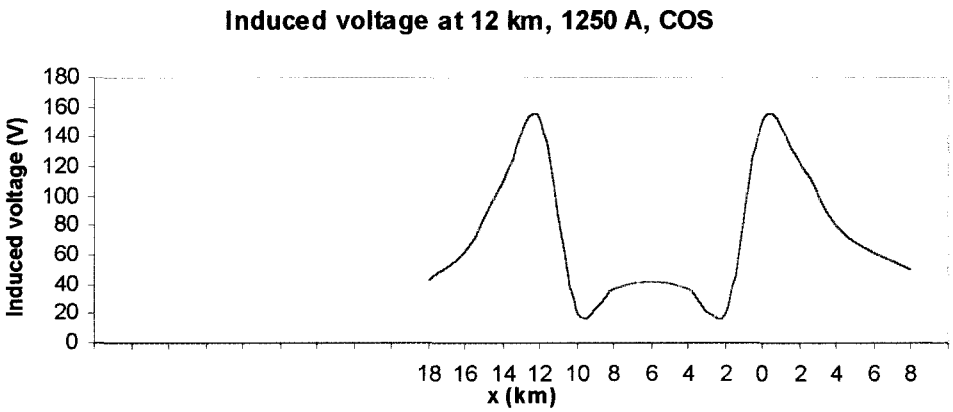

Figure 3.9: Induced voltage at 12 km exposure (1250 A) other side cable position

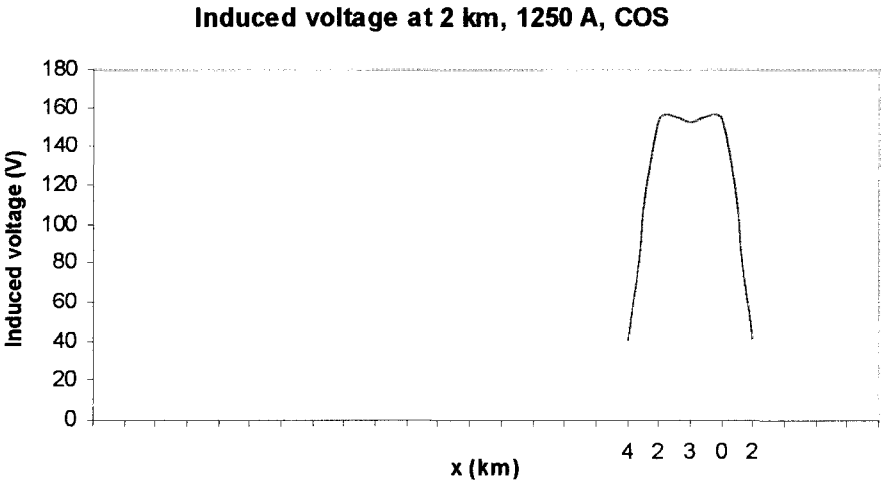

Figure 3.10: Induced voltage for 2k exposure (1250 A) other side cable position

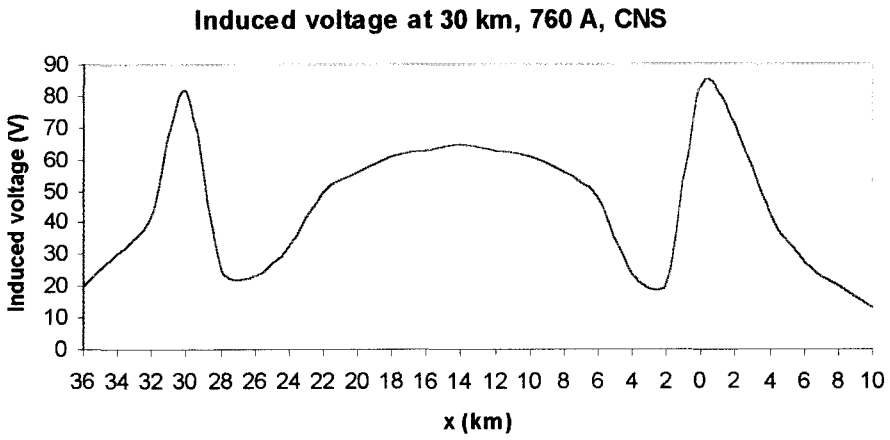

Figure 3.11: Induced voltage at 30 km exposure (760 A) normal cable position

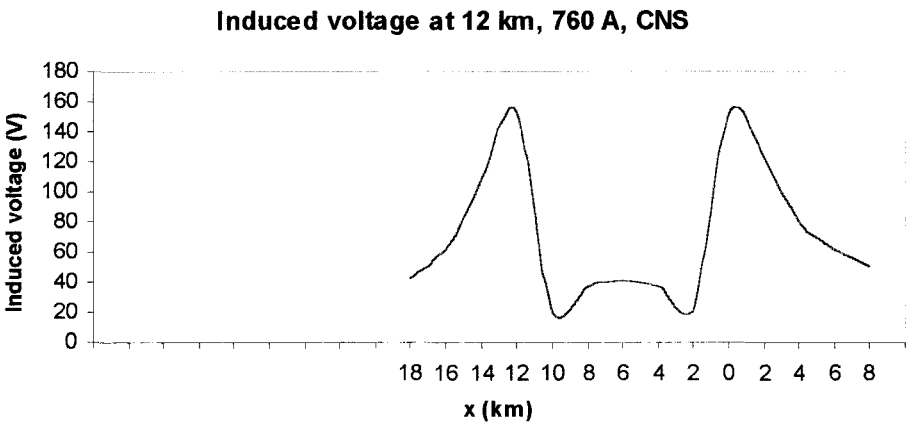

Figure 3.12: Induced voltage at 12 km exposure (760 A) normal cable position

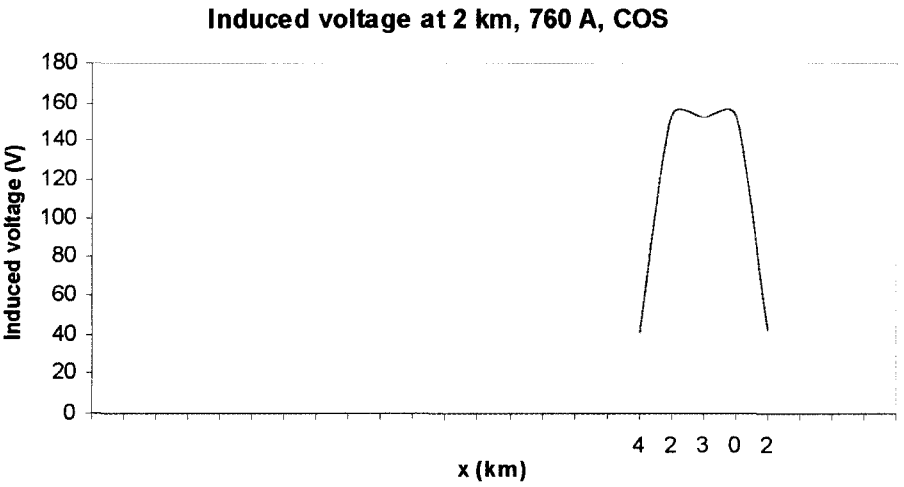

Figure 3.13: Induced voltage at 2 km exposure (760 A) normal cable position

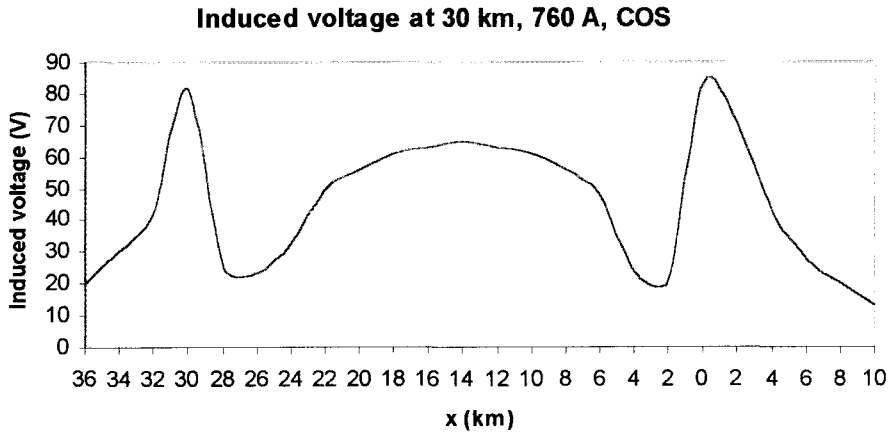

Figure 3.14: Induced voltage at 30 km exposure (760 A) cable on the other side position

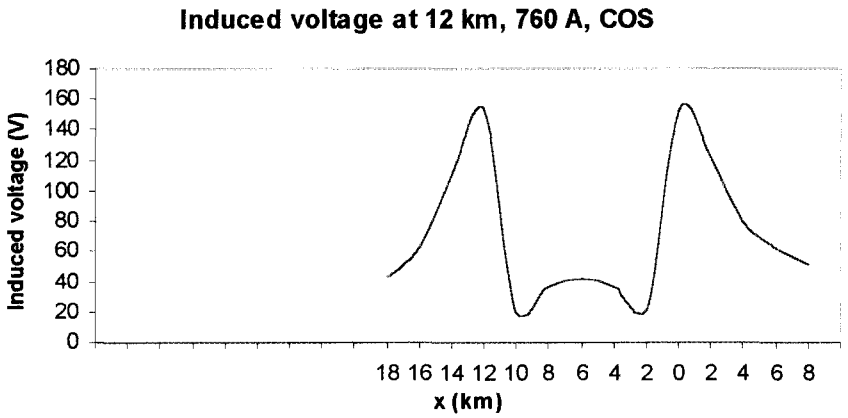

Figure 3.15: Induced voltage at 12 km exposure (760 A) other side cable position

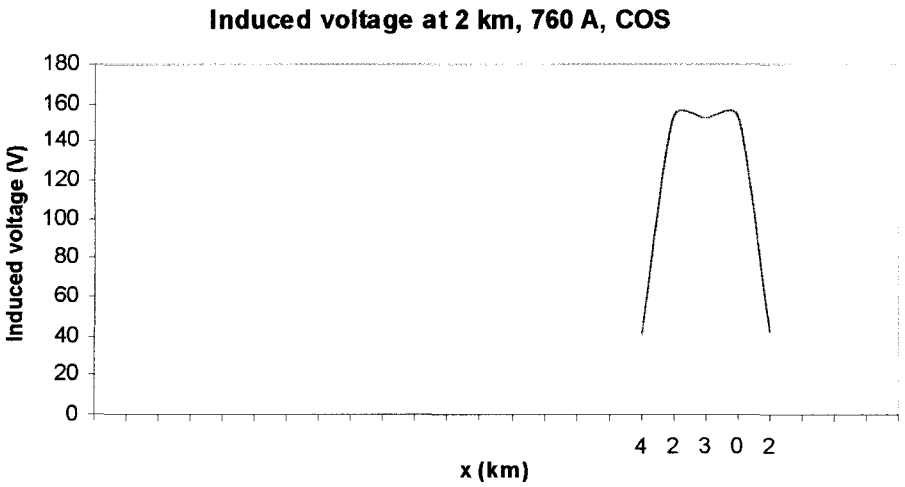

Figure 3.16: Induced voltage for 2k exposure (760 A) other side cable position

The following section deals with calculations and results for one-rail return systems.

3.3 One-rail return configuration

In one-rail traction return system, the traction currents returns to the sub-station in one rail only, while both running rails are used for track circuits.

3.3.1 Method of calculations for one-rail system

The method of calculation of induced voltage for one rail track follows the same approach as two rail return system described in chapter 2, once the rails, which do not carry the traction current, are eliminated.

Elimination of rails:

Using matrix elimination approach, R1 is eliminated from the complete impedance matrix, shown below.

$$\begin{array}{c} \\ R_1 \\ R_2 \\ B_1 \\ EW_1 \\ EW_2 \\ M \\ CW \\ F \end{array} \begin{array}{c} \begin{array}{cccccccc} R_1 & R_2 & B_1 & EW_1 & EW_2 & M & CW & F \end{array} \\ \begin{bmatrix} Z_{11} & Z_{12} & Z_{13} & Z_{14} & Z_{15} & Z_{16} & Z_{17} & Z_{18} \\ Z_{21} & Z_{22} & \cdots & \cdots & \cdots & \cdots & \cdots & \cdots \\ Z_{31} & \vdots & \ddots & \vdots & \vdots & \vdots & \vdots & \vdots \\ Z_{41} & \vdots & \vdots & \ddots & \vdots & \vdots & \vdots & \vdots \\ Z_{51} & \vdots & \vdots & \vdots & \ddots & \vdots & \vdots & \vdots \\ Z_{61} & \vdots & \vdots & \vdots & \vdots & \ddots & \vdots & \vdots \\ Z_{71} & \vdots & \vdots & \vdots & \vdots & \vdots & \ddots & \vdots \\ Z_{81} & \vdots & \vdots & \vdots & \vdots & \vdots & \vdots & \ddots \end{bmatrix} \end{array}$$

Eliminating rail1 (R1) from the above matrix gives;

$$\begin{array}{c} \\ R_2 \\ B_1 \\ EW_1 \\ EW_2 \\ M \\ CW \\ F \end{array} \begin{array}{c} \begin{array}{ccccccc} R_2 & B_1 & EW_1 & EW_2 & M & CW & F \end{array} \\ \begin{bmatrix} Z'_{22} & Z'_{23} & Z'_{24} & Z'_{25} & Z'_{26} & Z'_{27} & Z'_{28} \\ Z'_{32} & Z'_{33} & \cdots & \cdots & \cdots & \cdots & \cdots \\ Z'_{42} & \vdots & \ddots & \vdots & \vdots & \vdots & \vdots \\ Z'_{52} & \vdots & \vdots & \ddots & \vdots & \vdots & \vdots \\ Z'_{62} & \vdots & \vdots & \vdots & \ddots & \vdots & \vdots \\ Z'_{72} & \vdots & \vdots & \vdots & \vdots & \ddots & \vdots \\ Z'_{82} & \vdots & \vdots & \vdots & \vdots & \vdots & \ddots \end{bmatrix} \end{array}$$

RR, FF, RF matrices can now be extracted as below:

$$RR = \begin{array}{c} \begin{array}{cccc} R_2 & B_1 & EW_1 & EW_2 \end{array} \\ \begin{bmatrix} Z'_{22} & Z'_{23} & Z'_{24} & Z'_{25} \\ Z'_{32} & Z'_{33} & Z'_{34} & Z'_{35} \\ Z'_{42} & Z'_{43} & Z'_{44} & Z'_{45} \\ Z'_{52} & Z'_{53} & Z'_{54} & Z'_{55} \end{bmatrix} \begin{array}{c} R_2 \\ B_1 \\ EW_1 \\ EW_2 \end{array} \end{array}$$

RR matrix for one-rail traction return system (return conductor impedance)

$$RF = \begin{array}{c} \begin{array}{ccc} CW & M & F \end{array} \\ \begin{pmatrix} Z'_{26} & Z'_{27} & Z'_{28} \\ Z'_{36} & Z'_{37} & Z'_{38} \\ Z'_{46} & Z'_{47} & Z'_{48} \\ Z'_{56} & Z'_{57} & Z'_{58} \\ Z'_{66} & Z'_{67} & Z'_{68} \\ Z'_{76} & Z'_{77} & Z'_{78} \\ Z'_{86} & Z'_{87} & Z'_{88} \end{pmatrix} \begin{array}{c} R_2 \\ B_1 \\ EW_1 \\ EW_2 \\ CW \\ M \\ F \end{array} \end{array}$$

RF matrix for one-rail traction return system (feed conductors against return)

$$FF = \begin{array}{c} \begin{array}{ccc} CW & M & F \end{array} \\ \begin{pmatrix} Z'_{66} & Z'_{67} & Z'_{68} \\ Z'_{76} & Z'_{77} & Z'_{78} \\ Z'_{86} & Z'_{87} & Z'_{88} \end{pmatrix} \begin{array}{c} CW \\ M \\ F \end{array} \end{array}$$

FF matrix for one-rail traction return system (feed conductors impedance)

3.3.2 Results obtained for one-rail return system

For one rail return systems, the induce voltage results for one-track layouts in open areas are given below; the exposure considered are:

1. That which gives highest induced voltage inside the exposure
2. That which gives highest induced voltage outside exposure
3. The maximum exposure, i.e. 30 km.

The above results also represent a broken rail situation for two-rail return system, where one of the two rails is broken and the other carries the traction return current.

One track in an open area

As in two rail systems, the maximum voltage induced inside the exposure is at 2 km, and maximum outside exposure is at 12 km. However the results for one rail are greater than those for two rails.

From an induction point of view two rail return systems are better than one-rail. In one rail, it is better if the rail on the farther side of the cable carries the traction return current.

In order to consider the effect of a broken rail, elimination of each rail has been carried out one by one. The case of two broken rails has also been considered, even though this situation has an unlikely occurrence.

In all cases 2 km exposure gives the highest voltage induced inside the exposure, and 12 km exposure gives the highest voltage induced outside the exposure.

Results obtained are shown in Figures 3.17-3.24 below.

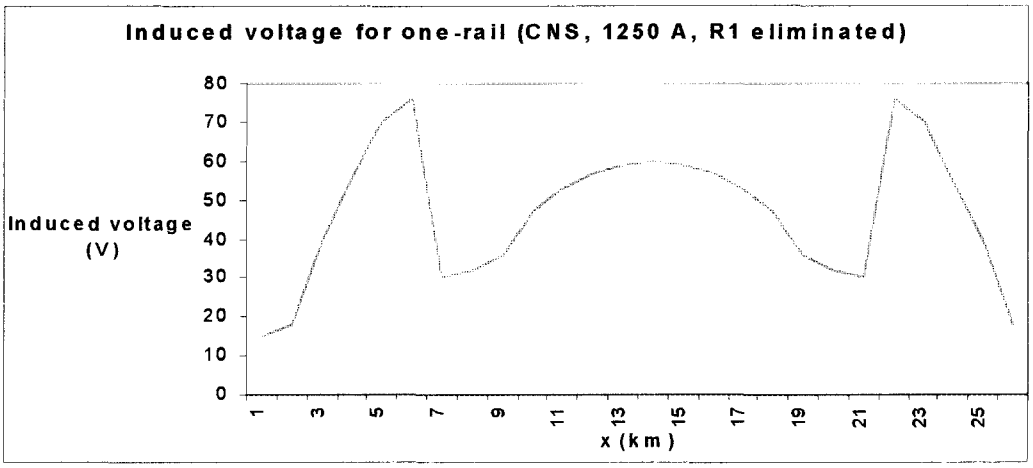

Figure 3.17: Induced voltage, open track, 1250 A, CNS, R1 eliminated

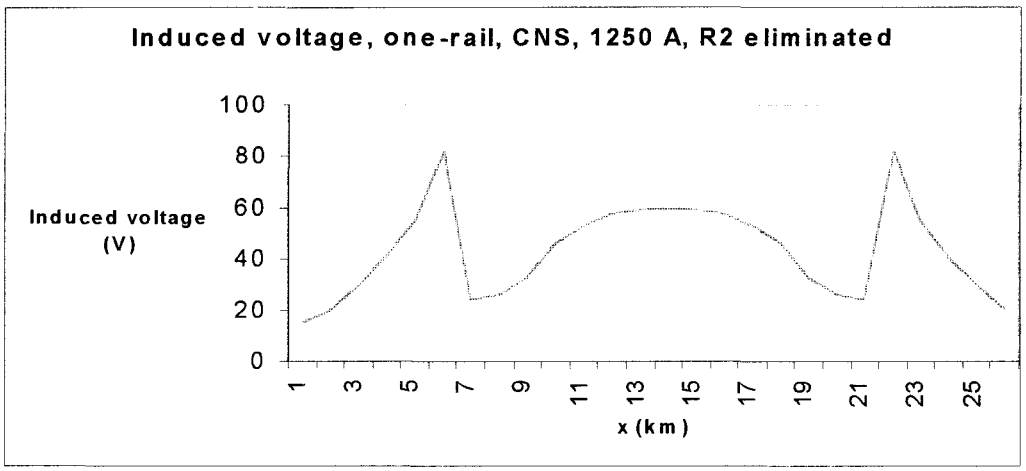

Figure 3.18: Induced voltage, open track, 1250 A, CNS, R2 eliminated

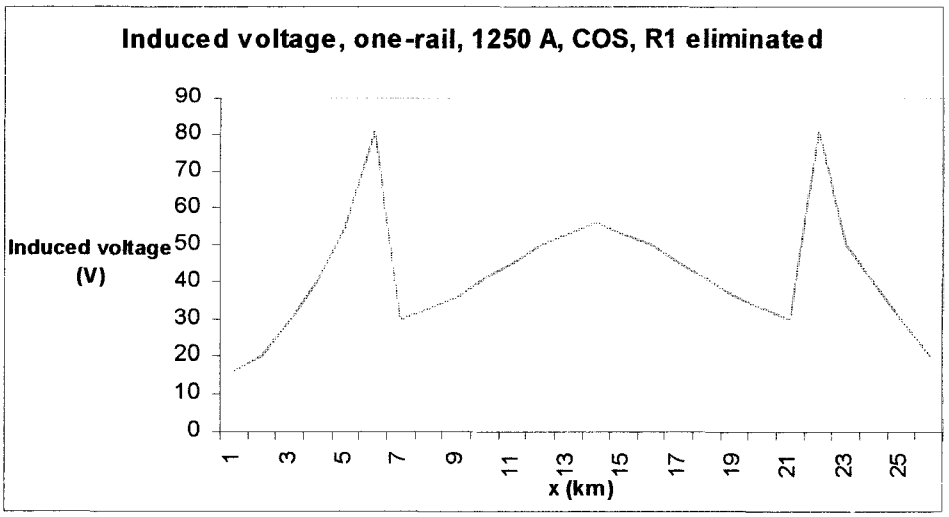

Figure 3.19: Induced voltage, open track, 1250 A, COS, R1 eliminated

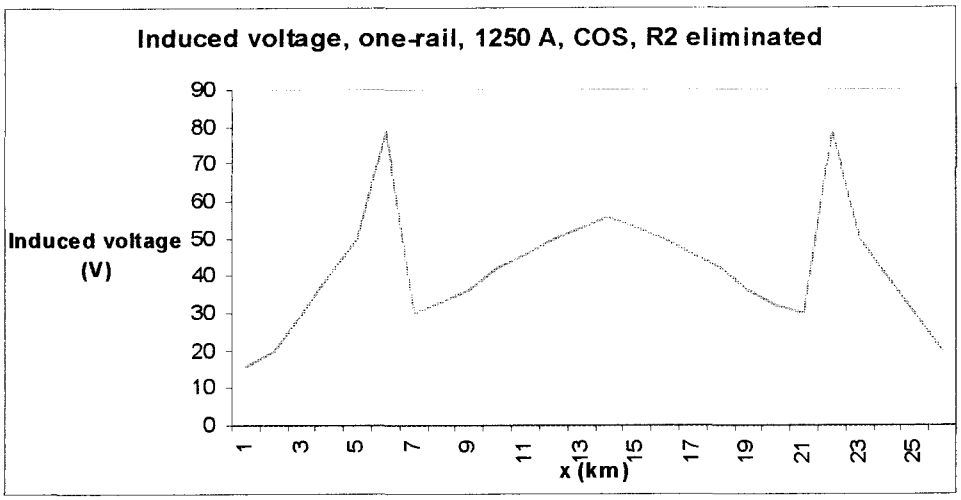

Figure 3.20: Induced voltage, open track, 1250 A, CNS, R2 eliminated

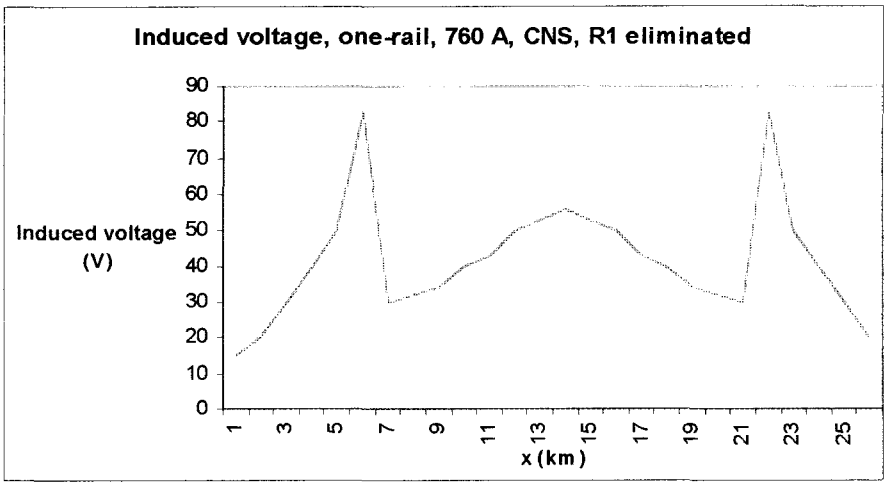

Figure 3.21: Induced voltage, open track, 760A, CNS, R1 eliminated

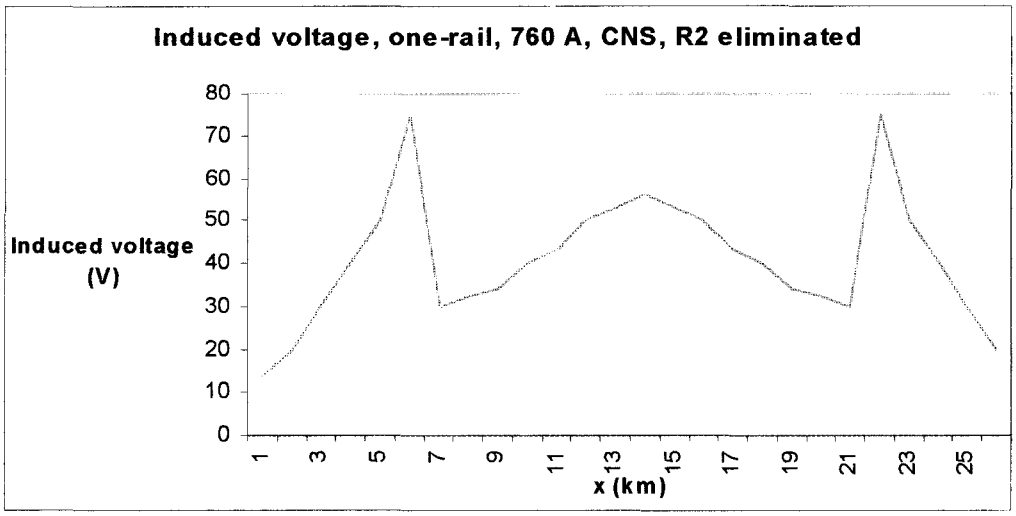

Figure 3.22: Induced voltage, open track, 760A, CNS, R2 eliminated

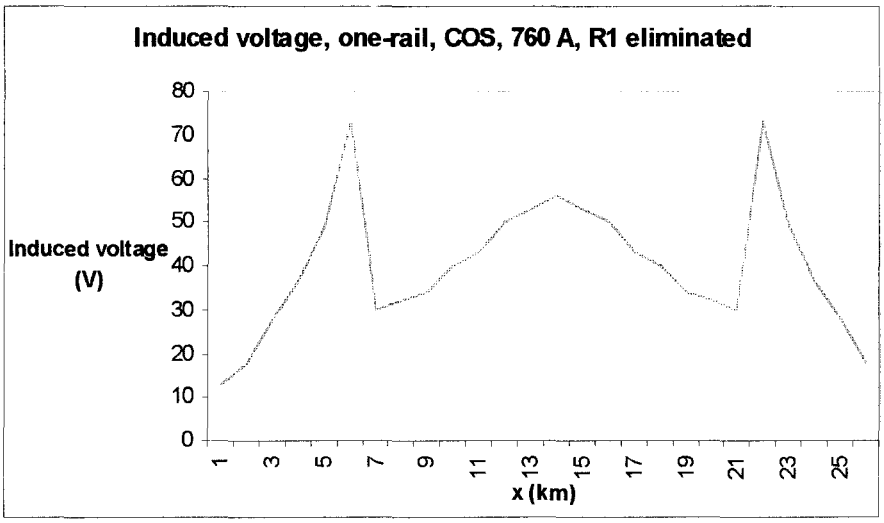

Figure 3.23: Induced voltage, open track, 760 A, COS, R1 eliminated

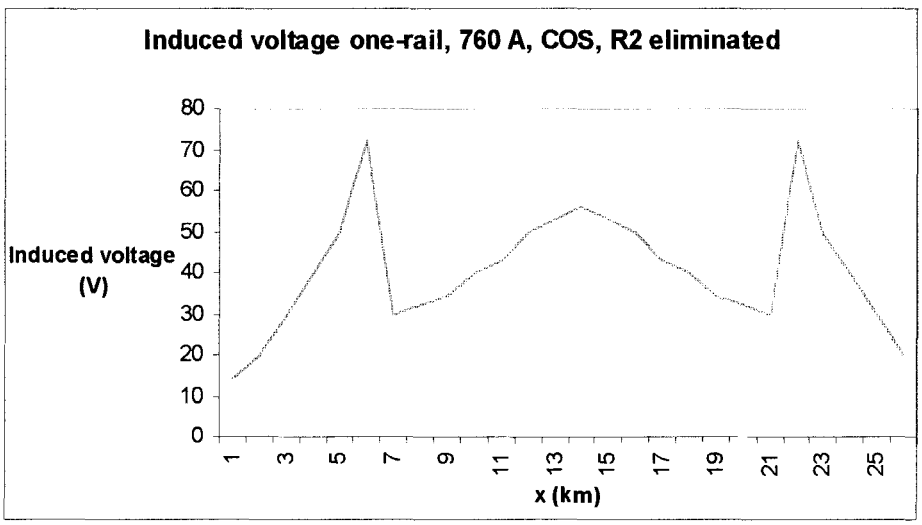

Figure 3.24: Induced voltage, open track, 760 A, COS, R2 eliminated

3.4 Summary

The induced voltages for uncompensated systems under normal operation conditions have been calculated for one and two track layouts and two different overhead ratings (1250, & 760 Amps). The induced voltages have been analysed for inside exposure where the return induction is more dominant and outside exposure where the feed conductor effect is more obvious. The position of the signalling cable, whether it is on the normal or other side of the track has also been considered.

Induced voltage curves of this chapter follow the established trend[47]; however, the calculated values for the curves are different. This is because the impedance values used are different and have been calculated by FDTD method, described earlier in this thesis.

CHAPTER (4)

Induced Voltage in Uncompensated Systems Under Fault Condition: A Touch Potential Effect

Introduction

The previous chapter dealt with the calculation of induced voltage for uncompensated systems under normal operation conditions. In order to establish a complete analysis of the system, it is important to understand the behaviour of the system under fault conditions, namely touch potential fault. In this section the induced voltage under fault conditions is analysed and calculations are given for one and two track layouts.

4.1 Touch Potential

The maximum voltage at different points either inside or outside exposures, induced into a section of the unscreened signalling cable in an open area is known from chapter (3) above.

If a cable fault develops due to contact between a conductor and the return system, the signalling equipment will be subjected to the sum of potentials set up in the conductive loop formed. This is known as the touch potential voltage in respect to danger to personnel and is also known as stress voltage in respect to equipment, it is therefore very important to know its level (Figure 4.1)[47].

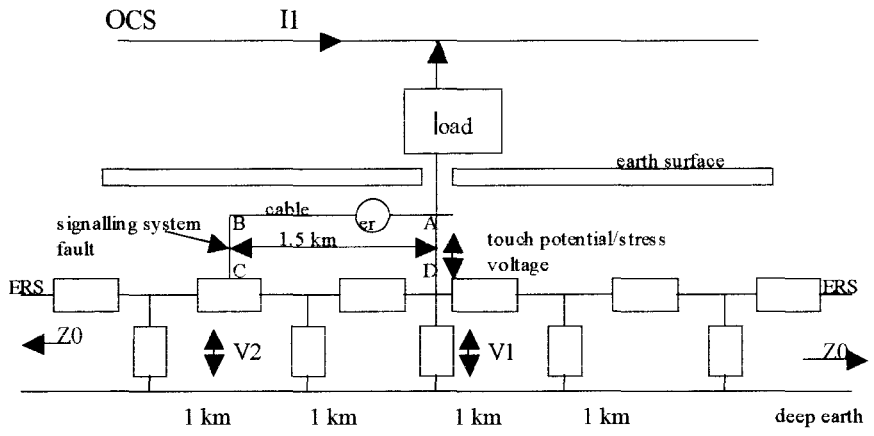

Figure 4.1: Signaling system in contact with ERS (Touch potential effect)

4.1.1 Formulation of touch potential

The first step for the calculations of the touch potential voltage is the total current inside and outside the exposure which are given below;

Total current I_T (comprises of induction Ii and conduction I_c);

$$I_t = -\frac{E_i}{Z_s} - (I - \frac{E_i}{Z_s})e^{-\gamma\left|\frac{d}{2}\right|} \cdot \cosh(\gamma x) \text{ ------(4.1) (for inside exposure)}$$

$$I_t = (I - \frac{E_i}{Z_s})e^{-\gamma|x|} \cdot \sinh(\gamma\left|\frac{d}{2}\right|) \text{ ------(4.2) (for outside exposure)}$$

From the formula above, it can be interpreted that; in entering the rails the primary current I splits up into the induced rail current $-E_i / Z_s$ and the return rail current -(I-E_i / Z_s)

The induced rail current flows only between feeding and loading points with constant intensity, as if the rails were perfectly earthed. Also it does not produce any voltage between rails and ground. The return rail current divides equally inside and outside and produces a potential drop in the rails as well as a potential between the rails and the ground, which is known as rising earth potential and is given by;

$|x| \leq |d/2|$

---------(4.3) (between the load and the sub-station)

$$V = Z_0 (I - \frac{E_i}{Z_s}) e^{-\gamma |d/2|} \sinh(\gamma x)$$

$|x| \geq |d/2|$

--------(4.4) (outside the load or sub-station)

$$V = Z_0 (I - \frac{E_i}{Z_s}) e^{-\gamma |x|} \sinh(\gamma |d/2|)$$

Referring to Figure 4.1 above, if the B end of the cable comes into contact with the return system at C, the resultant potential set up due to the conductive fault loop, identified by points A B C and D, will be given by the vectorial sum of potentials V_1, V_2 and e (V_1,V_2 are the rising earth potentials at the two ends and e is the total induced voltage in the cable). V_1 & V_2, when drawn with respect to deep earth as origin, may be regarded to be in the 1st quadrant as shown in Figure 4.2.

On the other hand vector e may lie in any of the quadrants 1, 2,or 3, but its origin has to be shifted to coincide with the end of vector V_2 because the cable comes into contact with return system at the V_2 end

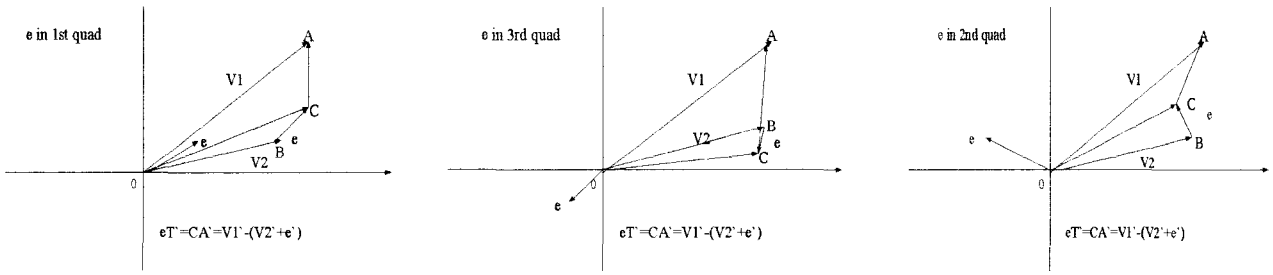

Figure 4.2: Voltage position in different quadrants

The touch potential in all cases, is the same and is given by;

$\hat{e}_T = \hat{V}_1 - (\hat{V}_2 + \hat{e})$ --------(4.5)

4.1.2 Determination of touch potential

Consider the Figure 4.3 below, to determine the touch potential for the cable AB, positioned as shown in Figure 4.3;

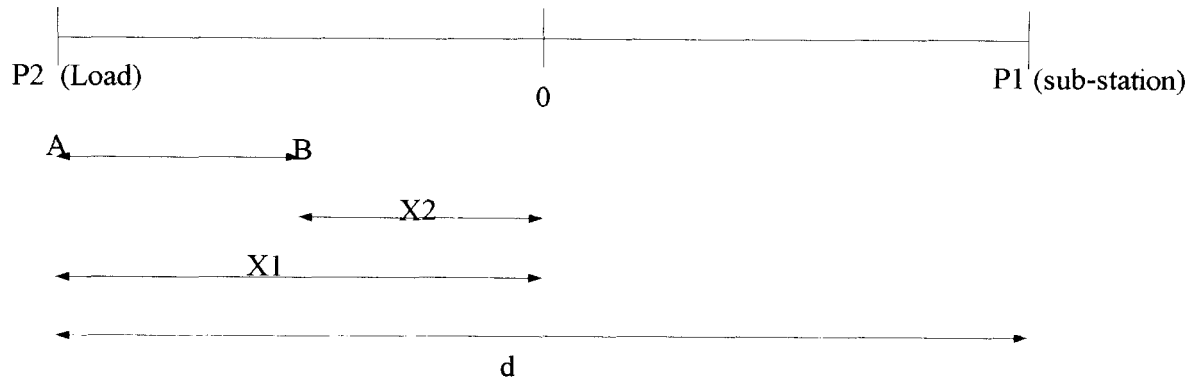

Figure 4.3: Position of the cable of length AB (inside exposure)

The sum of conduction and induction current It at any distance x inside the exposure is given by equation;

$$I_t = -\frac{E_i}{Z_s} - (I - \frac{E_i}{Z_s})e^{-\gamma|d/2|}\cosh\gamma x \quad \text{---------(4.6)}$$

for cable AB;

$$I_{t_{AB}} = \int_{x_2}^{x_1} -\frac{E_i}{Z_s} - (I - \frac{E_i}{Z_s})e^{-\gamma|d/2|}\cosh\gamma x \cdot dx$$

or -------(4.7)

$$I_{t_{AB}} = -\frac{E_i}{Z_s}(x_1 - x_2) - \frac{1}{\gamma}(I - \frac{E_i}{Z_s})e^{-\gamma|d/2|}(\sinh\gamma x_1 - \sinh\gamma x_2)$$

Calculations for current in section 3.1.1, may now be repeated by substituting I_t by I_{tAB}.

Note: e_r calculated in this case, will be for the full length of the cable and not for its unit length, as in section 3.1 since the integration is carried out over the entire length.
Voltage induced from the feed system e_f in this case will be e_f of step 10 in section 3.1 multiplied by the length of the cable $(x_1 - x_2)$. Hence, resultant voltage e induced in a length $(x_1 - x_2)$, will be known.

From equation, V_1 and V_2 are

$$V_1(A) = Z_0(I - \frac{E_i}{Z_s}) \cdot e^{-\gamma|d/2|} \cdot \sinh(\gamma \cdot x_1)$$
$$V_2(B) = Z_0(I - \frac{E_i}{Z_s}) \cdot e^{-\gamma|d/2|} \cdot \sinh(\gamma \cdot x_2) \quad \text{----------(4.8)}$$

Knowing e, V_1 and V_2, the touch potential e_{TP} for an OCS current of 1 A, may now be determine by;

$e_{TP} = V_1 - (V_2 + e)$ --------(4.9)

Multiplying equation 4.9 above by the total OCS current gives the total touch potential.

TP for a cable situated outside the exposure, as shown in the above figure is exactly the same. The only difference lies in that It, the total current (conduction + induction) and rising earth potentials v1 and v2 are all to be used as for the outside exposure (see Figure 4.4).

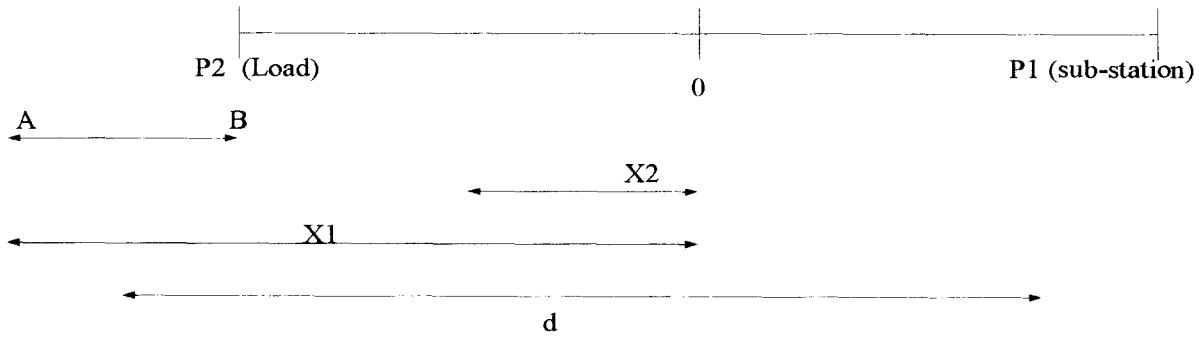

Figure 4.4: Position of the cable AB (outside exposure)

$$I_t = \int_{x_2}^{x_1} (I - \frac{E_i}{Z_s}) \cdot e^{-\gamma|x|} \cdot \sinh(\gamma|d/2| \cdot dx \text{ -------(4.10)}$$

hence

$$I_t = -\frac{1}{\gamma}(I - \frac{E_i}{Z_s}) \cdot \sinh(\gamma \cdot d/2) \cdot (e^{-\gamma|x_1|} - e^{-\gamma|x_2|}) \text{-------(4.11)}$$

therefore;

$$V_1(A) = Z_0(I - \frac{E_i}{Z_s}) \cdot e^{-\gamma|x_1|} \cdot \sinh(\gamma \cdot d/2)$$
$$V_2(B) = Z_0(I - \frac{E_i}{Z_s}) \cdot e^{-\gamma|x_2|} \cdot \sinh(\gamma \cdot d/2) \quad \text{--------(4.12)}$$

4.1.3 Results

On the basis of results obtained for one track and two track, it has been established that the touch potential maintains the same profile irrespective of the exposure and the OCS configuration or track layout.

Touch potential inside the exposure (Figure 4.5 & Table 4.1)) is minimum at the centre of exposure. It rises gradually on moving away from the centre on either side to a maximum value at the load or sub-station. Outside exposure (Table 4.2), touch potential decays rapidly from a maximum value at load or sub-station to almost nothing at about 10 km away from load or sub-station.

	Inside exposure		Outside exposure	
Configuration Figures	x (km) (exposure)	Max. TP (V)	x (km)	Max. TP (V)
2.15	2	142	13	19
2.16	2	139	13	21
2.17	2	131	12	16
2.18	2	135	12	16

Table 4.1: maximum touch potential (TP)

	Inside exposure		Outside exposure		Inside exposure		Outside exposure	
Configuration Figures	x (km)	Max. IV (V)	x (km)	Max. IV (V)	x (km)	Ma. TP (V)	x (km)	Max. TP (V)
2.15	2	1158	12	152	2	145	13	19
2.16	2	158	12	149	2	140	13	21
2.17	2	148	12	145	2	131	12	16
2.18	2	140	12	141	2	135	12	16

Table 4.2: comparison of Maximum TP against Max induced voltage (IV)

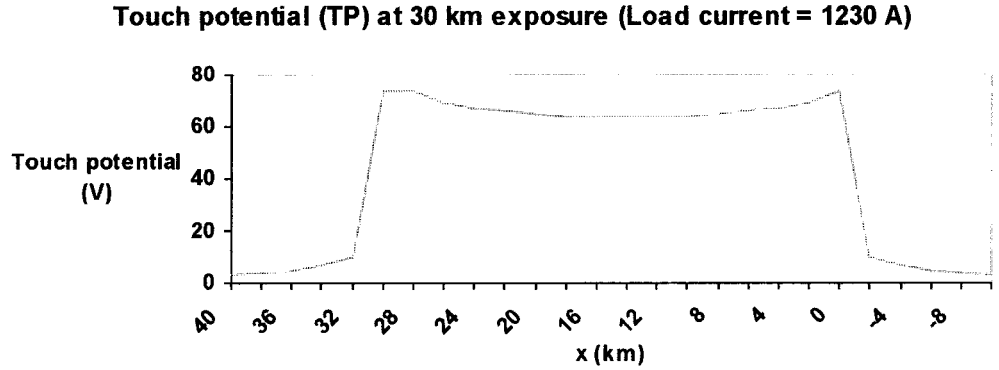

Figure 4.5: TP open track, 1250 A cable on normal side, 30 Km exposure

From Figure 4.5 above; with the contraction of exposure, the touch potential curve inside the exposure rises higher. For the range of exposure considered 2 –30 km, the shortest exposure i.e. 2 km gives the highest touch potential. While Figure 4.6 shows touch potential at different exposures for inside exposure and Table 4.3 for outside exposure.

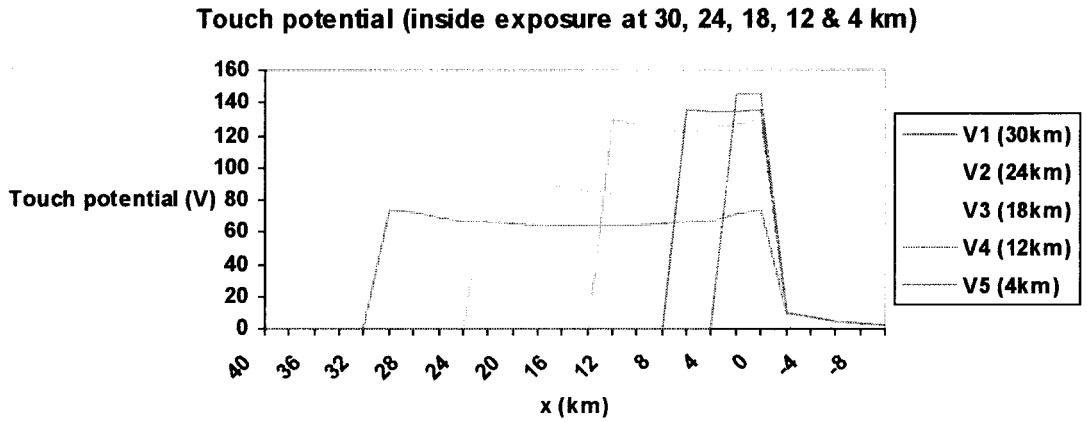

Figure 4.6: TP inside exposure, cable on normal side, 1250 A

V_1 (V)	x (km)
4	36
6	34
8	32
10	30

V_2 (V)	x (km)
4	28
6	26
10	24
14	22

V_3 (V)	x (km)
6	20
7	18
14	16
19	14

V_4 (V)	x (km)
7	12
9	10
15	8
17	6

V_5 (V)	x (km)
6	4
7	2
10	0

Table 4.3: TP outside exposure, cable on normal side for V1, V2, V3, V4, & V5

Outside the exposure, the touch potential is maximum in the mid exposure range (e.g. 13 km), its value decreases with the increase or decrease of exposure, beyond this range so that with the increasing exposure, it is minimum for 30 km exposure and with decreasing exposure, it is minimum for 2 km exposure.

4.2 One-rail touch potential

It can be calculated in the same manner as for two-rail return system. The three basic matrices, RR, RF, FF of the two-rail for the relevant OCS configuration and track layout are modified in order to include for the elimination of rails, which no longer would carry the traction current. The new sets of matrices are substituted for the old one and the same method is applied as before. Elimination is carried using standard matrix elimination method.

4.2.1 Results

As it would be expected the profiles of the touch potential curves, whether for inside or outside the exposure, remain the same as those in a two-rail return system. The maximum touch potential values inside and outside, however are greater than the corresponding values in a two-rail system. Results are shown in tables 4.4-4.7 and Figures 4.7 & 4.8 below.

	Inside exposure		Outside exposure	
Configuration Figures used	x (km)	Max. TP (V)	x (km)	Max. TP (V)
2.15	2	192	12	43
2.16	2	183	12	43
2.17	2	178	12	39
2.18	2	178	13	36

Table 4.4: maximum TP (R1 eliminated)

	Inside exposure		Outside exposure	
Configuration figures	x (km)	Max. TP (V)	x (km)	Max. TP (V)
2.15	2	186	12	43
2.16	2	191	12	48
2,17	2	174	13	36
2.18	2	185	12	41

Table 4.5: Maximum TP (R2) eliminated

	Inside exposure		Outside exposure		Inside exposure		Outside exposure	
Configuration Figures	x (km)	Max. IV (V)	x (km)	Max. IV (V)	x (km)	Ma. TP (V)	x (km)	Max. TP (V)
2.15	2	153	12	130	2	192	13	44
2.16	2	175	12	134	2	183	13	44
2.17	2	153	12	132	2	178	12	40
2.18	2	159	12	141	2	178	12	36

Table 4.6: comparison of maximum TP against Max IV (R1 eliminated)

	Inside exposure		Outside exposure		Inside exposure		Outside exposure	
Configuration Figures	x (km)	Max. IV (V)	x (km)	Max. IV (V)	x (km)	Ma. TP (V)	x (km)	Max. TP (V)
2.15	2	174	12	142	2	185	13	44
2.16	2	160	12	127	2	189	13	48
2.17	2	178	12	145	2	176	12	36
2.18	2	150	12	131	2	185	12	41

Table 4.7: maximum TP against Max IV (R2) eliminated)

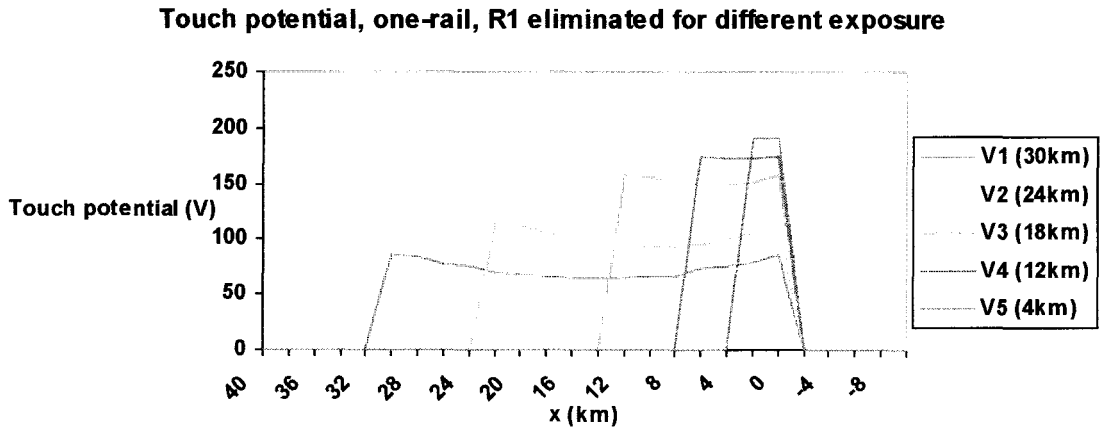

Figure 4.7: TP inside exposure, 1250 A, cable on normal side R1 eliminated

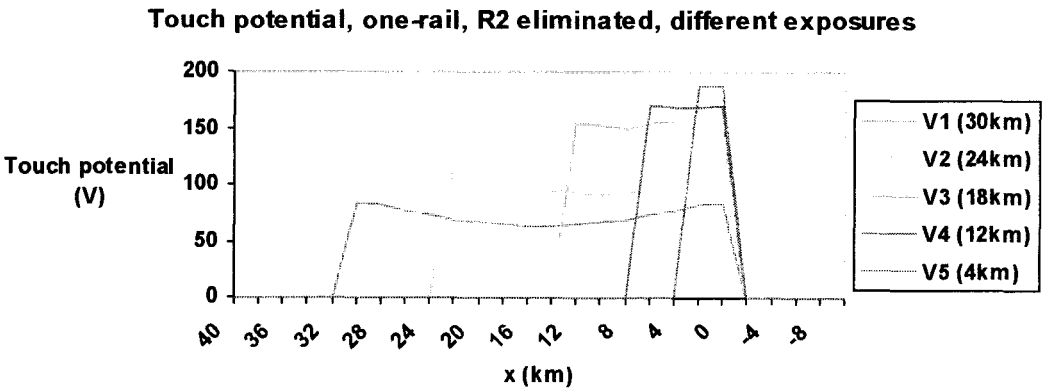

Figure 4.8: TP inside exposure, 1250 A, cable on normal side R2 eliminated

CHAPTER (5)

Induced Voltage in Compensated systems Under Normal Operation Conditions: A Booster Transformer Compensations

Introduction

The level of induced voltage due to the ac-single-phase, 25 kv, 50 Hz, should not exceed certain limits. The European Directive (CCITT)[19] for the protection of signalling and telecommunication lines sets these limits against harmful effects from the overhead power lines and are as given below:

1. 60 V rms under normal conditions (100 V rms for signalling cables)
2. 430 V rms under power systems fault conditions

To fulfil these requirements further suppression of any induction is needed. This is achieved by using booster transformers (BTs) connected to the contact wire and either directly to the rail or via a special return conductor. BTs were first introduced to suppress any interference caused to the post office lines (unbalanced lines), due to their effectiveness it was decided that they should be used in all major railway lines. Booster transformer suppression is now one of the most commonly used methods to constrain the level of induced voltage to the required limits.

The BTs are in effect current transformers with a 1:1 ratio. Their function is to force the return current to flow along a special return or rail to which the secondary of the transformer is connected.

As mentioned before their connection can be achieved in two different ways, either directly to the rail (Rail connected BT), where almost all of the return current is confined to the rails (Figure 5.1) small part flows through earth. In Britain the distance between two such transformers is 1 mile. It is apparent that this system is not effective, due to the difference between the distances of two current carrying conductors (catenary and rail) from the cable is very large and hence the residual resultant induced voltage in the cable is high. Also the impedance of the rails rises with frequency and causes a greater loss. For these reason suppression using the rail connected booster transformers has proved unreliable.

The second connection can be achieved by connecting the BT to a special return conductor. This type of connection provided better suppression when tested at the beginning of electrification and it is now widely used in the UK and Overseas. In this thesis only the latter is investigated.

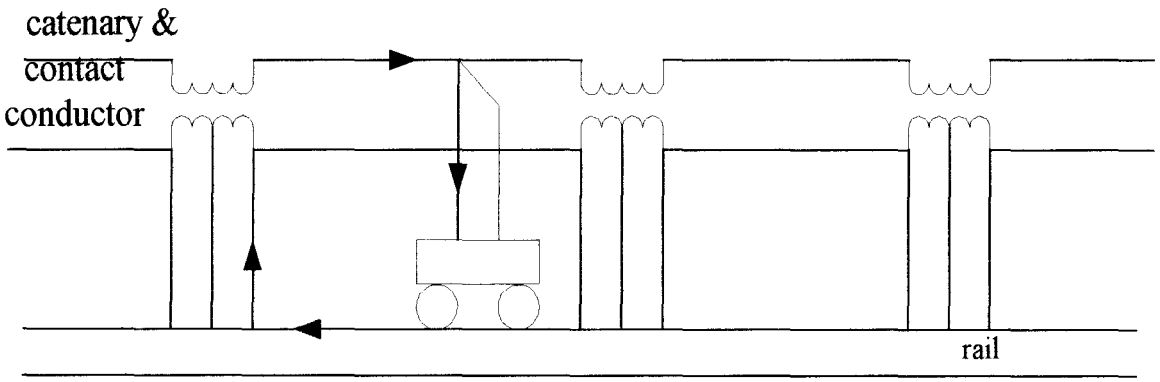

Figure 5.1: Rail connected BT

5.1 Booster Transformer (BT) with a special return conductor

A typical booster transformer with a special return conductor is shown in Figure 5.2. It is important that the return conductor should be placed as close as possible with the contact wire in order to reduce magnetic coupling between the power line and signalling/telecommunication cables. In practice however, the configuration of the conductors provide an inducing loop, which causes induced current in adjacent conductors and in traction rails. The value of this current depends on the rail impedance and rail-to-earth leakage resistance[69].

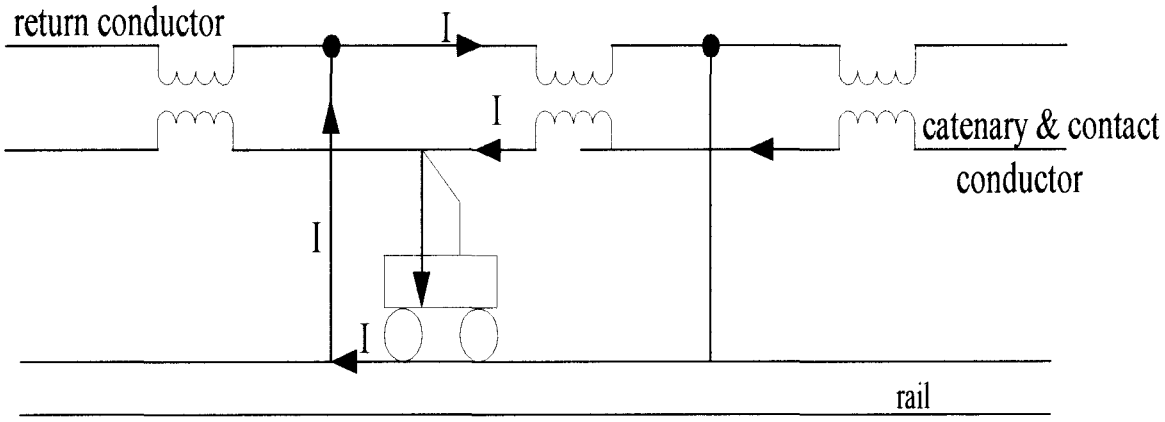

Figure 5.2: BT with a special return conductor

The connection of the rails to the return conductor is midway between consecutive BTs. The return path of the magnetising current is via the rails. This magnetising current is very small under normal condition. For the short circuit faults, saturation occurs in the transformer core and higher magnetising currents results.
The effect of the magnetising current under fault condition can be very severe hence further precautions are required. This is established by providing insulated overlaps across BT primary sides in the overhead line.

The magnitude of the BT magnetising current affects its size. Employing high magnetising current can reduce the size of the BT, but this could affect the current balance between primary and secondary, which in effect will contribute towards magnetic induction.
The series connection of the BTs with the supply system, can cause some voltage drop in the overhead line, this is due to leakage impednaces. The impedance of the simple feeding circuit is less by about 30% than that of this system[70].

5.1.1 Induction effect from BT system

For booster transformer systems with a return conductor, two main effects need to be considered. The first is induction from through currents, i.e. those currents taken by the trains well beyond the parallelism and confided wholly to the contact wire and return conductor (Figure 5.3). The second is induction due to a train in section, i.e. where the train is within or near to parallelism, and current flows along the rails (Figure 5.4).

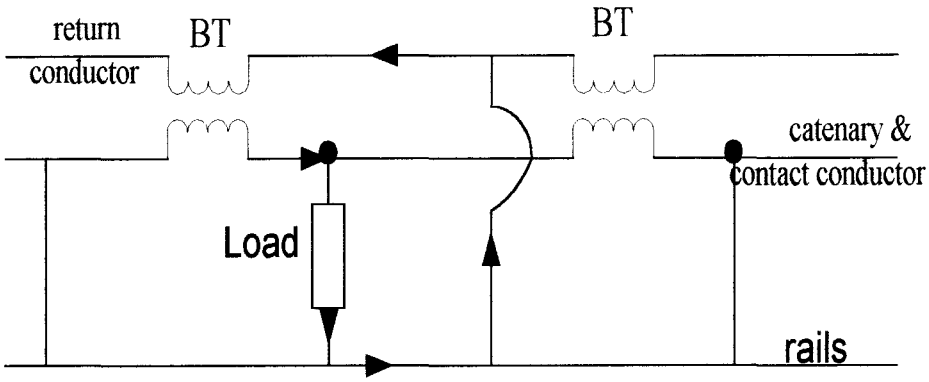

Figure 5.3: Train in section effect: case 1

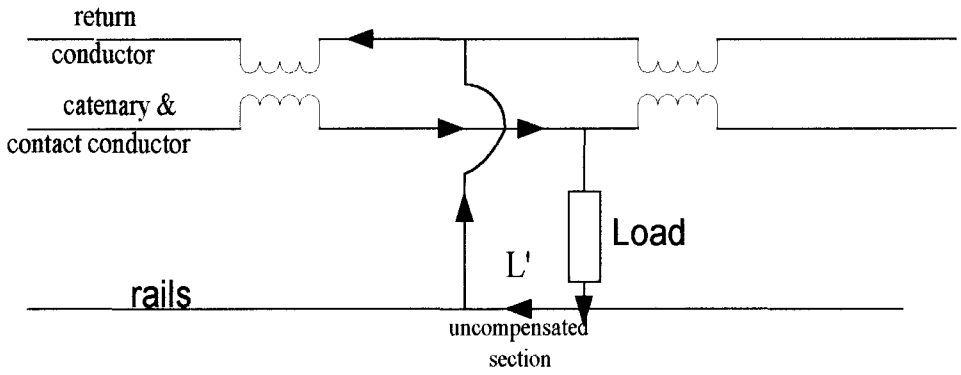

Figure 5.4: Train in section effect: case 2

The BT has also an effect on the increase of the impedance of the power circuit. The impedance of a single track system employing BT and return conductor is about 505% more than that of the non-boostered system (simple feeding system)[71]. This increase of the system impedance results in the need for closer ac substations.

Another effect is the size of the return conductor, since the secondary voltage of BT varies with the impedance of the return conductor and consequently the capacity of the transformer varies with the size of the conductor.

5.1.2 BT and its Mathematical model formation

Consider the equivalent ideal transformer shown in Figure 5.5.

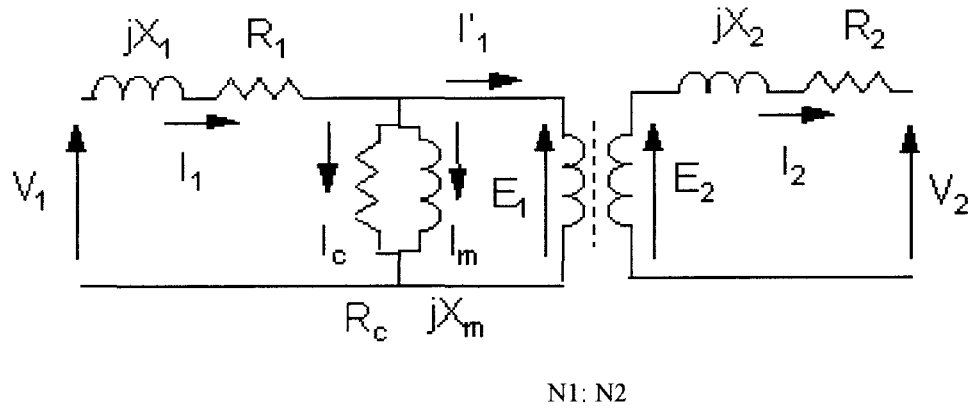

Figure 5.5: Ideal transformer equivalent circuit

And the simplified circuit below (Figure 5.6) for impedance calculations.

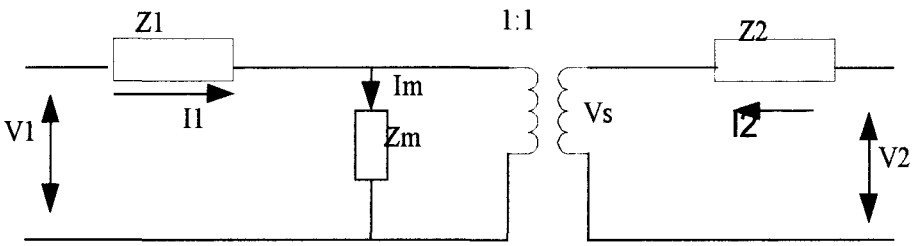

Figure 5.6: BT system for impedance calculations

From the above circuit, the impedance of the BT can be calculated as;

$$\begin{aligned} V_1 &= I_1(Z_1 + Z_m) + I_2 Z_m \\ V_2 &= I_1 Z_m + I_2(Z_2 + Z_m) \end{aligned} \quad \text{--------(5.1)}$$

where,

$I_1 = I_c$ (contact/catenary current)

$I_2 = I_{rt}$ (return conductor current)

Writing the above equation in matrix form gives;

$$[Z_b]=\begin{pmatrix}(Z_1+Z_m)Z_m \\ Z_m \qquad (Z_2+Z_m) \\ 0 \qquad 0\end{pmatrix} \text{--------(5.2)}$$

For the railway system with booster transformers and a special return conductor, the components involved are the catenary (C), return conductor (re) and rail conductor (R), the equivalent circuit for the calculation of the admittance and current of the BT in shown in Figure 5.7 below.

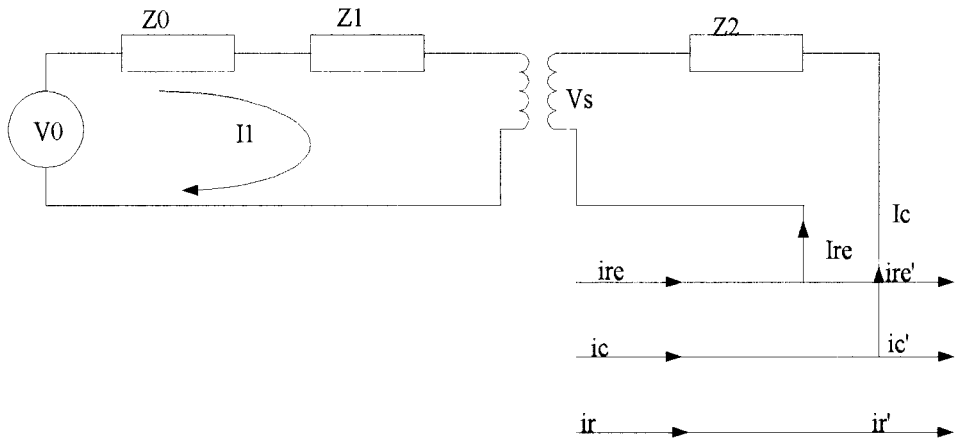

Figure 5.7: Component involved for BT system

Where, Z_0 = input source impedance

Z_1, Z_2 = primary and secondary impedance of feeding transformer.

From the circuit;

$$V_0^{'} = \frac{n_2}{n_1} V_0 \quad ---(5.3)$$

$$Z_1 = (\frac{n_2}{n_1})^2 (Z_0 + Z_1) \quad ---(5.4)$$

$$I_1 = -\frac{n_2}{n_1} I_c \quad ---(5.5)$$

$$V_s = \frac{n_2}{n_1}(V_0 - I_1(Z_0 + Z_1) \quad ---(5.6)$$

$$I_c + I_{re} = 0 \quad ---(5.7)$$

$$V_c - V_{re} = Z_2 * I_{re} + V_s \quad ---(5.8)$$

$$V_{re} - V_c = Z_2 * I_{re} - V_s \quad ---(5.9)$$

Substituting (5.3), (5.4), (5.5), in (5.6) gives:

$$V_s = \frac{n_2}{n_1}[\frac{n_1}{n_2} V_0^{'} - \frac{n_2}{n_1}(\frac{n_1}{n_2})^2 * Z_1^{'} * I_c] \quad ---(5.10)$$

$$V_s = V_0^{'} + I_c * Z_1^{'} \quad ---(5.11)$$

or

$$V_s = V_0^{'} - I_{re} * Z_1 \quad ---(5.12)$$

and;

$$V_c - V_{re} = V_0^{'} + I_c * Z_1^{'} + I_c * Z_2 \quad ---(5.13)$$

$$V_{re} - V_c = -V_0^{'} + I_{re} * Z_1^{'} + I_{re} * Z_2 \quad ---(5.14)$$

$$V_c - V_{re} = V_0^{'} + I_c(Z_1^{'} + Z_2) \quad ---(5.15)$$

$$V_{re} - V_c = -V_0^{'} + I_{re}(Z_1^{'} + Z_2) \quad ---(5.16)$$

In matrix form;

$$\begin{pmatrix} V_c - V_{re} \\ V_{re} - V \end{pmatrix} = \begin{pmatrix} V_0^{'} \\ -V_0^{'} \end{pmatrix} + \begin{pmatrix} Z_1^{'} + Z_2 & 0 \\ 0 & Z_1^{'} + Z_2 \end{pmatrix} * \begin{pmatrix} I_c \\ I_{re} \end{pmatrix} \text{-----(5.17)}$$

Using matrix manipulation the above can be rearranged to the required formula, and hence the admittance of the circuit can be obtained as:

$$[Y_s]=\begin{bmatrix} V_c \\ V_{re} \\ V_r \end{bmatrix}=\begin{bmatrix} i_c \\ i_{re} \\ i_r \end{bmatrix}-\begin{bmatrix} i_c' \\ i_{re}' \\ i_r' \end{bmatrix}+[J_s]\text{-------(5.18)}$$

For the ac single-phase 25 kV, 50 Hz system with booster transformers connected to a return conductor, the above calculations are carried out using Mathcad and some of the results obtained are given below (Figure 5.8-5.11).

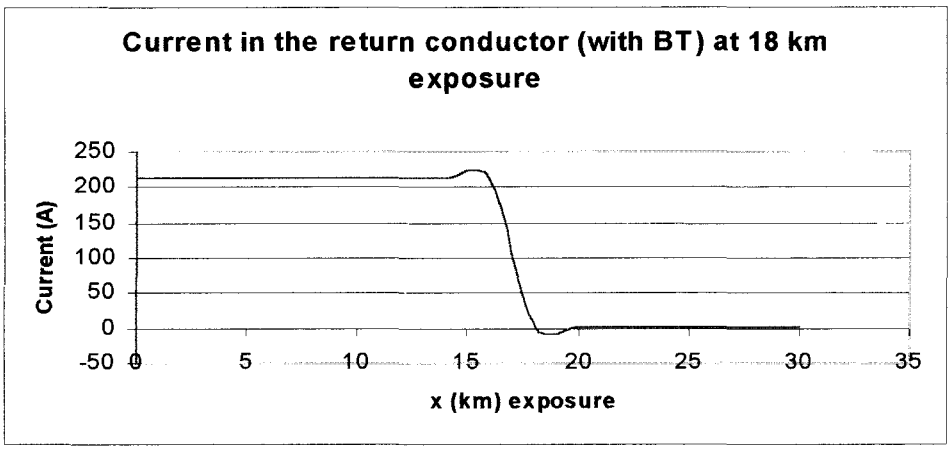

Figure 5.8: Current in the return conductor for BT spacing 3.2 km, train position at 18 km

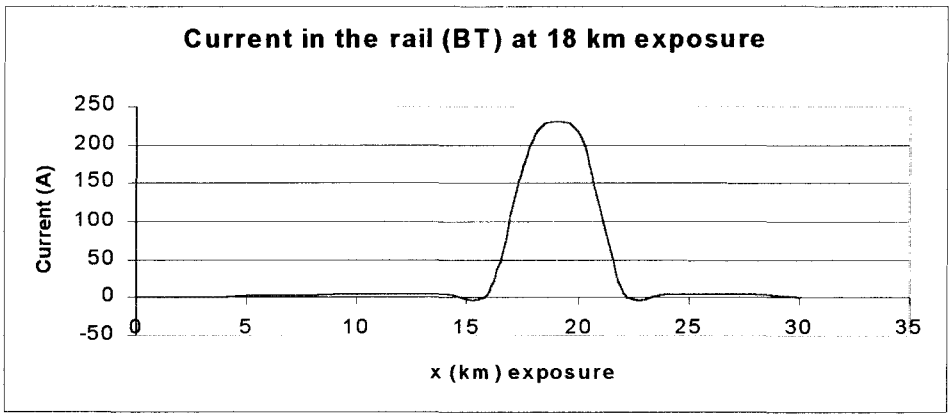

Figure 5.9: Rail current for BT 3.2 km spacing, train position at 18 km

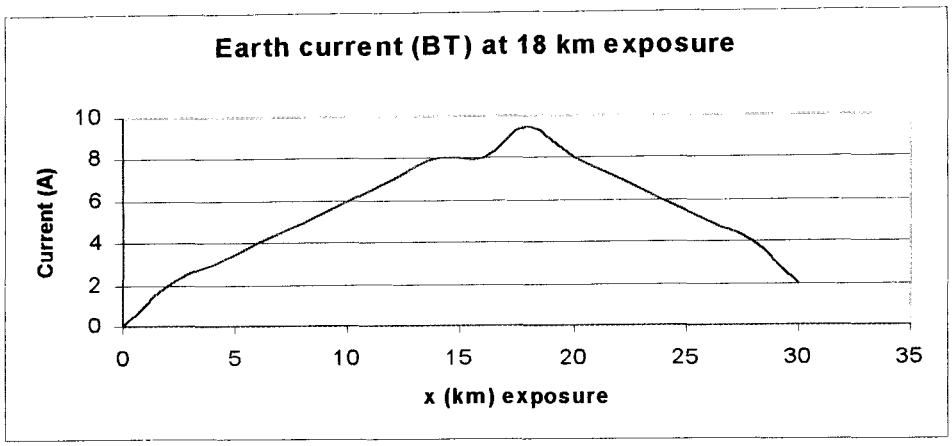

Figure 5.10: Earth current for BT 3.2 km spacing, train position at 18 km

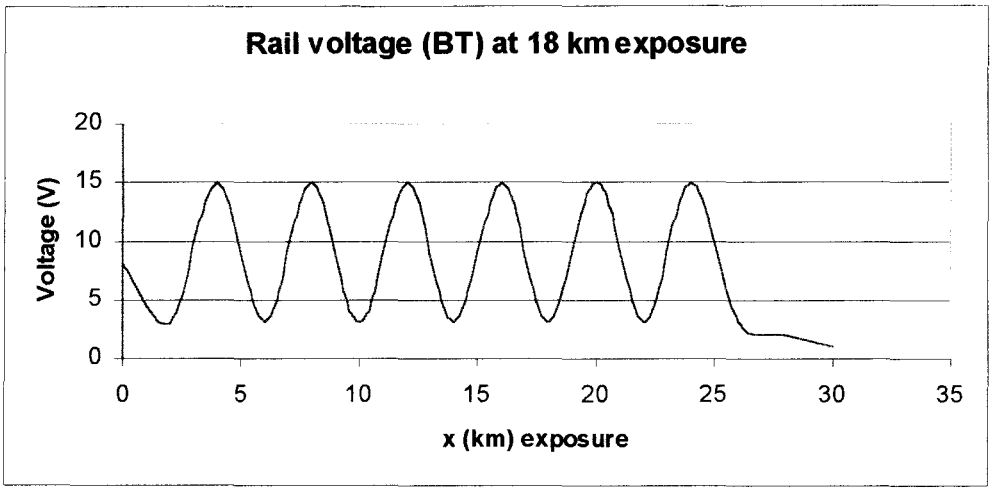

Figure 5.11: Rail voltage with BT system with rail return (train position at 18 km)

The above section shows the calculation for the booster transformer it self. The calculations of the induced voltage in the nearby signalling cables for one and two track layouts under normal operation conditions are given in the following section (5.5, 5.6 & 5.8).

5.2 Compensated systems under normal operation

As mentioned before interference with signalling and communication circuits is a problem that has been greatly accentuated with advent of 50 Hz traction supply.

There are many different possible remedial measures that can be adopted for the prevention of any interference these are[72]:

1. To connect booster transformers with their primary windings connected in series with overhead line and their secondary windings connected either directly to the running rails or connect to a special return conductor as shown above.
2. To provide heavy magnetic and electric shielding on signalling and telecommunication cables which parallel the track.
3. To design signal and telecommunication circuits, which would be immune from the effects of, induced voltage and thus save cost of providing series booster transformers and special shielding of the cables.
4. To sectionalise the cable with the use of a device such as an isolating transformer, which may be provided in the cable circuits to act as barrier to the induced voltage. The device at most allows a small fraction of this voltage to reach the terminal apparatus or personnel working on the termination of the circuit.

All of the methods mentioned above have been tried in different lines at the beginning of electrification project in Britain. The most effective method was found to be booster transformers connected to a special return conductor. Shielding and good grounding have also been used to provide further suppression. With the introduction of electromagnetic compatibility EMC Directive (January 1996) it is now required by law that all new electric and electronic equipment should be immune from the effect of interference as well as having little interference produced by them. Unfortunately, many of the old equipment are still in use now a day[73].

The European directive concerning the protection of telecommunication lines against harmful effects from power lines, specify that cables which are not terminated by suitably constructed transformers should not be subject to longitudinally induced voltage in excess of the limits mentioned earlier. Where transformers of suitable construction are employed to terminate the cable circuit, the CCITT[19] directive recommend that under fault conditions, the maximum

possible longitudinally induced voltage may be increased to 60% of the cable conductor sheath-test voltage.

If the calculated values of induced voltage exceed the limit set by the CCITT, one of the options of remedial measure mentioned above has to be considered. It is desirable first to see if the induction can be reduced to the safe limits by sectionlisation of the cable. In such an event the cost is likely to be significantly less than incurred using BT, if they are to be employed. However, this may be true for cases where only a reasonable number of sections are necessary. In other cases, it may very well be possible that the findings show a balance in favour of the use of BT on the grounds of economy.
Since the booster transformer suppression is commonly used in the UK, this project concentrated on the analysis of such system.

5.3 BT with return conductors

Reducing the magnetic field caused by the current flowing in the traction line can reduce induced voltage to an acceptable level.
Theoretically this field can be reduced to zero in the space around the traction line if the current of the same magnitude and phase as the traction current, but in the opposite direction flows through a conductor in the immediate vicinity of the OHL.

The aim therefore, is to pass the return current through a special return conductor, running parallel and as close as possible to the OHL, thereby reducing the leakage current to a minimum, which returns to the sub-station via earth or the running rails. This is achieved by having BT in the circuit as shown in Figure 5.2. In Britain the distance between two BT with return conductor is 2 miles. The return current flows in the rail up to the nearest point at which the return conductor is bonded to the rails. From there it flows through the return conductor back to the feeder point (Figures 5.3 & 5.4).

Two limitations of suppression at source using BT with return conductor may be mentioned here;
Considering a single-track line with BT return, the field produced by the current in the return conductor is 180° out of phase with the field produced by the current in the catenary system.

If the whole of the return current flowed in the return conductor and if there were no other parallel conductors to carry induced currents, the field produced respectively by the catenary current and the return current would sum to zero at all points that were equi-distant from the two conductors. These points would lie on a neutral plane that passed mid-way between the catenary and the return conductor and was as right angles to the line joining them. For any point in this plane there is a perfect suppression at source.

- The first limitation of suppression at source occurs when there is more than one track. The induced field at any given point is the vector sum of the fields produced by all the catenary systems to several tracks, as well as by all the return conductors and other current-carrying conductors. For such a system a neutral plane is no longer relevant.
- The second limitation is set by the fact that the return current after leaving the wheels of the electric vehicle does not reach the return conductor until the nearest point at which this conductor is bonded to the rails (the return conductor is connected to the rails at every mid-point between two transformers).

Hence between the load and the nearest mid-point connection or in a train section as it is commonly referred to, the return current is confided mainly to the rails (a small part flows through earth). Although the currents in the two current-carrying conductors (catenary & rail, return conductor & rail) are equal in magnitude and phase but opposite in direction (assuming no current flowing into earth), the level of induced voltage is very high in a train section. This is because of a large difference in the distance between the two current carrying conductors and the cable, which subsequently causes a large difference in two opposing mutual induction.

The longest train section therefore, gives the worst-case scenarios and the shortest is the best case. With a distance of 2 miles between two BTs, the maximum length of a train section is 1 mile.

This condition is achieved when the train is at the BT and is commonly known as 1-mile effect. On the other hand the shortest train section length is fulfilled when the train is at the mid-point connection. Hence the nearer the train is to the BT, the less perfect is the compensation.

5.4 Rail connected BT

Even though this type of connection has proved unreliable as motioned earlier, a brief description is given here. With this scheme nearly all the return current is confided to the rails. In Britain distance between two such transformers is 1 mile[74].

From the diagram (see Figure 5.1) it is apparent that this system is not as effective as the BT return system, this is due to;

1. The difference between the distances of the two current-carrying conductors (OH catenary and rail) from the cable is very large. Thus residual resultant induced voltage in the cable is very high.
2. The impedance of the rails rises with frequency and causes a greater loss of current from the track
3. Between BT locations, the return traction current tends to find its own low impedance path down all the running rails. This means that the return traction current tends to leave a single-rail track circuit and join a double rail track because of its lower impedance. The result of these transverse current is to raise the potential difference between the rails on double-rail track circuit.
4. There is also the effect on rail potential to earth. The potential of the rail when several trains are taking current steps progressively higher until the feeder station is reached.

In the following sections, the calculation of induced voltage under normal for compensated return conductor only, has been considered, since this system is the most widely used due to efficiency compared to BT running rail. Fault conditions in the form of short circuit faults for compensated systems are given in the next chapter (6).

As in an uncompensated system the starting point in the calculation is the determination of self and mutual impedance values for track layouts and OCS configurations considered.

5.5 Two-rail return compensated system

In uncompensated systems, the distribution of current in a multi-track case follows the same rule as in a one-rail track case as far as the direction of currents in different conductors is

connected. In other words, in such systems, as a general rule, it can be said that the currents in feed conductors are always in one direction and those in return conductors in the other.
This general rule however, does not apply for compensated systems, because as it will be seen later, the current distribution pattern in these systems is different for different number of tracks considered.

As a result in contrast to uncompensated systems, where the method of calculation has been explained by taking one case (i.e. one-track as an example), here in compensated systems each track case will have to be considered separately.

In this section the method of calculation for one-track and two-track cases for the track layout and OCS configuration in given in chapter 2 (Figures 2.11, 2.12) are considered receptively.

Furthermore, in compensated systems induced voltage to be calculated is twice the number of times as in uncompensated systems. This is due to the fact that two different situation arise in this type of systems, depending on whether the load is positioned at the feed end or the far end of the transformer. Both position of the load have been considered.
It is noteworthy that, irrespective of the position of the load it is always the length of the cable between the load and the nearest connection of the return conductor to the rail (cable within train section), which is the subject to the most severe induction. The maximum possible length of such cable is 1 mile, since the BTs are spaced at 2 miles apart and the return conductor is connected to the rail at every mid point between two transformers (Figure 5.2). The induction outside the train section at the feed end is independent of the load position and so is the induction outside at the far end[75].

In the calculations of this and next chapter, it has been assumed that the currents in the rails remain confided to the rails (no flow to earth). This assumption is valid since in normal operation the magnetising current of the BT is very small and can be neglected. In short circuit conditions, however, as well be seen later, magnetising current is very important factor of consideration and cannot be ignored. In both normal load and s/c calculations the impedance of the transformer has to be taken into account. If this impedance is to be included, then it's value per km is to be added to the impedance values per km of the conductors, to which the windings of these transformers are connected.

It is some times convenient if two or more conductors, which are in effect s/c by zero impedance, are bundled together. This also has the advantage of reducing the number of conductors to be dealt with.

Using standard method of bundling, the conductors from RR, RF and FF matrices may be bundled as shown below.

Bundling of conductors from RR, RF, FF matrices:

RR, RF, and FF matrices are considered as;

$$RR = \begin{array}{c} \begin{matrix} R_1 & R_2 & R_T & R_{CAB} \end{matrix} \\ \begin{pmatrix} Z_{11} & Z_{12} & Z_{13} & Z_{14} \\ Z_{21} & Z_{22} & Z_{23} & Z_{24} \\ Z_{31} & Z_{32} & Z_{33} & Z_{34} \\ Z_{41} & Z_{42} & Z_{43} & Z_{44} \end{pmatrix} \end{array} \begin{matrix} R_1 \\ R_2 \\ R_T \\ R_{CAB} \end{matrix} \quad \text{-------(5.19)}$$

R_1 & R_2 = rails

R_T = return conductor

R_{CAB} = cable

$$RF = \begin{array}{c} \begin{matrix} CW & F \end{matrix} \\ \begin{pmatrix} Z_{15} & Z_{16} \\ Z_{25} & Z_{26} \\ Z_{35} & Z_{36} \\ Z_{45} & Z_{46} \end{pmatrix} \end{array} \begin{matrix} R_1 \\ R_2 \\ R_T \\ R_{CAB} \end{matrix} \quad \text{------(5.20)}$$

CW = contact wire

F = feeder wire

$$FF = \begin{array}{c} \begin{matrix} CW & F \end{matrix} \\ \begin{pmatrix} Z_{55} & Z_{56} \\ Z_{65} & Z_{66} \end{pmatrix} \end{array} \begin{matrix} CW \\ F \end{matrix} \quad \text{--------(5.21)}$$

Combing the above matrices (5.19-5.21) to form one large symmetrical matrix (M_T) as:

$$M_T = \begin{bmatrix} (RR) & (RF) \\ (RF^T) & (FF) \end{bmatrix} = \begin{pmatrix} Z_{11} & Z_{12} & Z_{13} & Z_{14} & Z_{15} & Z_{16} \\ Z_{21} & Z_{22} & Z_{23} & Z_{24} & Z_{25} & Z_{26} \\ Z_{31} & Z_{32} & Z_{33} & Z_{34} & Z_{35} & Z_{36} \\ Z_{41} & Z_{42} & Z_{43} & Z_{44} & Z_{45} & Z_{46} \\ Z_{51} & Z_{52} & Z_{53} & Z_{54} & Z_{55} & Z_{56} \\ Z_{61} & Z_{62} & Z_{63} & Z_{64} & Z_{65} & Z_{66} \end{pmatrix} \text{--------(5.22)}$$

where, M_T = total of matrices (RR, RF, & FF)

Hence any two conductors can easily be bundled at a time, using standard method.

5.6 One-track case

5.6.1 Load at the feed-end of the BT

Consider Figure 5.12[47], the calculations are carried out for the two current-carrying zones as shown below;

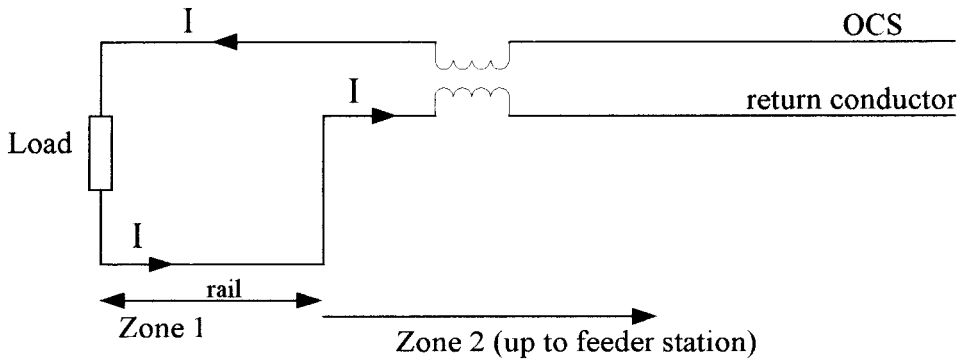

Figure 5.12: One-track case for load at the feed end of the BT

It may be noted that only the current-carrying conductors are shown in each zone.

From the computed self and mutual impedance of all conductors using their co-ordinates, the matrices of the RR, RF, FF are formed in the same manner as uncompensated system. For

easiness of the calculation the cable CAB is considered to be one of the return conductors, hence as are all other conductors, it is to be included in the RR and RF matrices.

R_1 & R_2 in the RR matrix can be bundled together and represented by a single conductor R. similarly contact wire and feeder wires in FF matrix can be bundled together and represented by a single conductor OCS. The resulting matrix is;

$$M_T = \begin{pmatrix} Z_{77} & Z_{73} & Z_{78} & Z_{74} \\ Z_{37} & Z'_{33} & Z_{38} & Z'_{34} \\ Z_{87} & Z_{83} & Z_{88} & Z_{84} \\ Z_{47} & Z'_{43} & Z_{48} & Z'_{44} \end{pmatrix} \text{--------(5.23)}$$

5.6.1.1 Zone 1 calculation

Here the return conductor carries no current; hence it is eliminated from the total matrix (5.23), giving the resulting matrix as;

$$M'_T = \begin{pmatrix} Z'_{77} & Z'_{78} & Z'_{74} \\ Z'_{87} & Z'_{88} & Z'_{84} \\ Z'_{47} & Z'_{48} & Z''_{44} \end{pmatrix} \text{-------(5.24)}$$

For a current I in the OCS, the rail current =-I (opposite direction of the OCS current, the function of the BT)

From the matrix above, the mutual impedance between the cable and OCS = Z'_{48} and the mutual impedance between cable and rails = Z'_{74}

Hence the total voltage induced in the cable

$$e_{CAB} = -I \cdot Z'_{48} + I \cdot Z'_{74}$$

$$e_{CAB} = I(Z'_{74} - Z'_{48}) \quad \text{---------(5.25) (V/km)}$$

For the current in OCS I =1

The total voltage in the cable is:

$$e_{CAB} = Z'_{74} - Z'_{48} \quad \text{------(5.26) (V/km)}$$

5.6.1.2 Zone 2 calculations

The rails in this case carries no current, hence R is eliminated from the total matrix (5.23) above, giving:

$$M_T'' = \begin{pmatrix} Z_{33}'' & Z_{38}' & Z_{34}'' \\ Z_{83}' & Z_{88}'' & Z_{48}'' \\ Z_{43}'' & Z_{48}'' & Z_{44}''' \end{pmatrix} \text{--------(5.27)}$$

If the current in return conductor =-I

and mutual impedance between cable and OCS = Z_{48}''

and mutual impedance between cable and return conductor = Z_{34}''

The total voltage in the cable;

$$e_{CAB} = I(Z_{34}'' - Z_{48}'')$$

$$I = 1 \qquad \text{--------(5.28) (V/km)}$$

$$e_{CAB} = Z_{34}'' - Z_{48}''$$

5.6.2 Calculations for load at the far-end of the BT

Referring to Figure 5.13[47], the calculation are carried out for two current carrying zones;

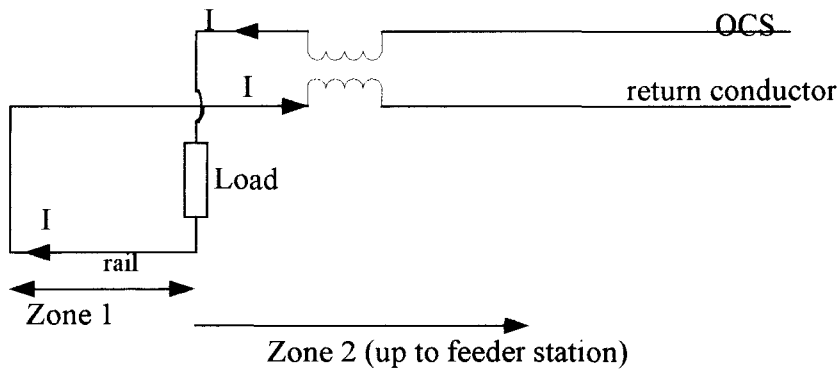

Figure 5.13: One-track case, load at the far end of the BT

5.6.2.1 Zone 1

OCS current =0, hence when it is eliminated form the total matrix (5.23) the following is obtained;

$$M_T''' = \begin{pmatrix} Z_{77}'' & Z_{77}' & Z_{74}'' \\ Z_{73}' & Z_{33}''' & Z_{34}''' \\ Z_{74}'' & Z_{34}''' & Z_{44}''' \end{pmatrix} \text{-------(5.29)}$$

For the current in rails =I

The current in return conductor =-I

The mutual impedance between cable and rail $= Z_{74}''$

The mutual impedance between cable and return conductor = Z_{34}'''

Hence total voltage is:

$$e_{CAB} = I(Z_{34}''' - Z_{74}'') \text{-------(5.30) (V/km)}$$
$$e_{CAB} = Z_{34}''' - Z_{74}''$$

5.6.2.2 Zone 2

The calculations and results are the same as in the case of load at the feed end of the transformer.

5.7 Two track case

5.7.1 Load at the feed end of the BT

There are three zones in this case and are as shown in Figure 5.14[47] below;

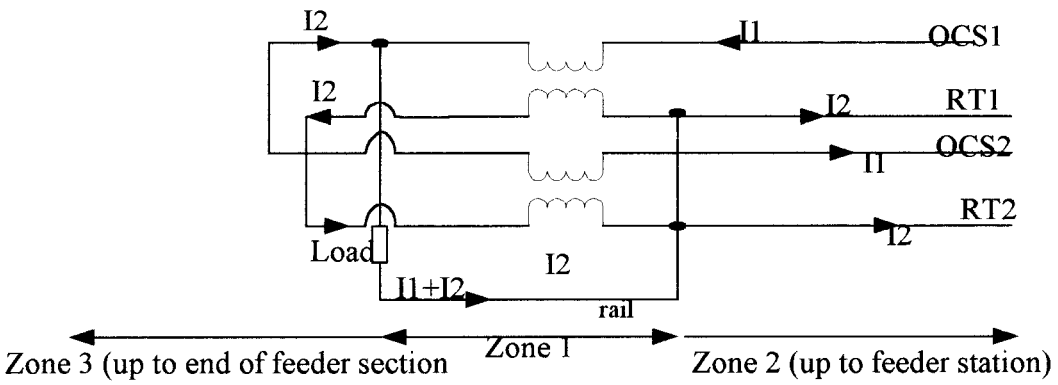

Figure 5.14: Two-track case, load at the feed end of the BT.

Note: only current carrying conductors are shown in the above figure.

The RR, FF, RF can be composed from the computed self and mutual impedance from chapter (2),

$$RR = \begin{array}{c} \begin{matrix} R_1 & R_2 & R_3 & R_4 & R_{T1} & R_{T2} & R_{CAB} \end{matrix} \\ \begin{pmatrix} Z_{11} & Z_{12} & Z_{13} & Z_{14} & Z_{15} & Z_{16} & Z_{17} \\ Z_{21} & Z_{22} & Z_{23} & Z_{24} & Z_{25} & Z_{26} & Z_{27} \\ Z_{31} & Z_{32} & Z_{33} & Z_{34} & Z_{35} & Z_{36} & Z_{37} \\ Z_{41} & Z_{42} & Z_{43} & Z_{44} & Z_{45} & Z_{46} & Z_{47} \\ Z_{51} & Z_{52} & Z_{53} & Z_{54} & Z_{55} & Z_{56} & Z_{57} \\ Z_{61} & Z_{62} & Z_{63} & Z_{64} & Z_{65} & Z_{66} & Z_{67} \\ Z_{71} & Zz_{72} & Z_{73} & Z_{74} & Z_{75} & Z_{76} & Z_{77} \end{pmatrix} \end{array} \begin{matrix} R_1 \\ R_2 \\ R_3 \\ R_4 \\ R_{T1} \\ R_{T2} \\ R_{CAB} \end{matrix} \quad \text{---------(5.31)}$$

RR matrix consists of the return conductors impedance.

$$RF = \begin{pmatrix} Z_{18} & Z_{19} & Z_{1,10} & Z_{1,11} \\ Z_{28} & Z_{29} & Z_{2,10} & Z_{2,11} \\ Z_{38} & Z_{39} & Z_{3,10} & Z_{3,11} \\ Z_{48} & Z_{49} & Z_{4,10} & Z_{4,11} \\ Z_{58} & Z_{59} & Z_{5,10} & Z_{5,11} \\ Z_{68} & Z_{69} & Z_{6,10} & Z_{6,11} \\ Z_{78} & Z_{79} & Z_{7,10} & Z_{7,11} \end{pmatrix} \text{--------(5.32)}$$

RF matrix consists of feed against return conductors impedance.

$$FF = \begin{pmatrix} Z_{88} & Z_{89} & Z_{8,10} & Z_{8,11} \\ Z_{98} & Z_{99} & Z_{9,10} & Z_{9,11} \\ Z_{10,8} & Z_{10,9} & Z_{10,10} & Z_{10,11} \\ Z_{11,8} & Z_{11,9} & Z_{11,10} & Z_{11,11} \end{pmatrix} \text{--------(5.33)}$$

FF matrix consists of feed conductor impedance.

Form the above the following conductors are bundled;

1. R_1, R_2, R_3 & R_4 to make R (conductor no.12)
2. CW_1 & F_1 to make (OCS_1) (conductor no.13)
3. CW_2 & F_2 CW2 (OCS_2)(conductor no.14)

The new matrices are;

$$RR' = \begin{matrix} \\ \begin{pmatrix} Z_{12,12} & Z_{12,5} & Z_{12,6} & Z_{12,7} \\ Z_{5,12} & Z'_{55} & Z'_{56} & Z'_{57} \\ Z_{6,12} & Z'_{65} & Z'_{66} & Z'_{67} \\ Z_{7,12} & Z'_{75} & Z'_{76} & Z'_{77} \end{pmatrix} \end{matrix} \begin{matrix} R \\ R_{T1} \\ R_{T2} \\ R_{CAB} \end{matrix} \text{-------(5.34)}$$

The new matrix RR` consists of the bundled return conductor impedance.

Where, Z_{12} = The results of the bundled rail conductors R_1, R_2, R_3 & R_4

Z' = The new value as a result of bundling

$$RF' = \begin{pmatrix} Z_{12,13} & Z_{12,14} \\ Z_{5,13} & Z_{5,14} \\ Z_{6,13} & Z_{6,14} \\ Z_{7,13} & Z_{7,14} \end{pmatrix} \text{-------(5.35)}$$

The new RF` matrix consist of the bundled feed against return conductors impedance.

Where, Z_{13} = The result of the bundled feed conductors CW_1 & F_1

$$FF' = \begin{pmatrix} Z_{13,13} & Z_{13,14} \\ Z_{14,13} & Z_{14,14} \end{pmatrix} \text{-------(5.36)}$$

The new FF` matrix consists of the bundled feed conductors impedance.

Where, Z_{13} = The result of the bundled feed conductors CW_1 & F_1

Z_{14} = The result of the bundled feed conductors CW_2 & F_2

The total new matrix (combining 5.34-5.36) is:

$$M_T''' = \begin{pmatrix} Z_{12,12} & Z_{12,5} & Z_{12,6} & Z_{12,13} & Z_{12,14} & Z_{12,7} \\ Z_{5,12} & Z'_{55} & Z'_{56} & Z_{5,13} & Z_{5,14} & Z'_{57} \\ Z_{6,12} & Z'_{65} & Z'_{66} & Z_{6,13} & Z_{6,14} & Z'_{67} \\ Z_{13,12} & Z_{13,5} & Z_{13,6} & Z_{13,13} & Z_{13,14} & Z_{13,7} \\ Z_{14,12} & Z_{14,5} & Z_{14,6} & Z_{14,13} & Z_{14,14} & Z_{14,7} \\ Z_{7,12} & Z'_{75} & Z'_{76} & Z_{7,13} & Z_{7,14} & Z'_{77} \end{pmatrix} \text{------(5.37)}$$

5.7.1.1 Calculations for zone 1

mutual impedance between cable and $OCS_1 = Z_{7,13}$

" " " $OCS_1 = Z_{7,14}$

" " " $R_{T1} = Z'_{75}$

" " " $R_{T1} = Z'_{76}$

" " " rails = $Z_{7,12}$

Current I_1 and I_2 in OCS may be assumed to be equal, $I_1 = I_2 = I/2$ (I = total current).

Hence the current in R_{T1} = I/2,

The current in R_{T2} = -I/2,

And the current in the rails = -I.

The total induced voltage in the cable;

$$e_{CAB} = -\frac{I}{2}\cdot Z_{7,13} - \frac{I}{2}\cdot Z_{7,14} + \frac{I}{2}\cdot Z'_{75} + \frac{I}{2}\cdot Z'_{76} + I\cdot Z_{7,12}$$

or ------(5.38) (V/km)

$$e_{CAB} = \frac{I}{2}(2Z_{7,12} + Z'_{76} + Z'_{75} - Z_{7,13} - Z_{7,14})$$

5.7.1.2 Calculation for zone 2

In this case the rails carry no current, hence eliminating the 1st row and column from the above matrix (5.37) gives;

$$M''_T = \begin{pmatrix} Z''_{55} & Z''_{56} & Z'_{5,13} & Z'_{5,14} & Z''_{57} \\ Z''_{65} & Z''_{66} & Z'_{6,13} & Z'_{6,14} & Z''_{67} \\ Z'_{13,5} & Z'_{13,6} & Z'_{13,13} & Z'_{13,14} & Z'_{13,7} \\ Z'_{14,5} & Z'_{14,6} & Z'_{14,13} & Z'_{14,14} & Z'_{14,7} \\ Z''_{75} & Z''_{76} & Z'_{7,13} & Z'_{7,14} & Z''_{77} \end{pmatrix} \text{--------(5.39)}$$

Z' & Z'' are the new values resulting from eliminating the rail (first raw & column) from the matrix in (5.37).

Mutual impedance between cable and $OCS_1 = Z'_{7,13}$

" " " $OCS_2 = Z'_{7,14}$

" " " $R_{T1} = Z''_{75}$

" " " $R_{T2} = Z''_{76}$

Current I_1 and I_2 in OCS may be assumed to be equal, $I_1 = I_2 = I/2$ (I = total current)

Hence the current in R_{T1} = I/2,

The current in R_{T2} = -I/2,

And the current in the rails = -I.

The total induced voltage in the cable;

$$e_{CAB} = -\frac{I}{2}\cdot Z'_{7,13} - \frac{I}{2}\cdot Z'_{7,14} - \frac{I}{2}\cdot Z''_{75} + \frac{I}{2}\cdot Z''_{76}$$

or -------(5.40) (V/km)

$$e_{CAB} = \frac{I}{2}(2Z''_{76} + Z''_{75} + Z'_{75} - Z'_{7,13} - Z'_{7,14})$$

5.7.1.3 Calculations for zone 3

In this case the rails do not carry any current therefore the same matrix for zone 2 calculations has been used.

Hence the total induced voltage in the cable;

$$e_{CAB} = \frac{I}{2}\cdot Z'_{7,13} - \frac{I}{2}\cdot Z'_{7,14} - \frac{I}{2}\cdot Z''_{75} + \frac{I}{2}\cdot Z''_{76}$$

or ---------(5.41) (V/km)

$$e_{CAB} = \frac{I}{2}(Z'_{7,13} - Z'_{7,14} - Z''_{75} + Z''_{76})$$

5.7.2 Calculations for load at the far end of the BT

Again there are three zones in this case as shown in Figure 5.15[47] below.

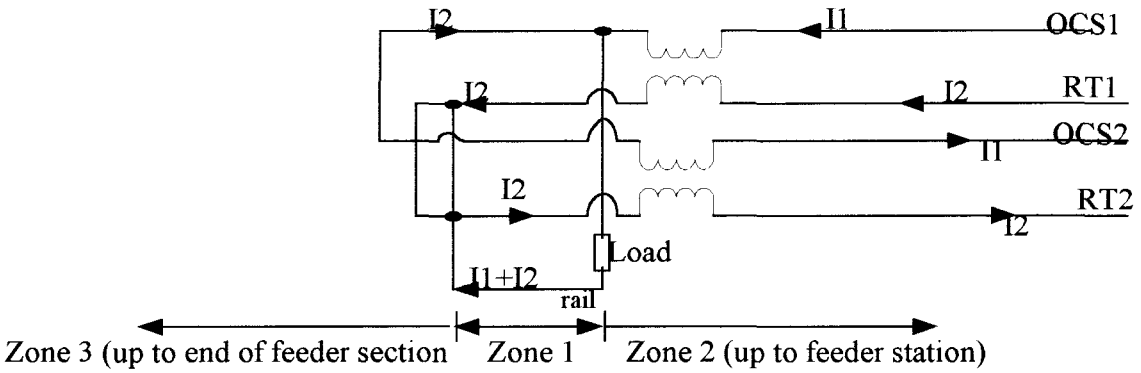

Figure 5.15: Two-track case, load at the far end of the BT

5.7.2.1 Zone 1

The mutual impedance are obtained from the original matrix (5.37) for;

Cable & OCS_1 $= Z_{7,13}$

CAB & OCS_2 $= Z_{7,14}$

CAB & R_{T1} $= Z'_{75}$

CAB & R_{T2} $= Z'_{76}$

CAB & rail $= Z_{7,12}$

The total induced voltage is;

$$e_{CAB} = \frac{I}{2}\cdot Z_{7,13} - \frac{I}{2}\cdot Z_{7,14} + \frac{I}{2}\cdot Z'_{75} + \frac{I}{2}\cdot Z'_{76} - I\cdot Z_{7,12}$$

or --------(5.42) (V/km)

$$e_{CAB} = \frac{I}{2}(Z_{7,13} - Z_{7,14} + Z'_{75} + Z'_{76} - 2Z_{7,12})$$

5.7.2.2 Zone 2

Calculations are the same as for load at the feed-end.

5.7.2.3 Zone 3

The same also follows as for load at the feed-end.

5.7.3 Results

It is only within a train section (between load and the nearest mid-point rail to return conductor connection) that the rails carry current. Rails being much closer to the cable induce a much higher voltage, which pre-dominates the induction from the other conductors.
The current in the rails, reverses in direction as the load moves from one position to another, i.e. from the feed-end to the far-end side of the transformer and vice versa. Therefore, the resultant voltages have opposite signs in the two load positions.

Outside the section, the induction is much lower than inside, this is because the rails do not carry current and the induction due to OCS is to a great extent cancelled by the induction from the return conductors, the two induction's being opposite in direction.

The induction outside a train section on the feed-end side of the transformer, are same for both load positions. Similarly the induction outside on the far end side of the transformer are independent of the side of the transformer on which the load is. Results obtained are shown in tables 5.1 and 5.2 below.

	Induced voltage (V)		
Outside induction	Two track	One track	
		CNS	COS
At feed end of BT	-0.00057+0.00373i	-0.00097+0.00867i	-0.00122-0.00935i
At far end of BT	0.00011+0.0073i		

Table 5.1: Induced voltage outside for load at either end: feed-end of the transformer

	Induced voltage (V)		
Outside induction	Two track	One track	
		CNS	COS
At feed end of BT	0.00038+0.05073i	-0.00191+0.07109i	-0.00167-0.07004i
At far end of BT	-0.00255-0.04291i	0.00251-0.06763i	0.00226-0.08565i

Table 5.2: Induced voltage inside, when load is at: feed-end and far-end of the transformer

5.8 One-rail Return systems

Calculations in this case can be carried out using the same approach as for two-track system described above, provided that the rails, which do not carry traction current, are eliminated from the relevant matrices. The remaining rails, which do carry the traction current, may then be bundled together to from a single conductor, which carries the total rail current.

In order to consider the effects of broken rails, such rails are to be eliminated and all the current carrying rails can be bundled together. Results obtained are shown in tables 5.3-5.6.

5.8.1 Results

Eliminated rails	Induced voltage (V)		
	Two track	One track	
		CNS	COS
R_1	0.00289+0.04883i	0.00539+0.0203i	0.0045+0.05461i
R_2	0.00477+0.03311i	0.0071+0.05489i	0.0059+0.01656i
R_3	0.00415+0.01264i		
R_4	0.00391+0.02195i		
R_1 & R_3	0.00455+0.01012i		
R_2 & R_4	0.00357+0.02343i		

Table 5.3: Induced voltages inside when load at the feed end of the BT

Eliminated rails	Induced voltage (V)		
	Two track	One track	
		CNS	COS
R_1	-0.0042-0.04244i	-0.00402-0.01511i	-0.00202-0.07064i
R_2	-0.00608-0.02614i	-0.00225-0.05008i	-0.00438-0.03127i
R_3	-0.00535-0.0079i		
R_4	-0.00516-0.01551i		
R_1& R_3	-0.00554-0.0018i		
R_2 & R_4	-0.00451-0.01382i		

Table 5.4: Induced voltages inside when load at the far end of the BT

Eliminated rails	Induced voltage (V)		
	Two track	One track	
		CNS	COS
R_1	-0.00056+0.00374i	-0.00097+0.00868i	-0.00122-0.00935i
R_2	-0.00057+0.00375i	-0.00097+0.00867i	-0.00121-0.00936i
R_3	-0.00056+0.00375i		
R_4	-0.00056+00375i		
R_1 & R_3	-0.00056+0.00374i		
R_2 & R_4	-0.00056+0.00375i		

Table 5.5: Induced voltages outside at the feed end with load at either end

Eliminated rails	Induced voltage (V)		
	Two track	One track	
		CNS	COS
R_1	0.00014+0.00728i		
R_2	0.00012+0.00728i		
R_3	0.00013+0.00729i		
R_4	0.00013+0.00728i		
R_1 & R_3	0.00013+0.00728i		
R_2 & R_4	-0.00012+0.00729i		

Table 5.6: Induced voltages outside at the far end with load at either end

The above results are for one rail return systems and broken rail situations.

For one track case

Within a train section (between load and mid point rail connection to the return conductor) induced voltages are still higher than those outside.

The level of induction is considerably reduced if the rail nearer to the cable is eliminated. This holds true irrespective of whether the load is at the feed-end or far-end of the BT

There is no induction outside a train section at the far end because there are no current carrying conductors in this zone. Outside a train section at the feed end, the results are unaffected and remain the same as in a two rail return system, since the rails do not carry any current irrespective of which rail is eliminated.

For two-track case

Within a train section, the results follow the same trend as in a one-track case. If one of the rails were to be broken, the induced voltage is highest when the rail farthest from the cable is eliminated. Since R_3 is nearest to the cable, followed in succession by R_4, R_2 and R_1, the induced voltage increases in progression from a minimum value when R_3 is eliminated, to a maximum when R_1 is eliminated. This is true irrespective of whether the load is at the feed-end or far end. However the corresponding values are higher when the load is at the feed end position.

In a one rail return system, either rails R_2 and R4 or rails R_1 and R_3, will carry the traction return current. In the first case, rails R_1 and R_3 will have to be eliminated and in the second case rails R_2 and R_4.

Induced voltage with R_2 and R_3 eliminated is considerably less than that with R_2 and R_4 eliminated, this is true for both load positions. However as seen in the case of a broken rail situation, the corresponding values are higher when the load is at the feed end than those when it is at the far end.

As in one track case, the induced voltage outside a train section is the same irrespective of whether it is a two rail or a one rail return system, or a broken rail situation, because the rails outside a train section do not carry any current. However, on contrast to a one-track case, in a two-track case there is induction on the feed end as well as the far end. This is because the OCS and return conductors overhead have currents flowing in them. The level of induction is greater outside at the far end than at the feed end.

5.9 Summary

The induced voltage in compensated systems (with BTs) under normal operation conditions for one and two track layouts have been calculated in this chapter. For two-rail return system, the highest induction occur within a train section (train in-section), since the rails carry current in this section. The direction of the rail current changes as the load moves from one position to another (feed-end to the far-end side of the BT and vice versa), hence the voltage have different sign for the two load positions. For outside section (out-section of the train) induction is much lower than that of in-section (no current in the rail). Induction for out-section is the same for the both load positions.

One-rail return systems, the highest induction is the same as two-rail. There is no induction in the out-section of the train for load at the far-end of the booster transformers, while for the load at the feed-end the results are the same as for two-rail systems. The level of induced voltage is at its highest when the rail farthest from the cable is eliminated. It can be concluded that induction in compensated systems under normal operation conditions is dependent on the position of the load with respect to the booster transformer. Calculations under short circuit fault conditions are discussed in the following chapter (6).

CHAPTER (6)

Induced Voltage in Compensated Systems: Short Circuit Condition

Introduction

The effect of the inducing current in a booster transformer with return conductor is divided into three parts[47]:

1. A compensated component, in which equal and opposite currents flow in the catenary and return conductor between the supply transformer and the load.
2. An uncompensated component due to the magnetising current in the BT, which flows in the catenary between the same points and returns via rails and earth.
3. An uncompensated component due to current which flows in the catenary or return conductor between the load point and the nearest mid-point strap and returns via rails and earth.

In normal conditions, the magnetising current effect is small and can be neglected, whereas for short circuit conditions, the magnetising current is of such importance that, from a first approximation, the compensated component can be neglected. In short circuit conditions therefore, a booster transformer does not give perfect results because the magnetising current of the BT returns via the running rails and earth. This gives rise to problems because of the rather severe interference in the nearby conductor under BT saturation conditions, when the magnetising current becomes very high. Thus knowledge of the magnetising current taken by BT with heavy load is essential for a pre-determination of the effect of short circuit[76].

To a certain extent, the magnetising components will depend on the type, make and rating of the transformer. The transformer used by BR is an oil-immersed current transformer, with 1:1 ratio. The current ratings of the BR are shown below (BR, B. spec AC 7/4, 1972)[63]

Continuous current (A)	peak current
100	500
150	600
200	600
300	600

The continuos' rating is the rms current, which the transformer can withstand continuously. The peak current rating is the maximum rms current that the transformer can withstand for a time of 15 minutes.

The primary side of the transformer is insulated for 44 kV, 50 Hz and the secondary side for 3.3 kV (encountered under fault condition), thus meeting the requirements of BS 233[63].

The overhead system is designed for spark-less current collection at all speeds, but under abnormal conditions a degree of sparking may occur and the equipment should be capable of withstanding the resultant transient effect. Finally the transformer should be capable of operating throughout the temperature range -25°C to 55°C in a polluted atmosphere.

From the current transformer theory, the main components are the magnetising and leakage impedance. The magnetising impedance appears due to the core properties of the transformer.

Consider the ideal transformer with no load connected across the secondary as shown in Figure 5.5. If a voltage is applied at the primary side, a current known as the exciting current flows in the circuit. Part of this current form the magnetising current, which produces magnetic flux in the core. For a load to be connected across the secondary windings, the exciting current will combine with the secondary current to give the total primary current.

The magnetising impedance consists of two components connected in parallel, a resistance R_m and an inductance L_m. The resistance represent the core losses (hystresis and eddy current). The inductance produces magnetic field inside the core that links the primary with the secondary winding. Both components are affected by the frequency. R_m is proportional to frequency while L_m is inversely. If the applied voltage exceeds a certain value the saturation of the transformer starts. This causes a sudden drop in the value of L_m and as a result the exciting current increases considerably depending on the degree of the core saturation.

The windings of the transformer are also not perfect due to the winding resistance and leakance flux. A component of the magnetic flux in the core will always link one winding without linking the other.

Under load conditions therefore the windings develop an electromotive force (emf), which acts in opposition to the applied voltage, producing voltage regulation.

The leakance flux can be represented by impedance Z_1 connected in series with the equivalent circuit of the transformer. This impedance is made up of R_1 and L_1. R_1 represents the winding resistance (dc resistance) and the eddy current losses developed in the windings when the transformer is in operation. L_1 is the opposing emf as mentioned.

In the event of short circuit (s/c) fault on the OHL, a high current several times the value of the normal operating current, will flow in the primary of the BT. this will cause saturation of the BT, its exciting impedance will be reduced suddenly and the BT efficiency will decrease dramatically. The magnetising current is very high and since this returns via the rails and earth only part of the total s/c current flows through the return conductor or in other words, is compensated. The current flowing in the return conductor or through the secondary of the transformer will be the total short circuit current less the magnetising current.
The system under these conditions behaves like a composite system, since it is partly compensated and partly uncompensated.

For the following calculations an s/c current of 6000 A has been assumed for the calculations. A typical value of the magnetising current for this value of s/c current will be 668 A, as given by one of the transformer manufacturer.

6.1 Method of calculations

Consider the circuit shown in Figure 6.1 below[47];

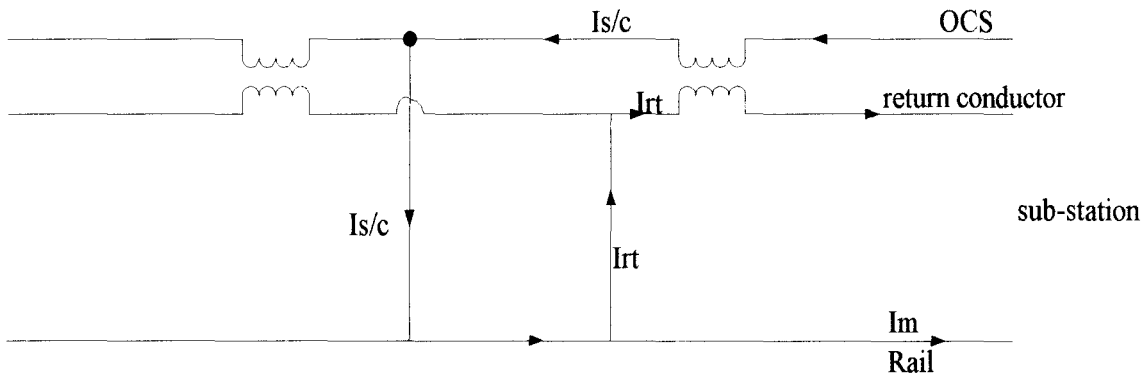

Figure 6.1: Compensated systems (with BT and return conductor) under s/c current

For a short circuit current $I_{s/c}$ = 6000 A and a magnetising current of the transformer I_m = 668 A, the current through the return conductor is obtained from the following relation;

$$I_{s/c} = I_m + I_{rt}$$

or --------(6.1)

$$I_{rt} = I_{s/c} - I_m$$

Hence, I_{rt} = 5332 A

Note: I_m reaches the sub-station via the rails and earth.

For simplicity, the above circuit is divided into two components;

(a) Compensated

(b) Uncompensated

6.1.1 Compensated components

Compensated components are as shown in Figure 6.2 below[47].

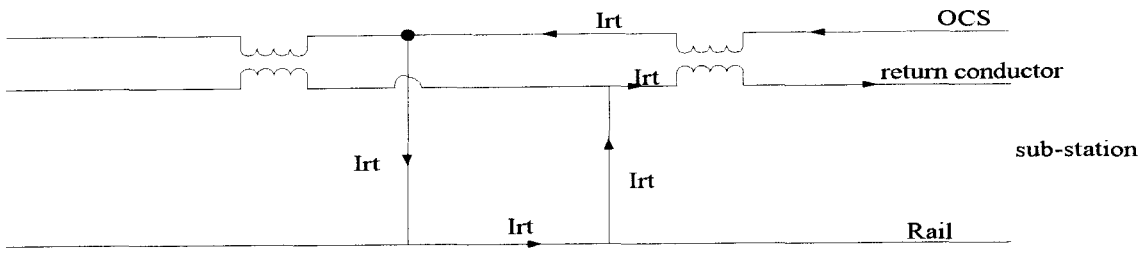

Figure 6.2: Compensated components

6.1.2 Uncompensated component

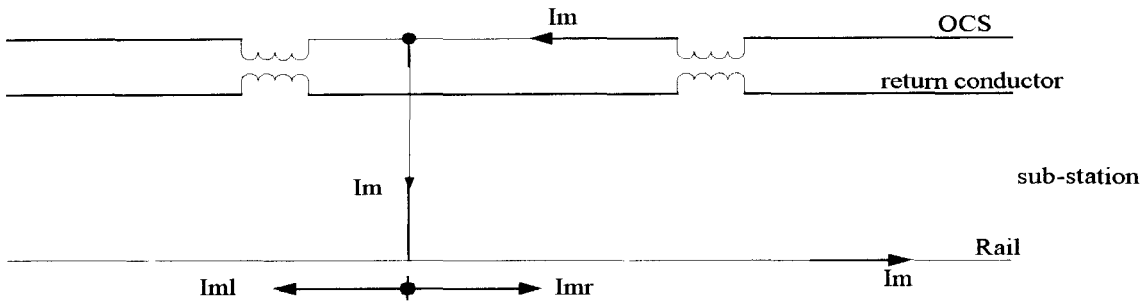

Figure 6.3: Uncompensated components

From the figure (6.3) the magnetising current I_m on entering the rails splits into I_{ml} on the left and I_{mr} on the right. I_{mr} reaches the sub-station via the rails and earth, and so eventually does I_{ml}. On reaching the sub-station, they combine to produce I_m again.

Calculations for compensated component can be carried out using the method described in chapter 5, and those for the uncompensated component by method in chapter 3.
The compensated and compensated may then be summed up to solve for short circuit situation.

6.1.3 Calculation examples

Consider a one-track configuration in an open area with cable on the normal side as shown in figure 2.17 in chapter 2. If the magnetising current is zero, the induced voltage results will be as in section 5.7.5 for two-rail return systems and 5.8.1 for one rail return configuration, which

are already known from the earlier study of compensated systems (chapter (5)). On the other hand if the entire s/c current was to be the magnetising current, then the induced curves of Figures 6.11, 6.12 are nothing but familiar results for an uncompensated systems[47].

If the compensated and magnetising currents are each assumed to constitute 50% of the total fault current, i.e. if compensated current = uncompensated current = 3000A for a fault current of 6000A, then the summation of the compensated and uncompensated will be as in Figures 6.7 and 6.8 and for the fault at the feed end and far end respectively.

For an assumed value of the magnetising current of 668 A, the induced voltage values are as shown in Figures 6.9 and 6.10.

It would appear from Figures 6.4, 6.5, 6.11 and 6.12, that the highest level of induced voltage is obtained either in a fully compensated system or in a fully uncompensated system and not in a composite system.

Using the same approach as in previous chapters and the computer programs that have been developed, the maximum induced voltage when a fault occurs can be calculated for inside and outside exposure for fault at the feed end and far end of the transformer, results obtained are shown in Figures 6.4-6.12.

6.1.4 Results

The results for one track and two tracks are given below. It can be seen that the induced voltage level decreases as the number of tracks increases.

For one-track case: cable on the normal side

The results are the same for faults at both the feed end and far end. The maximum voltage inside exposure is obtained when exposure = 32 km and the system is fully uncompensated. The maximum voltage outside exposure is obtained at 16 km and the system is fully uncompensated.

For cable on the other side: fault at feed end

The maximum voltage inside exposure is obtained when exposure = 32 km and the system is fully uncompensated.

The maximum voltage outside exposure is obtained when exposure = 16 km and the system is fully uncompensated.

For fault at the far end

For inside exposure the results are the same as above.

For outside exposure the maximum induced voltage is obtained at 32 km and the system is fully compensated.

For two-track case: fault at feed end

The maximum voltage inside exposure is obtained at 32 km fully compensated.

For outside exposure it was found at 19 km for a fully uncompensated components.

For fault at the far end

Inside exposure maximum voltage induced was at 32 km fully uncompensated and for the outside exposure was at 32 km for fully compensated components.

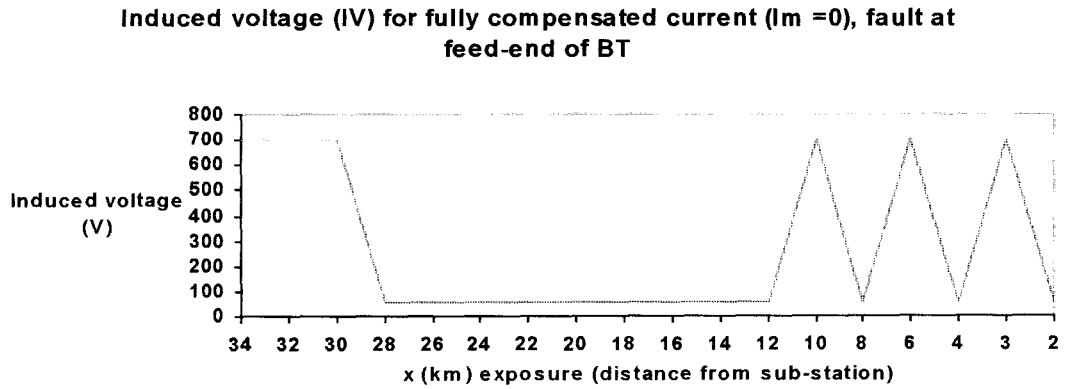

Figure 6.4: Induced voltage fault at feed-end, compensated I =6000A, I_m =0, one-track cable on normal side

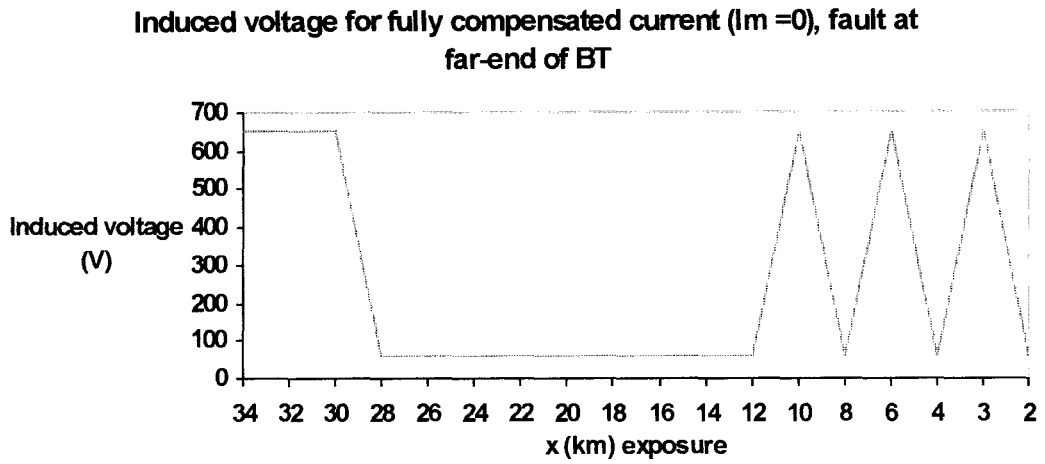

Figure 6.5: Induced voltage fault at far-end, compensated I =6000A, I_m=0, one-track cable on normal side

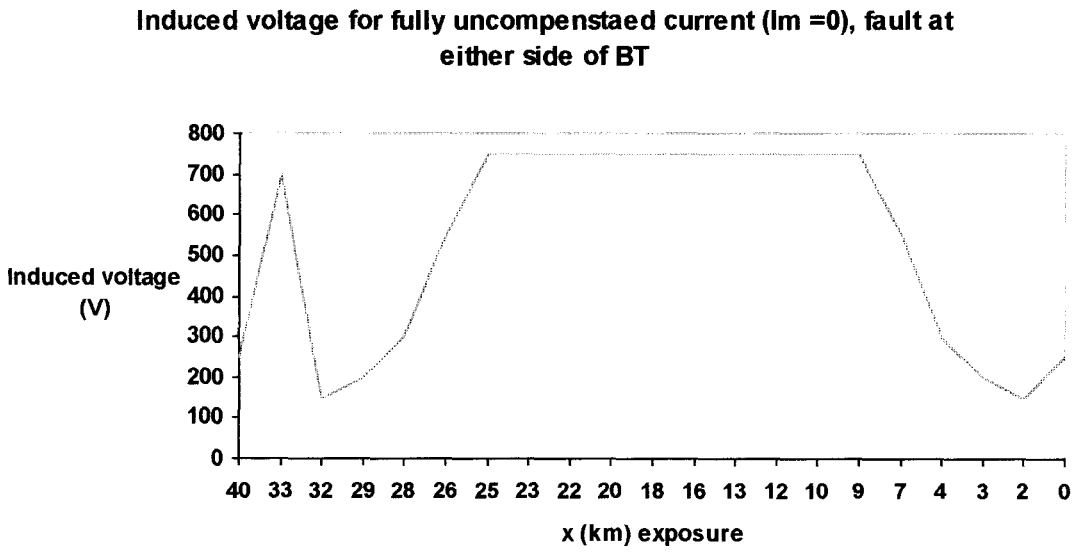

Figure 6.6: Induced voltage fault at either side, compensated I =0, I_m=6000A, one track cable on normal side

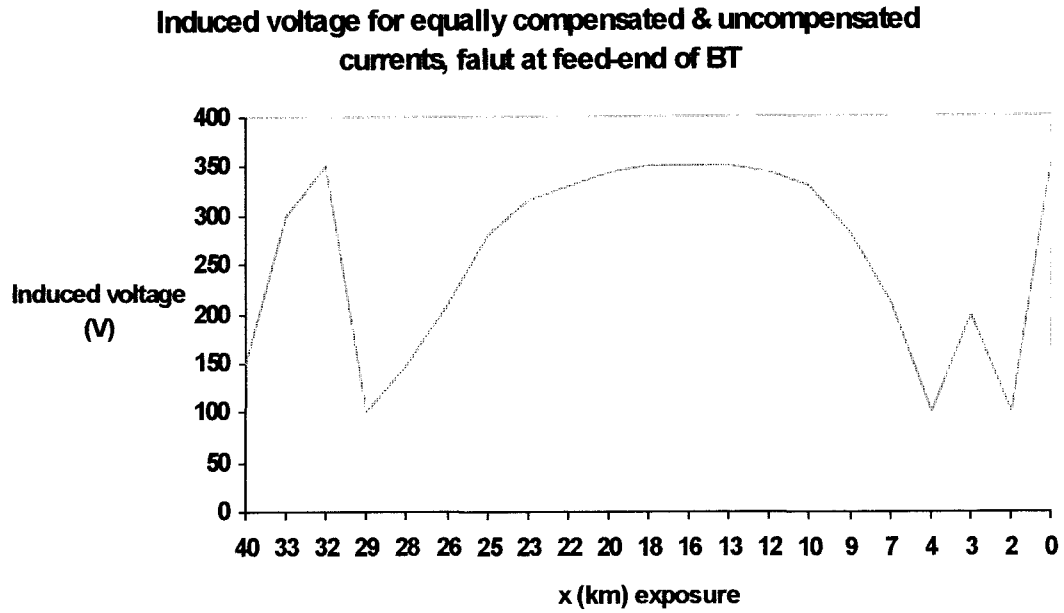

Figure 6.7: Induced voltage for fault at feed-end compensated I =3000A, I_m =3000A, one-track cable on normal side

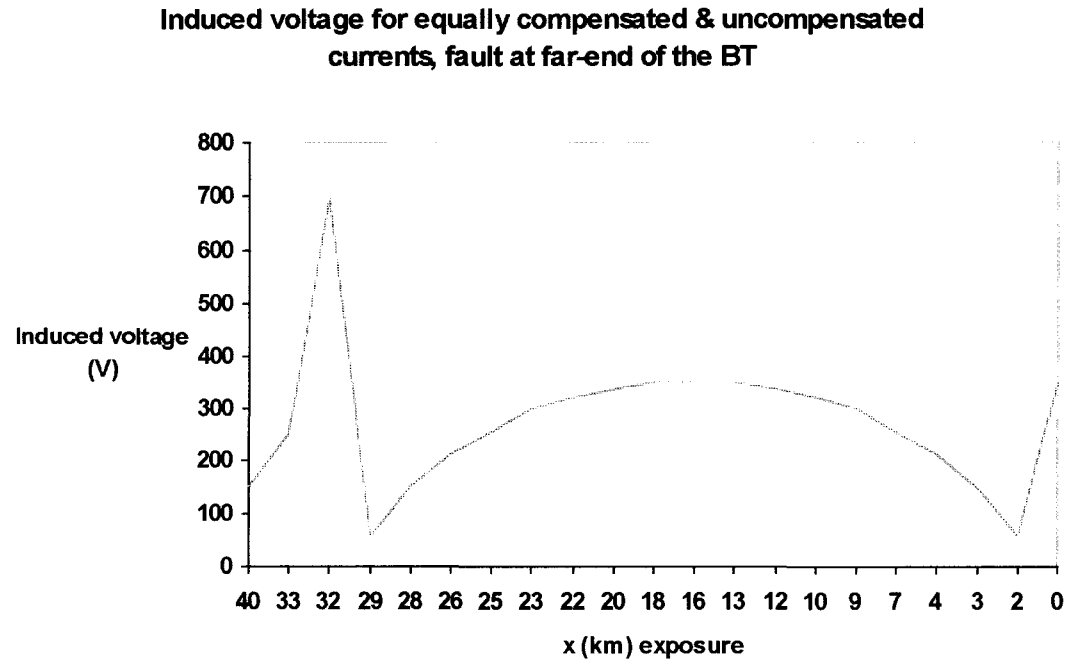

Figure 6.8: Induced voltage for fault at far-end compensated I =3000A, I_m =3000A, one track cable on normal side

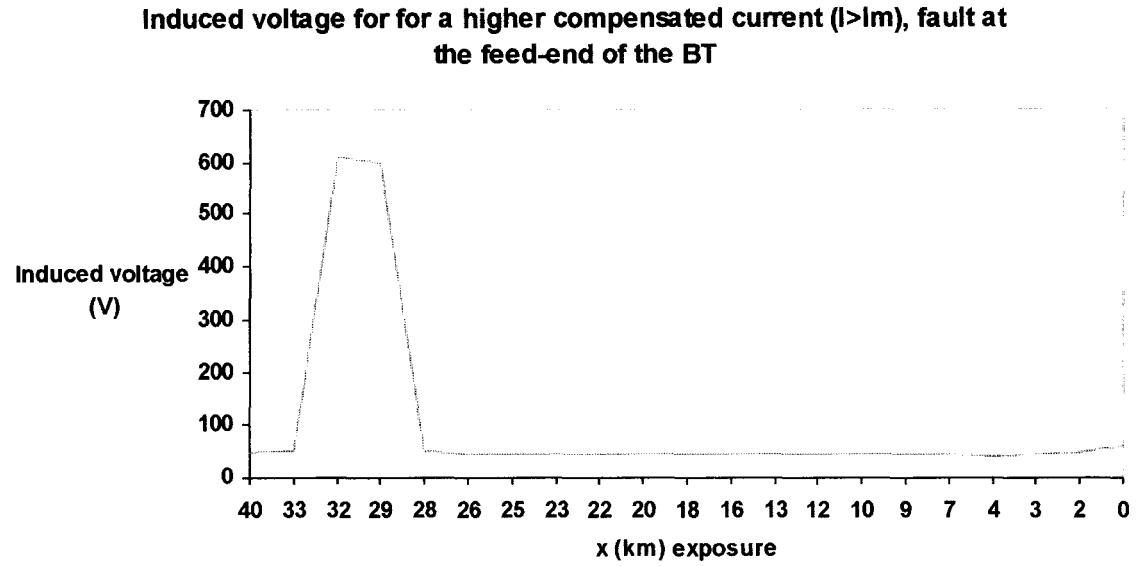

Figure 6.9: Induced voltage for fault at feed-end compensated I =5332A, I_m =668A, one track cable on normal side

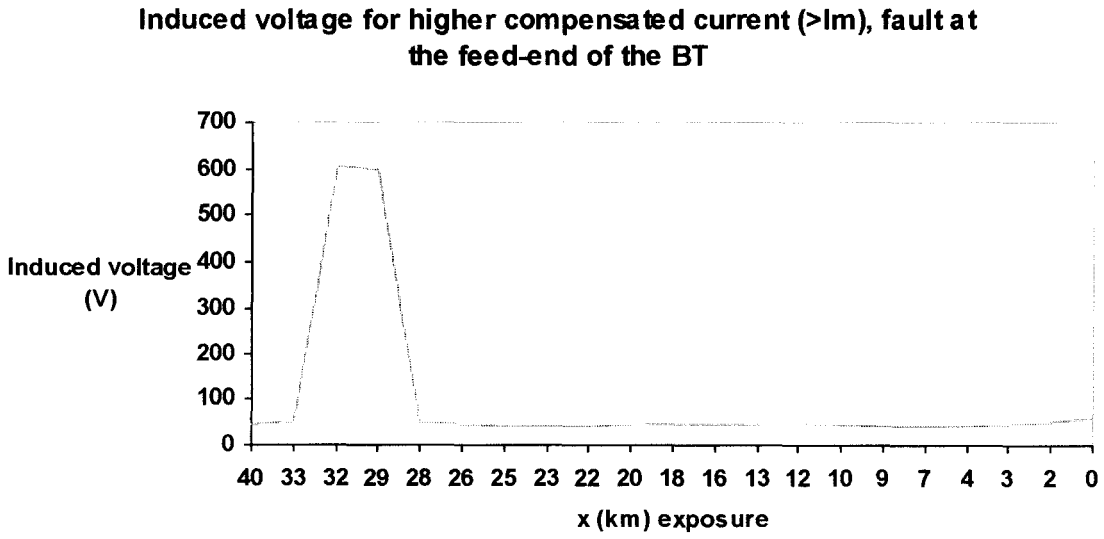

Figure 6.10: Induced voltage for fault at feed-end compensated I =5332A, I_m =668A, one-track cable on normal side

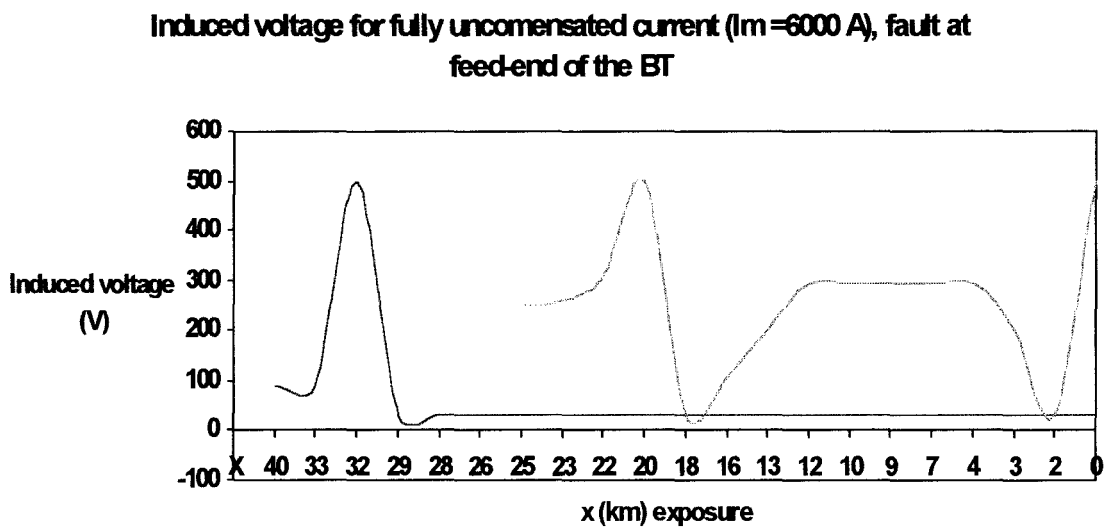

Figure 6.11: Induced voltage for fault at feed-end two-track for both inside exposure (compensated I =6000, I_m =0), and outside exposure (compensated I =0, I_m = 6000A)

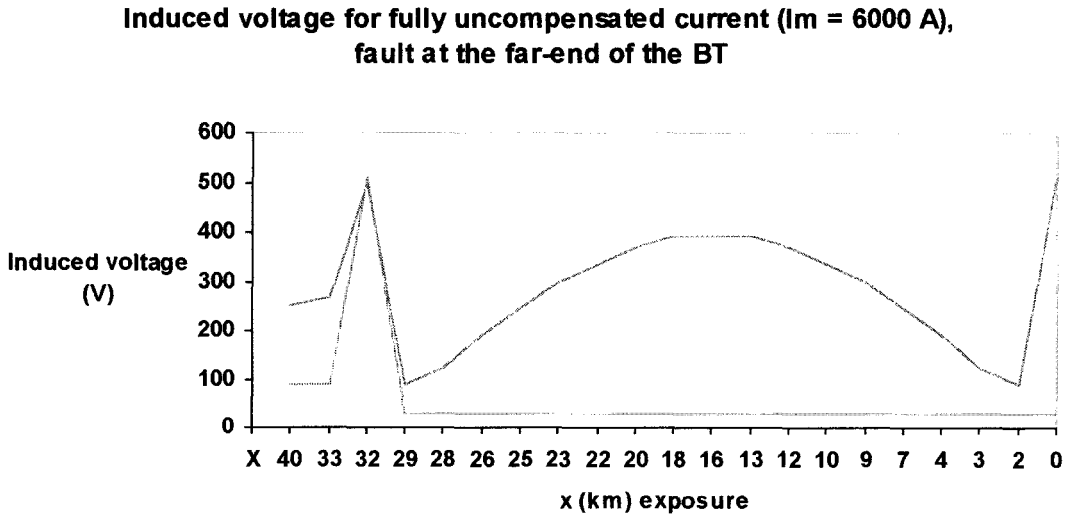

Figure 6.12: Induced voltage for fault at far-end, two-track, for inside exposure (I= 6000A, I_m =0), and outside exposure (I=0, I_m =6000A)

6.2 One rail return systems under short circuit condition

This follows the same method as for two rail return system. The rails that carry traction return current are bundled together to form a single conductor, which carries the total rail current. In one-rail systems some rails would not carry any current and these must be eliminated.

To consider a broken rail effect, they have to be eliminated, and all current carrying conductors are the bumbled.

6.2.1 Results

For one-track case: cable on normal side

The highest value of the induced voltage is the same irrespective of which rail is eliminated. This value is lower than the maximum value in a two rail return system.

The worst case always corresponds to a totally uncompensated system, i.e. when the entire fault is magnetising current Figures 6.13-6.15.

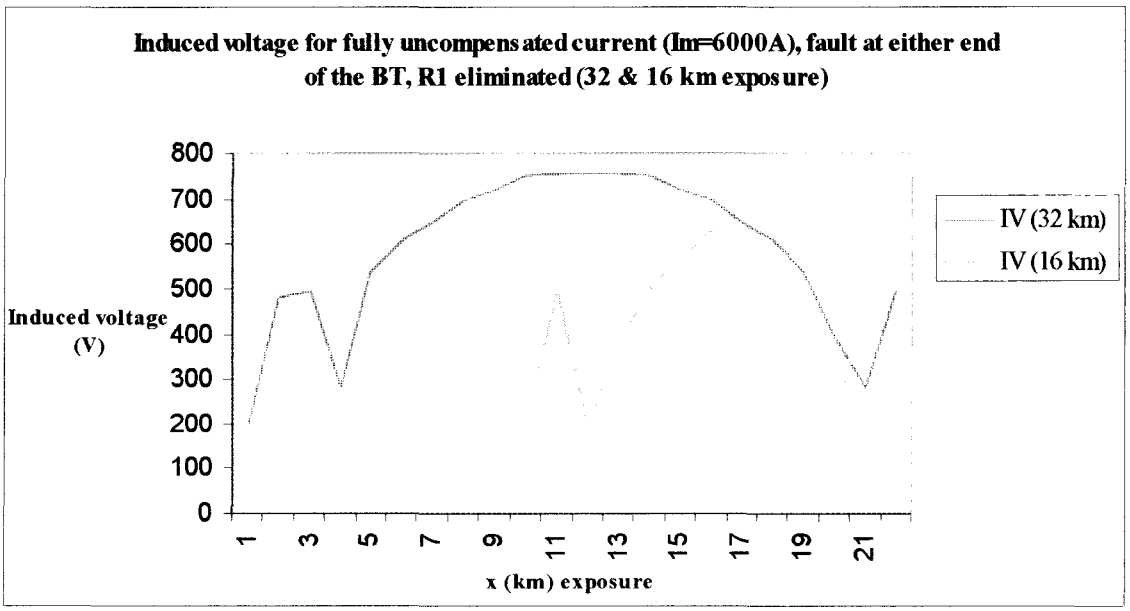

Figure 6.13: induced voltage fault at either end, compensated I =0, I_m = 6000A, one track, cable on normal side R_1 eliminated

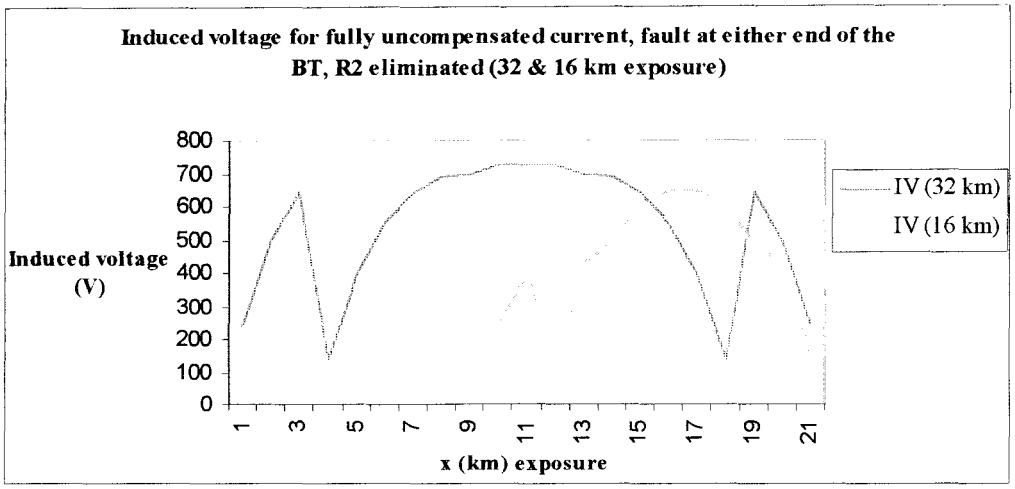

Figure 6.14: Induced voltage fault at either end, compensated I =0, I_m = 6000A, one track cable on normal side, R_2 eliminated

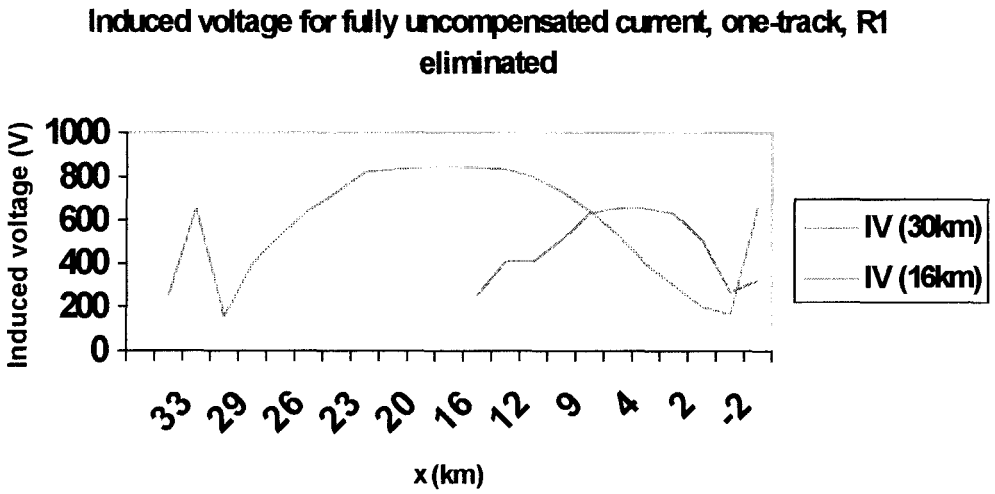

Figure 6.15: Induced voltage fault at feed-end, compensated I =0, I_m =6000A, one track, cable on the other side, R_1 eliminated

For cable on the other side

Highest of induced voltage is the same as above. This value is lower than the maximum value in the case of two rail return systems.

The highest induced voltage is always obtained in a totally uncompensated system with the exception of one case.

This occurs in the event of a fault at the far end and on elimination of rail R1, when the maximum induced voltage outside exposure will be obtained if the system was totally compensated, Figure (6.16).

For two-track case

With any rails (except R_1) eliminated the highest induced voltage is the same irrespective of the fault (feed or far) with R_1 eliminated the curve for maximum induced voltage within the exposure for fault at the feed end is different from that at the far end.

The highest induced voltage is obtained when R_1 is eliminated (which is lower than the maximum induced voltage in two rail return), Figures 6.13, 6.16.

The highest induced voltage when R_1 and R_3 (Figure 6.18) are eliminated is greater than that when R_2 and R_4 (Figure 6.19) are eliminated (lower than that obtained when R_1 is eliminated).

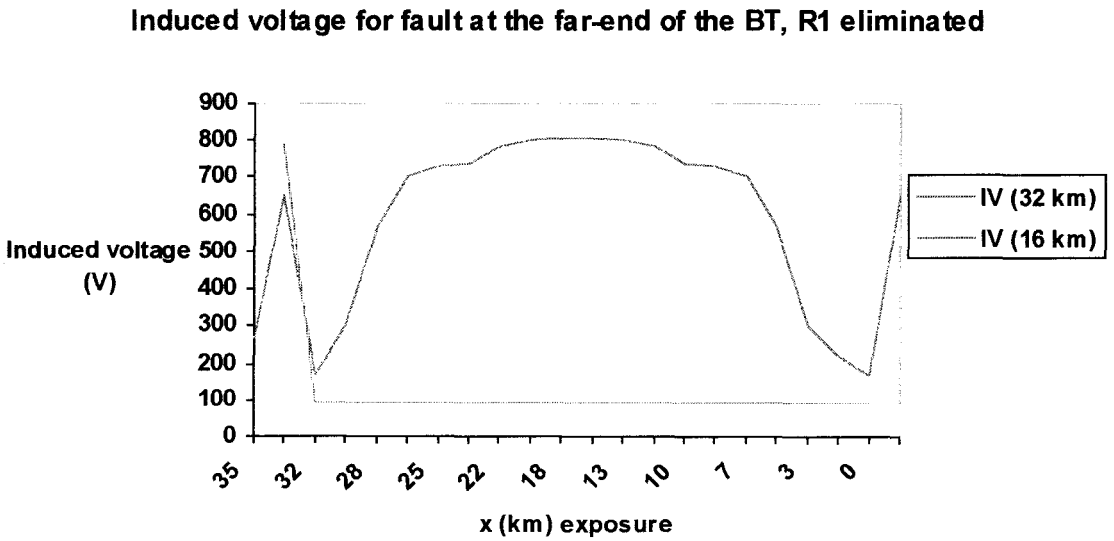

Figure 6.16: Induced voltage fault at far-end, one track, cable on the other side, R_1 eliminated

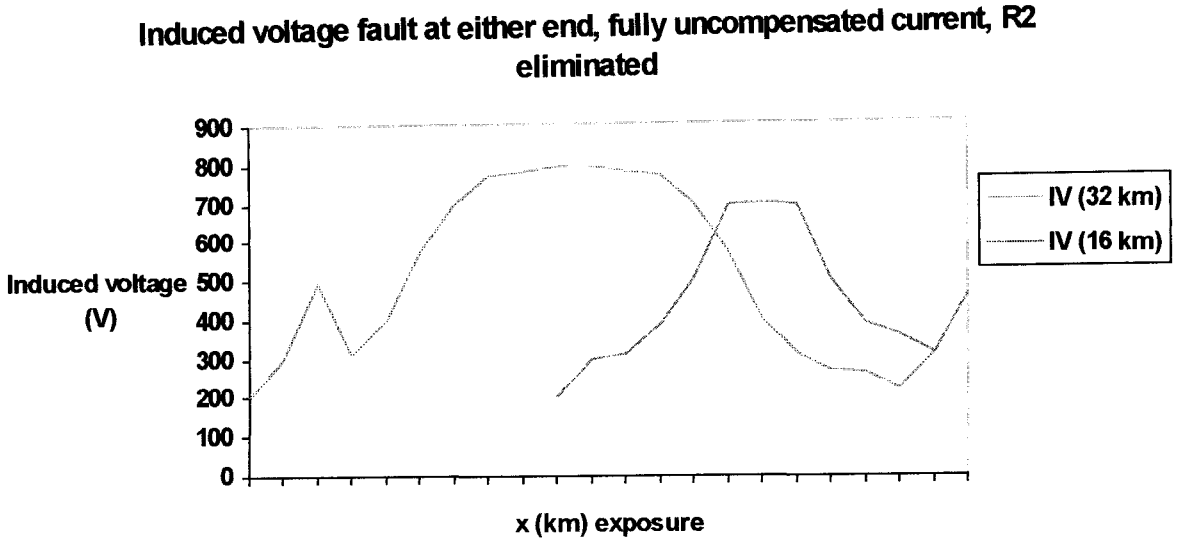

Figure 6.17: Induced voltage for fault at either end, I=0, I_m =6000A, one track, cable on the other side, R_2 eliminated

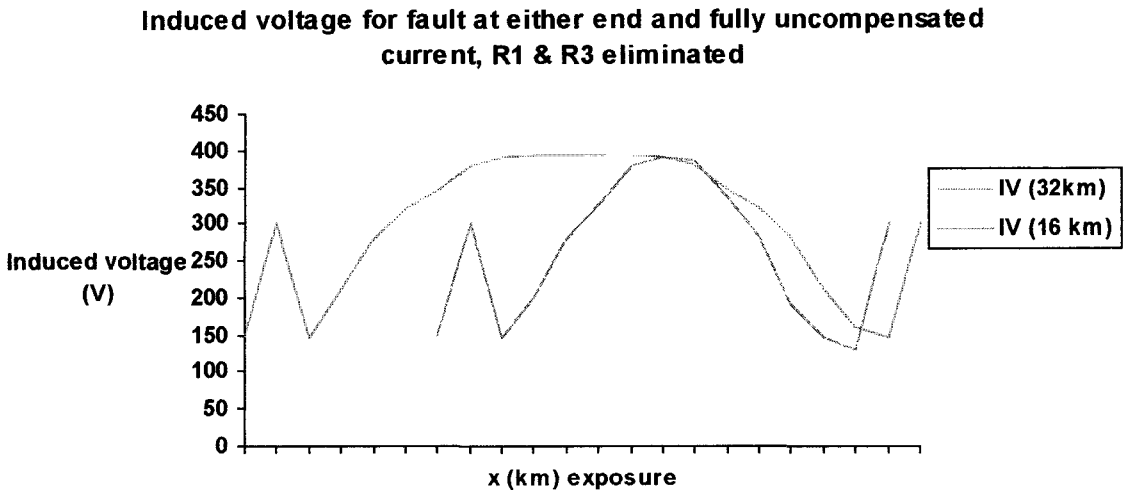

Figure 6.18: Induced voltage for fault at either end, I compensated = 0, I_m =6000A, two track, R_1 & R_3 eliminated

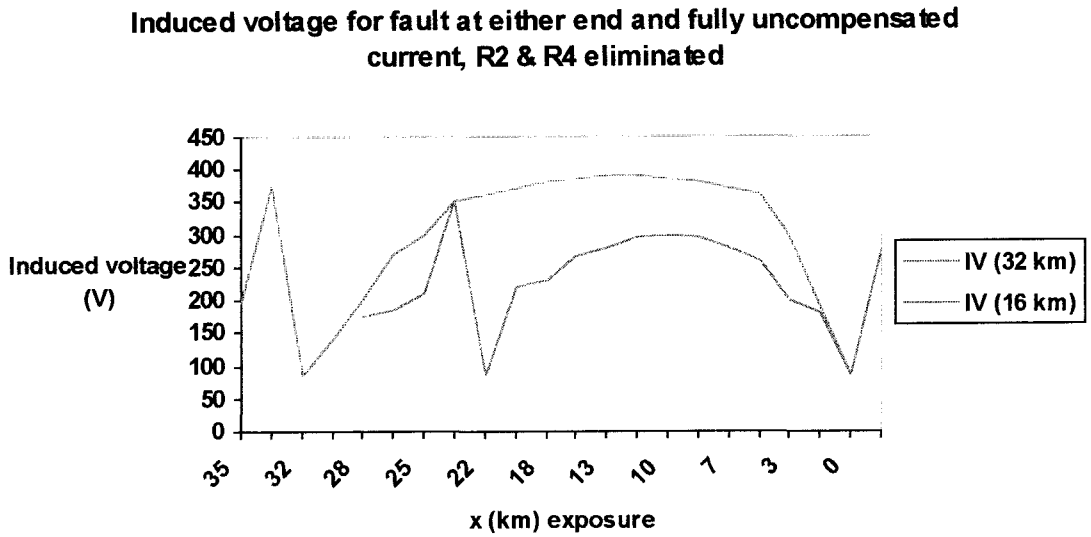

Figure 6.19: Induced voltage for fault at either end, I compensated = 0, I_m =6000A, two track, R_2 & R_4 eliminated

6.3 Validation of the FDTD Method

The method used in this thesis is a mathematical modelling technique based on the finite different time domain method. The main objectives of the project is to provide a reliable, easy to implement and cost effective approach for the calculations of the rail-track and overhead line impedance and hence better results and analysis of the induced voltage. This have been achieved and the FDTD provides comparable results to the finite element method and the well known Carson's correction method for the calculations of the impedances.

It is noteworthy that calculation of frequency-dependent impedance is important not only in power engineering, but also in other areas involving high frequency applications like communications and semiconductor microchip design. In fact, as the frequency increases to several GHz (10 9 Hz), a small segment of the conductor in a microchip behaves just like a 100-km-long power transmission line working at 60 Hz. Consequently, the methods for calculating power line frequency-dependent impedance are also applicable to the analysis of electromagnetic interference in printed circuit boards and integrated circuits.

To validate the FDTD method, calculations are carried out for the induced voltage in uncompensated and compensated systems under normal operation conditions for one-rail and two-rail return systems using the standard analytical approach (Carson's correction term). The results obtained are shown in Figures 6.20, 6.21 and Tables 6.1, 6.2 below.

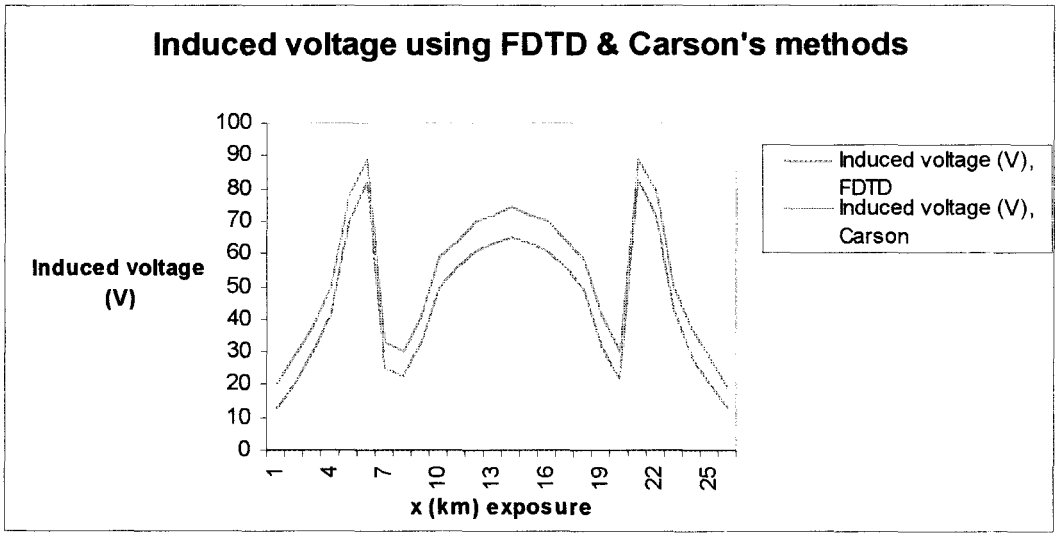

Figure 6.20: Induced voltage for two-rail return system in an open area (uncompensated, 1250 Amps ratings, 30 km exposure) using Carson's & FDTD methods

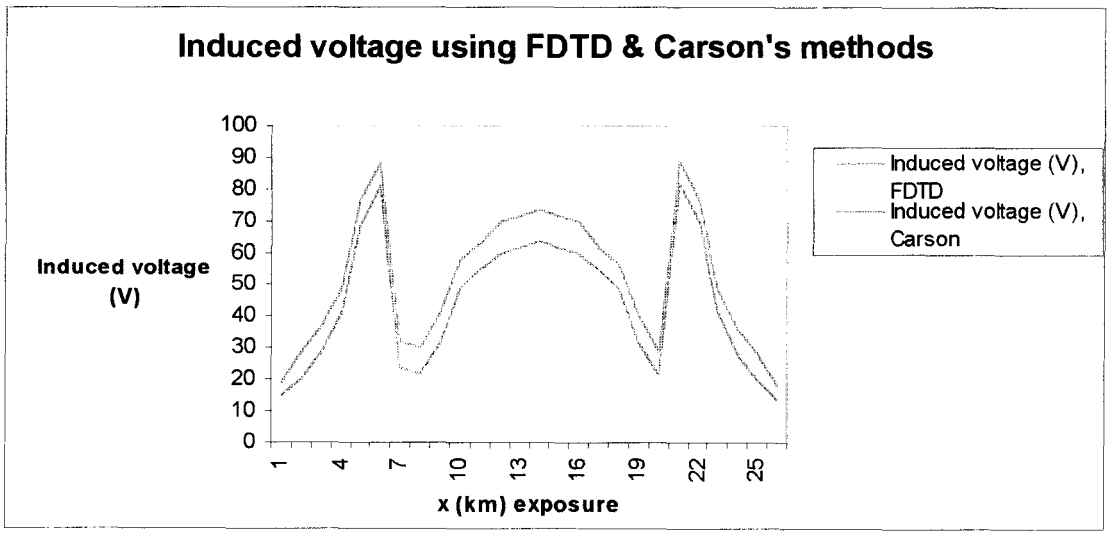

Figure 6.21: Induced voltage for one-rail return system in an open area (uncompensated,1250 A, 30 km exposure) using Carson's and FDTD methods

	Induced voltage (V)	
Outside induction	Two-track (FDTD)	Two-track (Carson)
At feed end of BT	0.00038+0.05073i	0.00062+0.0067i
At far end of BT	-0.00255-0.04291i	-0.00534-0.0063i

Table 6.1: Induced voltage inside for load at either end for two-rail return system (compensated, 1250 A) using Carson & FDTD methods

Eliminated rails	Induced voltage (V)	
	Two-track (FDTD)	Two-track (Carson)
R_1	0.00289+0.04883i	0.00539+0.0393i
R_2	0.00477+0.03311i	0.0071+0.05489i

Table 6.2: Induced voltages inside when load at the feed-end of the BT, for one-rail return system using Carson & FDTD methods

Comparison have also been made between the rail, earth and return current of the compensated systems obtained in (section 5.1.4) with published data[23], the results obtained are as follows:

Current	FDTD method	CAD method[23]
Earth current	10 (A)	16 (A)
Rail current	220 (A)	195 (A)
Return current	210 (A)	200 (A)

Table 6.3: Currents in the rails, earth and return conductor using FDTD & CAD method

It is always desirable to obtain measurements, however due to the complexity of the railway system this was not possible. Hence comparison can be achieved from published work, which in this case is slightly difficult since many of the publications deals with telecommunication (screened) cables rather than the unscreened signalling cables.

Models for induced voltage calculations for unscreened signalling cables were obtained and published for the first time by Gupta[47]. His work, however, uses Carson's method for impedance calculations. For the work in this thesis impedances were calculated by FDTD method. The shape of the induced voltage curves in this thesis are identical to those obtained by Gupta. Since the results obtained by two different approaches are identical it can be established that FDTD is a valid method. Moreover, it has been already shown that the method is more accurate than Carson's method. FDTD method has a wide scope for novel applications in EMC analysis in railway systems.

6.4 Summary

The induced voltages have been calculated for compensated systems under short circuit conditions. Two different track layouts have been investigated as well as the position of the cable. The results obtained showed that the induced voltage depends very much on the position of the fault where it is at the feed end or far end of the booster transformer. Results obtained here are based on the assumption that the short circuit current is 6000A. A different fault current can be tried easily by replacing the fault current in the program.

CHAPTER (7)

Conclusion

The aim of this project was to develop a mathematical tool for studying the interference problem caused due to the ac-single-phase, 25 kV, 50 Hz systems into line-side signalling systems. Knowing the magnitude of this induction is essential in understanding the behaviour of the systems to provide protection measures accordingly. Due to the complexity and the many components involved for such a system it has been difficult to provide a complete and reliable analysis of the longitudinal induced voltage. In particular, the primary objective has been to develop a mathematical model based on the finite difference time domain to provide reliable calculations of the self and mutual impedance of the conductors used, namely the rail track conductor (return) and feed conductor (overhead line).

Until recently, these parameters have been analysed using Carson's[21] correction term developed over seventy years ago. The method provides the only analytical calculation that includes the earth return effect and has been proved to be very reliable for calculations at the low frequency range (e.g. load flow studies, voltage drop, etc.). However, at a higher frequency range, >10kHz (section 2.2.1), the method converges very quickly with a high calculation error due to the assumption that the earth is semi-infinite.

For this reason it was very important to find an alternative approach especially for electromagnetic compatibility. The development in computer system speed has prompted engineers to find an alternative approach; mathematical modelling techniques. Another reason for the popularity of mathematical modelling is that it is not always possible to obtain results from direct measurement techniques. This is due the interaction problems that arise from the

complexity of the system as well as the measurement environment, which is impossible to control in a busy system like the railways. Therefore it is reasonable to obtain results via an alternative approach that enables us to represent the system and its parameters as accurate as possible. This cannot be achieved using the analytical approach.
Many researchers provided improvements in Carson's method and obtained better results for these calculations. One such a modification is Gray's[34] method, known as the complex return system, in which the skin depth effect is added to Carson's impedance method. This method received little attention because it was merely experimental and no mathematical proof was given. Wait[34] tested the method and obtained good results for frequencies higher than 10 kHz. Hill and Carpenter[23] on the other hand, took advantage of the development in mathematical modelling techniques and provided analysis for the rail track impedances using finite element method. The FEM is an electromagnetic method that is based on solving Maxwell's equations and from the stored energy results given; the impedance of the rail track can be extracted. The results obtained using this method have provided great accuracy and showed that Carson's method overestimates the values of the impedances. FEM has proved to be very reliable and takes into account the material properties of the conductor and its physical shape. However, it is a too complex procedure, requires long time simulation and introduces added cost in the form of the software and the training required to use the system.

An alternative approach, which has the same or close enough reliability as the FEM but requires less training and software cost, is now needed. This has been achieved in this project by using finite difference time domain method. The method is a direct solution of Maxwell's equations, hence it is easy to implement and understand. Furthermore, since it is a time domain method it covers a wide rang of frequencies with one simulation. The rail tack and overhead line impedance has been calculated using existing software therefore cost is greatly reduced. The software has built-in FDTD facilities and enables program writing according to required specifications. From Maxwell' equations the electric and magnetic field are solved for the required boundary conditions and the impedance of the conductor was extracted using Ampere's law.

The self and mutual impedance results were almost exactly the same as those obtained by FEM and Carson's up to 10 kHz, and the same as the FEM at frequencies >10 kHz (section 2.2.3).

Although the results obtained were very comparable to that published by other researchers, great care should be taken when applying the boundary conditions as incorrect application can result in great errors and increased simulation time. It is hoped that this can be overcome by trial and error through experience.

As mentioned before, the main objective was to find the level of induced voltage into signalling systems. The induced voltage was calculated for both compensated and uncompensated systems under normal and short circuit conditions for the two different track layouts and overhead rating. The position of the cable was also investigated.

7.1 Uncompensated systems

Analysis for this system was carried out for inside and outside exposure (also known as in-section and out-section). For long exposure where the outer section effect can be considered as negligible, the induced voltage was found to be maximal at the centre of the exposure (Figure 3.3). The voltage level starts to decrease towards the load or the sub-station until the induction from the feed conductors is greater than that of the return conductors. The voltage level rises again when the induction from the return conductors exceeds that from the feed one. In the case of short exposure, where the outer section effect can not be neglected, the return conductor induction is more dominant and the shape of the induced voltage is the reversed of that obtained for the long exposure (see Figure 3.7). For both cases the curve is symmetrical about the centre of exposure.

For outside exposure, the induced voltage is always maximal at the load or the sub-station but decreases later. The induction from the return conductor is more dominant in this case.
For fault condition when there is contact between the cable and the conductor, the induction is minimum at the centre with maximum values at the load or sub-station (Figure 4.2).
The induced voltage depends on many different effects, the maximum voltage induced for uncompensated systems was found to be 67 V rms. The induced voltage level depends on the position of the exposure (inside or outside), making its level maximal at the centre for outside exposure and minimal for inside exposure. Under fault conditions, namely touch potential; the induced voltage attained a maximum value at the load and sub-station. The value of the induced voltage varied between 470-500 V rms.

7.2 Compensated systems

For systems compensated with booster transformer connected to a special return conductor, two different situations arise depending on the position of the load. If the load is at the feed end of the transformer, the induced voltage is maximal within the exposure from the load up to the mid point of the rail return conductor connection (Figure 5.4). If the load is at the far end of the transformer, the maximum voltage is outside the exposure from the load to the outside connection (Figure 5.5). For both cases the zone between the load and the mid point connection is the most important, elsewhere induction is very small, hence we can say that the worse induction case occurs at this section.

Induced voltage outside at the sub-station end is zero. For one track at the load end, the voltage induced outside the sub-station is zero, while a small value is found for two track layouts.

Under short circuit conditions, a combination of uncompensated and compensated effect occurs. The compensated situation occurs as a result of the compensated current and the uncompensated situation is due to the magnetising current of the booster transformer.
For better understanding different theoretical considerations have been investigated. If the entire short circuit current is assumed to be the magnetising current, the induced voltage is at its worst level. For other cases, the worst induction is obtained between the load and mid point connection, the entire short circuit is assumed to be compensated.

For compensated systems using booster transformer method connected to a special return conductor, the induced voltage depends on the position of the load (far end or feed end of the transformer). For the load at far end induced voltage is maximum within exposure for the section between the load and the return conductor connection, the level was found to be 57 V rms. For far end load, the maximum voltage is outside the exposure, again from the load but to outside mid-point connection, the level was found to be 56 V rms. The induced voltage outside at the sub-station end is zero as well as at load end in a one-track case this is zero, but has small values in two-track.

For short circuit conditions the effect of the magnetising current of the booster is evident. Two different situations occur, the level of the induced voltage varies depending on the magnetising

current level and the compensated current. If the magnetising current is higher the worst induction occurs. On the other hand if the compensated current is greater the results are the same as above. It is therefore very important when designing the booster transformer that the no load current is made small to avoid any interference.

7.3 Limitations of the method

Higher frequency effect and harmonic studies have not been covered in this thesis, although higher frequency analysis can be done using the same approach by changing the frequency values. Also the analysis carried out mainly deals with unscreened signalling cables, but can be modified for analysing screened telecommunication cables. Due to the size of the model only one and two-track layouts have been considered.

It is always desirable to verify the numerical calculations by experiments. Unfortunately, however, due to the complexity of the systems and because it is not always easy to gain access to the railway lines for measurements, it was not possible to obtain experimental analysis. Nevertheless, the data used in this thesis is a real time data obtained from a Brazilian railway line.

Although not much research has gone into signalling systems, a valid comparison can, arguably, be made between the studies for induction into telecommunication systems that can be found in Kewle[15], Rosen[16], Mellitt[17], and Pickford[33]. It is not an easy task to carry out interference tests in a complex and busy railway network of today, due to the limits imposed on the amount of time available for extermination due to traffic and demands. Some of the results obtained, however, have been compared to similar test carried out in a German railway line and Hong Kong.

7.4 Future work

Although the emphasis of the methods presented in this thesis has been mainly on signalling cables, the work enables methods on similar lines to be devised for telecommunication cables, pipe-line cable etc. Analysis of tunnel and higher track lines can also make an area of future work.

Another area of future work will be the investigation of increasing the voltage level of the booster transformers for high-speed trains using power electronic techniques.
The effect of harmonics on the system behaviour and for compensated and uncompensated system is an area of a whole research in itself. Finally, the application of the method developed in this thesis to an autotransformer compensated systems would also be useful.

7.5 Summary

A mathematical modelling technique method that is different from the conventional standard method of calculating the induced voltage into line-side signalling cables has been developed and examined. The rail track impedance and overhead transmission line parameters have been calculated using finite difference time domain method over a frequency of 50Hz - 1MHz. The self and mutual impedance of the rail-track at system frequency (50 Hz), were, 0.67 and 0.87, respectively. The method used had an accuracy of ±0.5% in the determination of rail track impedance, and ±0.6% for over-head parameters compared to finite element approach and 0.1%-0.2%, compared to Carson standard approach. This in effect provided more accurate results for the calculations of induced voltage. The induced voltage has been calculated for one and two tracks in an open area, and for two different overhead ratings 1250 and 760 Amps. All calculations have been carried out for uncompensated (no Booster) and compensated systems under both normal and short circuit. The results obtained in this thesis provide a more detailed analysis of induced voltage calculations and provide improved calculations compared to the published work in this field.

CHAPTER (8)

References

1. Taflove A, Hagness S C, "Computational Electrodynamics: The Finite Difference Time Domain Method", Artech, London 2000.
2. Sullivan D M, "Electromagnetic Simulation using the FDTD Method", IEEE Press Series on RF and Microwave Technology, IEEE 2000.
3. Roters H C, "Electromagnetic Devices", John Wiley & Son, Inc, New York, 1992.
4. Grivet P, "The Physics of Transmission Lines at High and Very High Frequencies", Academic Press, London, 1991.
5. Perry G, C by Example, Que, 1992.
6. Karmel P R, Cole G D, and Camisa R L, "Introduction to Electromagnetic and Microwave Engineering", John Wiley & Sons, INC, 1998.
7. Magid L M, "Electromagnetic fields, energy and waves" (Wiley, 1968).
8. Yee K S, "Numerical Solution of Initial Boundary Value Problems Involving Maxwell Equations in Isotropic Media", IEEE Transaction on Antennas and Propagation, Vol. AP-14, No.3, May 1966.
9. Kurt L S and John B S, "A Survey of the Finite-Difference Time-Domain Literature", 1999.
10. Wedepohl L M and Efthymiadi A E s, "Wave Propagation in Transmission Lines Over Lossy Ground: A New Complete Field Solution", IEE Proc, Vol.125, No.6 June1978.
11. Galloway R H, Sharrocks W B, and LM Wedepohl, "Calculation of Electrical Parameters for Short and Long Poly-phase Transmission Lines", IEE PROC., Vol. 111, No.12, December 1964.
12. Dover A T, "Electric Traction", 4th Edition, Pitman,1963.
13. Partab H, "Modern Electric Traction", Pritam Surat, New Delhi, 1973.
14. "British Railway Electrification Conference", Publications by IEE, London 1960

15. Klewe H R J, "Interference Between Power Systems & Telecommunication Lines", Edward Arnold, 1958
16. Rosen A, "Interference in Railway Line-Side Telephone Circuits From 25 kV, 50 Hz Traction Systems", Proc.IRSE, 1956.
17. Mellitt B, Allan J, Johnston W B, "Software Modelling for Induced Voltage Calculations In Railways", Conference on Railway Engineering Perth, Sept 1987, pp. 87-11.
18. Mellitt B, Allan J, Shao Z Y, "CAD Techniques for Power Studies and electromagnetic Screening Calculations in AC Railways", Conference Paper 1987, pages: 145-172.
19. Mellitt B, Allan J, Shao Z Y, "Computer-based Methods for Induced-voltage Calculations in AC Railways", IEE Proc., Vol.137, Pt. B, No.1, January 1990.
20. "CCITT Directives Concerning the Protection of Telecommunication Lines against Harmful Effects from Electric Power and Electrified Railway Lines", (CCITT, Geneva, 1989), 9 Vols.
21. Treirney J R and Turner R, "Improvement to booster Transformer Return Conductor Method of Suppressing 50 Hz Interference From AC Electrified Railway Systems", IEE Discussion, AC Traction Interference, London, 1980, Paper No. 1, Railway Engineering Forum Meeting.
22. Carson J R, "Wave Propagation in Overhead wires with Ground Return", Bell System Technical Journal, 1926, 5, pp. 539-556.
23. Pollaczek F, "The Field in an Infinitely Long Conductor Carrying Alternating Current", Elec. 1926, 3, (9), pp. 339-359.
24. Hill R J, Carpenter D C, "Determination of Rail Internal Impedance for Electric Railway Traction System Simulation", IEE Proc-B, Vol.138, No.6, Nov.1991.
25. Buchanan W, "Analysis of Electromagnetic Wave Propagation Using The 3D Finite Difference Time Domain Method With Parallel Processing", PhD Thesis, Napier University, 1996.
26. Paul C R, "Introduction To Electromagnetic Compatibility", Wiley Series In Microwave and Optical Engineering, John Wiley, 1992.
27. Roden J A, Paul C R, Smith W T and Gedney S D, "Finite-Difference Time-Domain Analysis Of Lossy Transmission Lines", IEEE Trans. Electromag. Compat., Vol. 38, No. 1, pp.15-24, 1996.

28. Mur G, "Absorbing Boundary Condition for the Finite-Difference Approximation of the Time-Domain Electromagnetic Field Equations," IEEE Transactions on Electromagnetic Compatibility, pp. 377-382, November 1981.
29. Silvester P P, Ferrari R L, "Finite Elements for Electrical Engineers" (CUP, Cambridge UK, 1983).
30. Ruehli A E, "Circuit Oriented Electromagnetic Solutions in the Time and Frequency Domain", IEICE Trans. Commun., Vol. E80-B, No. 11, Nov. 1997.
31. Nonweiler T R F, "Computational Mathematics: An Introduction to Numerical Approximation", Ellis Horwood Ltd, 1984.
32. Abdulaziz I M and Gupta N K, "FDTD Method in Calculating Induced Voltage in Railways", IJEEE Journal, Submitted.
33. Bickford J P, "Transient in Power Systems: The Calculation of Transmission Line Constants", UMIST, 1983.
34. Alias Q M, "Calculation of Overhead Line Parameters with Particular Reference to Railway Systems", Msc Dissertation, UMIST, 1977.
35. Deri A, Teva G, Semlyen A and Castanheira A, "The Complex Ground Return Plane; A simplified Model for Homogenous and Multi-Layer Earth Return", IEEE Trans. Power Appa. Syst, 1981, 100 (8), pp. 3686-3693.
36. Agrawal A K, Price H J and Gurbaxani S H, "Transient Response of Multi-conductor Transmission Lines Excited by a Non-uniform Electromagnetic Field", IEEE Trans. EMC, Vol. 22, No. 2, pp. 119-129, 1980.
37. Trueblood H M and Waschek G, "Investigation of Rail Impedances", AIEE Trans, 1934, 53, pp. 1771-1780.
38. Butterworth S, Electrical Characteristics of Overhead Lines, Report, 1954.
39. Abdulaziz I M and Gupta N K, Rail Track Impedance Calculations using Carson's FE and FDTD Methods, IEE Proc. Elect. Power Applic., Under Review.
40. Macentee J A, Railway Track as a short Transmission Line, Msc Dissertation, University of Birmingham, 1972.
41. Siemens W A, "Will 50kv Become A World Standard?", Railway Gazette International, April 1978, pages: 201-204.
42. R J Hill and I H Cevik, "On-line Simulation of Voltage Regulation in Autotransformer-Fed AC Electric Railroad Traction Networks", IEEE Trans. Vehicular Technology, Vol.42, No.3, August 1993.

43. Allan J, Mellitt B, Brown J C, Taufiq J A, "A Computer-based Portable Analyser Assessment of Harmonic Effects in AC and DC Railways", Proc. Of International Comprail Conference, Frankfurt, 1987, pp.103-119.

44. Bozkaya H, Shao Z Y, Allan J, Mellitt B, "A Comparison Between Autotransformers and Booster Transformers for AC Traction Supply", Con.Paper, International Electric Railway Systems for A New Century, IEE, London, 1987, pp.114-118.

45. Abdulaziz I M, Gupta N K, Induced Voltage Calculations in Electrified Railways, University Power Engineering Conference (UPEC) Proceedings, University of Wales, Swansea, September 2001.

46. Brunton L J, "Earth-Leakage Problems and Solutions on the Tyne and Wear Metro", IEE PROC., Vol.136, Pt. B, No.3, May1989.

47. Gupta N K, "Inductive Interference into a Line-Side Signalling Cable in AC Electric Railway Systems", PhD Thesis, UMIST, October 1985.

48. Barnes R, Wong K T, "Unbalanced Tunnel Rail", IEE Proc-B, Vol.138, No.2, March1991.

49. Abdulaziz I M, and Gupta N K, Power Supply in Electric Railways, Energize Power Journal, SAIEE, March 2003.

50. Conlon M, Wilcox D and McGrath D, "Transient and Harmonic Induction from Underground Power Circuits into Parallel Communication Services", Proc. International Power Conference, 1984.

51. Shipp D G, "Track Circuit in DC Electrified Areas", Proc.IRSE, 1952, pp.108-134.

52. Mellitt B, "Electromagnetic Compatibility in DC railways Using Power Electronic Control. 'Railway Safety, Control and Automation Towards the 21st Century", IRSE International Conference, London, September 1984.

53. Abdulaziz I M and Gupta N K, Electromagnetic Interference in Electric Railway Systems, International Power Engineering Conference (IPEC) Proceedings, Singapore, May 2001.

54. Tierney J R and Grose B H, "Telecommunication Systems in Relation To 50 Hz AC Electric Traction", IEE Proc., Vol.119, (4), pp.441-455, 1972.

55. Wright A, "Current Transformers", 1st Edition, 1968, Chapman and Hall Ltd, London.

56. Hardman A R, "Interference and its Effects on Track Circuits", Proc. IRSE, 1976-77.

57. Nedelchev N, "Influence of Earth Connection on the Operation of Railway Track Circuits", IEE Proceeding (EPA), Volume 144, No. 3, May 1997

58. Hill RJ, Carpenter DJ, "Rail Track Transmission Line Distributed Impedance and Admittance Theoretical Modelling and Experimental Results", IEEE Trans, Veh. Technology, 1993, 42, (2), pp.225-241.

59. Abdulaziz I M and Gupta N K, "Booster Transformers in Railways", UPEC, University of Staffordshire, UK, September 2002.

60. Littler G E, "Harmonic Performance of an Autotransformer Type High Voltage AC Railway Electrification System", IEE Proc. Elect Energy Conference, pp.85-90, Australia, 1986.

61. Holtz J and Klein H J, "The Propagation of Harmonic Currents Generated by Inverter-Fed Locomotive in the Distributed Overhead Supply System, IEEE Trans. Power Electronics", Vol.4 APR, pp.168-174, 1989.

62. Pettersson G A and Svensson S, "Compensation from Rails, Return Conductor and Booster Transformers of Induction Caused By Electrified Railways, TELE, Pt.2, pp96-128, 1961.

63. Turner D R, "Interference from Power Lines and Traction Circuits", Proc. IRSE, 1953.

64. Efthymiadis A E, "Wave Propagation in Transmission Lines Over Lossy Ground", PhD Thesis, UMIST, 1977.

65. Helmer O, Petterson G A, and Swederborg, "The Induction Effects of Swedish Electrified Railways on Parallel Telecommunication Lines", Tele. English Edition, 1955.

66. Wilcox D J, "Implementation of non-homogenous Theory in Transient Analysis of Cross Bonded Cable Systems", Proc. IEE, Vol. 125, 1978.

67. Klewe H R, "The Interference Problem", Paper 9, BR Electrification Conference, London, 1960.

68. Webb W J, "The Power Supply", Paper 5, BR Electrification Conference, London 1960.

69. Cobbe D W, "Effect on Post Office Circuits", paper 37, BR Electrification Conference, London 1960.

70. Woodbridge A W, "Signalling and Telecommunication", Paper 10, BR Electrification Conference, London 1960.

71. Allen C E, and Goldring A G, "Overhead Equipment: The Catenary System", paper 33, BR Electrification Conference, London 1960.

72. Casson E, "Power Supply: The Railway Load", paper 28, BR Electrification Conference, London 1960.

73. KOSTIS A G, "Booster Transformers in British Rail Traction Systems", Msc Dissertation, UMIST, 1976.

74. Abdulaziz I M and Gupta N K, "Compensated Systems in Electrified Railways and the use of Booster Transformers", SAIEE Proceedings, Under Review.

75. Gergory N and Scott R, "Telecommunication in an AC Environment: Audio Frequency Interference into Line side telecommunication Cable Circuits", Railway Engineering Forum, London, 1980.

76. Woodbridge A W, Klewe H R, and Kapp R O, "Inductive Interference and its Measurement on Electrified Railways", Proc. IRSE, 1962.

77. Abdulaziz I M and Gupta N K, "EMC in Railways", Electronic Journal, SAIEE, In Print.

78. www.trainweb.com

APPENDIX

A

A.1 Data Used (Chapter (2))[47]

A.1.1 Uncompensated systems

Frequency = 60 Hz

Deep soil resistivity = 100000 ohm-m

Near soil resistivity = 3500 ohm-m

Length of cable = 1.5 km

Mutual impedance between cable and buried earth wire = 0.0922+0.99328i

Maximum exposure = 30 km

A.1.1.1 Data for rails

Weight = 130 lb/yard

Height = 0.1524 m

Internal reactance = 0.26 ohm/mile

Perimeter = 25.75 in

Permeability= 275 gauss

Resistivity= 20x10^-6 ohm-cm

DC resistance= 0.0386 ohm/mile

A.1.1.2Buried earth wire

No of strand = 7; 1 in layer 1 and 6 in layer 2

Radius of strand (a) = 1.75 mm

Overall radius of conductor (R) = 6.5 mm

A.1.1.4 Return conductor

No of strands = 23 ; 1 of steel in layer 1

6 of steel in layer 2

16 of aluminium in layer 3

Radius of steel strand (as) = 1.445 mm

Radius of aluminium strand (aa) =1.285 mm

Total radius = 8.15 mm

A.1.1.5 Messenger wire

No of strand 37; 1 in layer 1

6 in layer 2

12 in layer 3

18 in layer 4

Radius of strand = 1.21 mm

Total radius = 8.45 mm

A.1.1.6 Contact wire

N of strands = 1 (solid conductor)

Radius of strand (a) = 6.15 mm

A.1.1.7 Feeder wire

No of strands = 33; 1 of steel in layer 1

6 of steel in layer 2

10 of aluminium in layer 3

16 of aluminium in layer 4

Steel radius = 1.445 mm

Aluminium radius = 1.86 mm

Total radius = 23.5

A.1.1.8 Resistance to earth

Earthing resistance Re = pn/pi*L(Logh(2L/sqrt.(2rd)-2)

Pn = near soil resistivity

L = length

r= radius of buried earth wire

d= depth of buried earth wire

For L = 5000m, pn = 3500, r = 0.0065, d = 1.66

Re = 10.17 ohm/m

A.1.2 Data for compensated systems

Frequency= 50 Hz

Resistance to earth = 10.17

Length of cable in normal load calculations = 1 km

Length of cable in fault load calculations = 1.61 km

Mutual impedance between cable and buried earth wire = 0.0922+0.99328i

Maximum exposure = 32.18 km

A.1.2.1 Data for rails

Weight = 100 lb/yard

Height = 0.1524 m

Internal reactance = 0.30 ohm/mile

Perimeter = 24.63 in

Permeability = 300 gauss

Resistivity = 20x10^-6 ohm-cm

DC resistance = 0.0526 ohm/mile

A.1.2.2 Other conductor data

Conductor	Height (m)	Dc resistance (ohm/mile)	Internal reactance (ohm/mile)	Radius (mm)
Return conductor	5.7912	0.182735	0.0337	10.55
Contact wire	4.7244	0.27128	0.02528	6.17
Feeder wire	5.638	0.676	0.033	5.93

A.2 For Rail track impedance calculations using APLAC software (section 2.2), sample of written program:

```
#define freq 1kHz  "frequency setting"
#define DX  "cell size defined"
#define DY
#define DZ
#define EPSR 1        "permittivity"
Declare APLACVAR TT NL Z0 h w ereff
Declare VECTOR zaxis REAL 41
Declare VECTOR vect REAL 41
Call h = 3*DZ  "hieght of the cell"
Call w = 4*DX "cell wedth"
Call ereff = Mlin_epse((w/h),0,100,EPSR)
Call Z0 = Mlin_Z01((w/h), 0, 100, EPSR)/sqrt(ereff) "characteristic impedance"
ElectroMagnetics Rail "perform electromagnetic calculations"
+ HARMONIC freq
+ TIMESTEP MARGIN 99.9%  (time-step dt)
+ DIV 26 40 12
+ CELLSIZE DX DY DZ
+ SIMTIME LOOPS 1200
+ ABCTYPE ZHAO3 "Absorbing boundary condition"
```

```
+ ABCTRIM X ereff ereff
+ ABCTRIM Y ereff ereff
DefEMPort sequencer
+ NAME excitation1 NAME excitation2
+ SYMMETRIC
+ STORE sw2.s2p
EMPort excitation1
+ DIR +Z
+ SPAN 13 8 0 13 8 1
+ R Z0
+ STORE sw21.t
Patch pin_at_port_1
+ SPAN 13 8 1 13 8 3
EMPort excitation2
+ DIR +Z
+ SPAN 13 32 0 13 32 1
+ R Z0
+ STORE sw22.t
Patch pin_at_port_2
+ SPAN 13 32 1 13 32 3
Sleeper substrate
+ SPAN 0 0 0 26 40 3
+ ER EPSR
Patch ground_plane
+ SPAN 0 0 0 26 40 0
Rail
+ SPAN 11 8 3 15 32 3
+ SPAN 4 19 3 22 23 3
EndElectroMagnetics
Call TT = EMSimTime("Rail")
Call NL = EMSimLoops("Rail")
Sweep "Response of a rail conductor "
```

```
+ LOOP NL TIME LIN 0 TT
+ WINDOW 0
+ X "position" "cells" 0 42
+ Y "Voltage" "V" -1 1
+ WINDOW 1
+ X "time" "s" 0 1.0ns
+ Y "input voltage" "V" -1 1
+ Y2 "output voltage" "V" -1 1
Call Ev("Rail", 12, 0, 2, 12, 42, 2, Z, zaxis, vect)
Show WINDOW 0 VECTOR 41 XY zaxis (h*vect) ERASE
Show WINDOW 1 Y Vem("Rail", 12, 8, 0, 12, 8, 1) PEN 1
Show WINDOW 1 Y2 Vem("Rail", 12, 30, 0, 12, 30, 1) PEN 3
EndSweep
```

B.2.2 Similar approach is applied for overhead conductor (Conductor above ground)

```
$ define cell sizes
#define DX
#define DY
#define DZ
$ define the conductor permittivity
#define EPSR 1
$ define output axis vector
Declare VECTOR yaxis    REAL 41
$ define output value vector
Declare VECTOR ezfields REAL 41
Declare APLACVAR TT NL Z0 h w ereff
$ height of the conductor
Call h     = 3*DZ
$ length of the conductor
Call L     = 4*DX
$ epsilon_r_eff.
Call ereff = Mlin_epse((w/h), 0, 80, EPSR)
```

$ charac.imp.of T.line

Call Z0 = Mlin_Z01((w/h), 0, 80, EPSR)

Here is the Electromagnetics block initialisation for the upcoming structure.

Electromagnetics conductor

+ PULSED

+ TIMESTEP MARGIN 99.9%

+ DIV 26 40 12

+ CELLSIZE DX DY DZ

+ SIMTIME LOOPS 2400

+ ABCTYPE ZHAO3

+ ABCTRIM X ereff ereff

+ ABCTRIM Y ereff ereff

This means that:

- we launch a pulse (as opposed to a sinusoidal wave). This creates a wide band simulation (as opposed to harmonic simulation)

- the timestep size is 99.9% of the maximal

- there are 26 x 40 x 12 cells in the computation region (XYZ)

- cellsize is DX x DY x DZ (values defined above)

- the simulation is run for 2400 loops.

- ABC is "good", ZHAO 3rd order ABC

- the ABC X and Y walls are optimised to absorb a wave propagating at medium having ereff = ereff.

For S-parameter derivation, we can use these lines:

DefEMPort sequencer

+ NAME excitation1 NAME excitation2

+ SYMMETRIC

+ STORE OHA.s2p

+ FREQS 501 0 1MHz

Note the following:

- EMPorts of the structure are referred to with names (EMPorts will be defined below).

- Typically a 2-port is symmetric: S21 = S12, and S11 = S22. This cuts down the simulation time by half, since only one excitation is required.

- The S-parameters are always stored to a file, they can not be used directly in APLAC. However, they can be read with an Nport to an ordinary circuit related APLAC simulation.
- the EMPorts are directed so that the plus node of the port is in the +Z direction
- Span of e.g. the first port is from 0 to 3 at X = 13, Y = 8.
- The internal resistance is Z0 (defined elsewhere, often 41.6 Ohms).
- The time domain voltages and currents are stored to two datafiles.

Finally (very important):

EndElectroMagnetics

NOTE: Avoid placing small instances very close to and ABC plane (ABCs might get unstable). A small instance is anything that is to the direction of the ABC plane normal, thinner than the degree of the ABC in terms of cells, and smaller than the plane itself in the tangential directions.

The Sweep that runs the simulation is

```
Sweep "OH voltage "
+ LOOP NL TIME LIN 0 TT
+ WINDOW 0
+   X "position" "cells" 0 40
+   Y "voltage" "V" -1 1
+ WINDOW 1
+   X "time" "s" 0 1.92ns
+   Y "input voltage" "V" -1 1
+   Y2 "output voltage" "V" -1 1
Call Ev("OH", 13, 0, 2, 13, 40, 2, Z, yaxis, ezfields)
Show WINDOW 0
+ VECTOR 41 XY yaxis (h*ezfields) ERASE
Show WINDOW 1
+ Y   Vem("OH", 13, 8, 0, 13, 8, 3) PEN 1
Show WINDOW 1
+ Y2 Vem("OH", 13, 32, 0 ,13, 32, 3) PEN 3
```

NOTE: These two functions should be added in front of the Sweep statement:

```
Call TT = EMSimTime("OH")
Call NL = EMSimLoops("OH")
```

APPENDIX

B

B.1 Carson's Method (Chapter (2)[21]:

(A). Self Impedance

Self impedance includes three components: the reactance of the loop inductance *Lii* assuming that the line and the earth are perfect conductors, the internal impedance of line Zc, and the impedance of the ground Zg. The impedance of conductor *i* can then be written as

$$Z_{ii} = jL_{ii} + Z_c + Z_g \text{ ------(B.1)}$$

The loop inductance is given by

$$L_{ii} = \frac{\mu_0}{2\pi}\ln(\frac{2h_i}{r_i}) \text{ ---------(B.2)}$$

The internal impedance of conductor *Zc* is given by

$$Z_{ii} = R_d \frac{j}{2} mr(1-S^2) \times \frac{(ber \cdot mr + jbei \cdot mr) + \phi(\ker \cdot mr + jkei \cdot mr)}{(ber' \cdot mr + jber' \cdot mr) + \phi(\ker' \cdot mr + j\ker' \cdot mr)} \text{ -------(B.3)}$$

where *Rd* = 1/[ps *(r* 2^-*q* 2)] is the DC resistance of the conductor, *q* and *r* are the inner and outer radii of the conductor, *S* = q/*r* is the ratio of the inner to the outer radius, which is zero

for a solid line, m =. μ0s is a variable related to the frequency is the radian frequency, s is the conductivity and μ0 is the permeability of the conductor. The variable f in Equation (B.3) is given by

$$\phi = \frac{-ber' \cdot mq + jbei' \cdot mq}{\ker' \cdot mq + jkei' \cdot mq} \text{ ---------(B.4)}$$

where *ber*, *bei*, *ker* and *kei* are Kelvin's functions which belong to the Bessel function family, and ber', bei', *ker'* and *kei'* are their derivatives, respectively (Andrews, 1992). Kelvin's functions are often defined as

$$ber \cdot x + jbei \cdot x = I_0(x, \sqrt{j}) \text{ ---(B.5)}$$

$$ker \cdot x + jkei \cdot x = K_0(x, \sqrt{j}) \text{ ---(B.6)}$$

Where I0 and K0 are the modified Bessel functions of the 1st and the 2nd kinds of order zero, respectively. Many scientific Fortran libraries provide subroutines for calculation of Kelvin's functions with satisfactory accuracy, which makes application of the tubular conductor model easier. It is noteworthy that the inner radius q equals zero for a solid line, leading to the result f = 0.

The ground impedance *Zg* is expressed by

$$Z_g = R_g + jX_g \text{ ---------(B.7)}$$

Calculation of *Zg* will be discussed in the next section.

(B). Mutual Impedance

The mutual impedance *Zij* of two conductors *i* and j, both parallel to the ground with their respective heights above the ground being *hi* and hj, has two components. The first component is the mutual inductance *Lij* between the two conductors when the conductors and the ground are perfectly conductive.

The second component is the impedance of the earth return path *Zgm* that is common to the currents in conductors *i* and j. The mutual impedance *Zij* can be written as

$$Z_{ij} = jL_{ij} + Z_{gm} \text{--------(B.8)}$$

The mutual inductance *Lij* is given by:

$$L_{ij} = \frac{\mu_0}{2\pi} \ln(\frac{D_{ij}^{'}}{D_{ij}}) \text{------(B.9)}$$

where *Dij* is the distance between conductors *i* and j, and *D ij* ' is the distance between conductor *i* and the image of conductor *j*. The impedance of the earth return path *Zgm* is;

$$Z_{gm} = R_{gm} + jX_{gm} \text{--------(B.10)}$$

Carson's correction terms for the self and mutual impedances due to the earth path impedances *Zg* and *Zgm* are given by (Carson, 1926; Meliopoulos, 1988).

$$R_g = 4\omega * 10^{-7}(\frac{\pi}{8} - b_1 k + b_2[(C^2 - \ln k)k^2] + b_3 k^3 - d_4 k^4 - .....) - - - (B.12)$$

$$X_g = 4\omega * 10^{-7}\{\frac{1}{2}(0.6159315 - \ln k) + b_1 k - d_2 k^2 + b_3 k^3 - b_4[(C_4 - \ln k)k_4] + ...\} - - - (B.13)$$

$$R_{gm} = 4\omega \cdot 10^{-7}\{\frac{\pi}{8} - b_1 k_m \cos\theta + b_2[(C_2 - \ln k_m)k_m{}^2 \cos 2\theta + \theta k_m{}^2 \sin 2\theta]$$

$$+ b_3 k_m{}^3 \cos 3\theta - d_4 k_m{}^4 \cos 4\theta - ...\} - - - (B.14)$$

$$X_{gm} = 4\omega * 10^{-7}\{\frac{1}{2}(0.6159315 - \ln k_m) + b_1 k_m \cos\theta - d_2 k_m{}^2 \cos 2\theta + b_3 k_m{}^3 \cos 3\theta$$

$$- b_4[(C_4 - \ln k_m)k_m{}^4 \cos 4\theta + \theta k_m{}^4 \sin 4\theta] + ...\} - - - (B.15)$$

where;

$$b_1 = \frac{\sqrt{2}}{6} - - - (B.16)$$

$$b_2 = \frac{1}{16} - - - (B.17)$$

$$b_i = b_{i-2} \frac{sign}{i(i+2)} - - - (B.18)$$

$$C_i = C_{i-2} + \frac{1}{i} + \frac{1}{i+2} - - - (B.19)$$

$$C_2 = 1.3659315 - - - (B.20)$$

$$d_i = \frac{\pi}{4} b_i - - - (B.21)$$

In Equation (B.17), the *sign* of coefficient *bi* changes every four terms.
That is, *sign* = +1 when *i* = 1, 2, 3, 4; *sign* = -1 when *i* = 5, 6, 7, 8 and so on. Variables *k* and *km* in Equations. (B.11) & (B.14) are frequency-related and are given by:

$k = 4\pi\sqrt{5} * 10\text{^-}4\ (2h\ i)\ \sqrt{f/\rho}$---- (B22)

$k\ m = 4\pi\sqrt{5} * 10\ \text{^-}4\ D\ ij\ '\sqrt{f/\rho}$--- (B.23)

where *f* refers to the frequency and ρ to the resistivity of the ground. The angle θ is the angle between *I-I'* and *I-j'*, and is expressed by

$\theta = \sin\text{^} -1\ (x\ ij\ /D'\ ij\ )$------(B.24)

B.2 Skin effect and inductance of OHTL explanation (Section 2.3.1.2)[33]

Analytical and approximated methods for resistance ratio (Rac/Rdc) and internal inductance ratio (Liac/Lidc);

$$\frac{R_{ac}}{R_{dc}} = \frac{J_0(j\sqrt{j \cdot m \cdot r})}{J_1(j\sqrt{j} \cdot m \cdot r)}$$

where --------(B.25)

$$m = \sqrt{\frac{2\pi f \varpi}{\rho}}$$

J0 = Bessel function of first kind and zero order

J1= Bessel function of first kind and first order

For stranded conductors, because of the spiralling the increase of resistance, and the decrease in internal inductance caused by skin effect is appreciated and approximate calculation methods have been developed[54] for high frequencies. For low frequency (<2 kHz) and low number of strands in the conductor, the ratios can be acceptably calculated the same way as for solid round conductor of the same dc resistance.

For stranded conductor with steel core, the ratio formulas for a tubular conductor can be used at higher frequencies as an approximate method with small error. For large size solid conductors or at high frequencies an approximate method is adopted. This method uses an effective depth of penetration of current[56]. By which it is assumed that the effective ac resistance is the same as the dc offered by a hollow conductor of the same external dimension and thickness equal to;

$$\frac{50330\sqrt{\rho}}{\sqrt{\mu f}} \text{ ------(B.26)}$$

Another approximate method given by Butterworth[57] using a semi-empirical formulae for (ΔR) which is;

$$\frac{\Delta R}{R_{dc}} = \frac{\lambda^2}{180}\left[\frac{6720+47\lambda^2}{448+33\lambda^2}\right] \text{ ------(B.27)}$$

$$\lambda = \frac{0.001011f}{R_{dc}}$$

ΔR = increase in resistance due to skin effect (ohm/mile).

For iron and steel conductors the resistance and internal inductance ratios can be obtained by assuming an effective average value for the permeability to be constant through the conductor since both permeability and resistivity vary within wide limits according to the frequency, size of conductor and current flowing. When these conductors are carrying alternating currents, the

increase in their effective resistance is due principally to skin effect, but also to some extent to hysteresis.

Butterworth's formula are used for the calculations of ac resistance for all conductors in a traction system except for the rails. The method provide reliable results for frequencies up to 12kHz. For higher frequencies, Bessel's function as described in equation (2.10).
For internal inductance;

$$\frac{L_{iac}}{L_{idc}} = \frac{j\sqrt{jm}}{(2\pi)^2 r \cdot f(L_{dc})} \cdot \frac{J_0(j\sqrt{jmr})}{J_1(j\sqrt{jmr})} \text{-------(B.28)}$$

TL inductive reactance

When a magnetic flux links any electrical circuit, and e.m.f. proportional to the rate of change of the flux linkages is induced in the circuit. It is convenient to divide the current flow into elements, each of which are linked with some flux and then summing to find the total flux linkages.

Inductance due to flux linkages within the conductor (internal inductance):
Consider a long conductor worse cross section is shown Figure 2.12, the skin effect at the operating frequency is neglected, non-uniformity due to stranding or magnetisation of steel core if present is neglected, as well as the proximity effect due to the current in the return path.

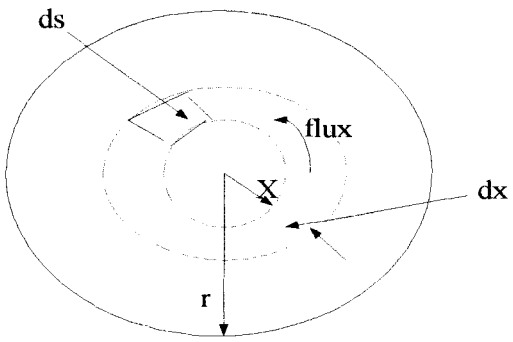

Figure B.1: internal inductance due to flux inside the conductor

The magneto-motive force mmf around any closed path is;

$$mmf = \oint H.ds = I \text{ -----(B.29)}$$

H = magnetic field intensity

S = distance along the path

I = current enclosed.

Integrating around the circular path concentric with the conductor x distance from the centre gives;

$$2\pi x H_x = I_x \text{-------(B.30)}$$

assume uniform current density give;

$$I_x = \frac{\pi x^2}{\pi r^2} I_t \text{-----(B.31)}$$

flux density at x distance from the centre of the conductor is;

$$B_x = \mu H_x = \frac{\mu I_t}{2\pi r^2} \text{------(B.32)}$$

the flux dϕ is;

$$d\phi = \frac{\mu_x I_t}{2\pi r^2} dx \text{------(B.33)}$$

now the flux linkage per unit length (PUL) of the fraction of current linked is;

$$d\psi = \frac{\pi x^2}{\pi r^2} d\phi = \frac{\mu I_t x^3}{2\pi r^4} dx \text{-----(B.34)}$$

integrating from the centre of the conductor to radius r to find total flux linkages inside the conductor gives;

$$\psi_{int} = \frac{\mu I}{8\pi}$$

hence ---------(B.35)

$$L_{int} = \frac{\mu}{8\pi}$$

Note: the above analysis assumes non-magnetic homogeneous conductor.

Inductance due to flux linkages outside the conductor (external inductance)

Consider Figure 2.13, in which a conductor of a radius r is carrying a current I.

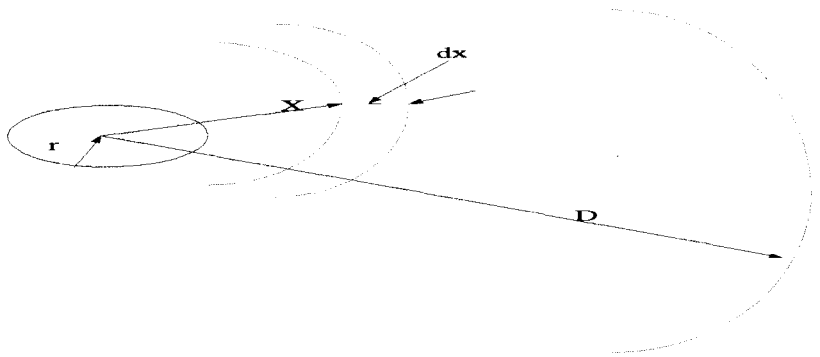

Figure B.2: Inductance due to external flux

The inductance of the conductor due to flux linkages surrounding the conductor up to a distance D from the centre is proved following the same principle as above.

Hence from the above equations;

$$H_x = \frac{I}{2\pi x}$$

and

$$d\phi = \frac{\mu I}{2\pi x} dx$$

so ------(B.36)

$$\psi_{12} = \frac{\mu I}{2\pi} \ln(\frac{D}{r})$$

and

$$L_{12} = \frac{\mu}{2\pi} \ln(\frac{D}{r})$$

Inductive reactance of a single-phase two conductor line

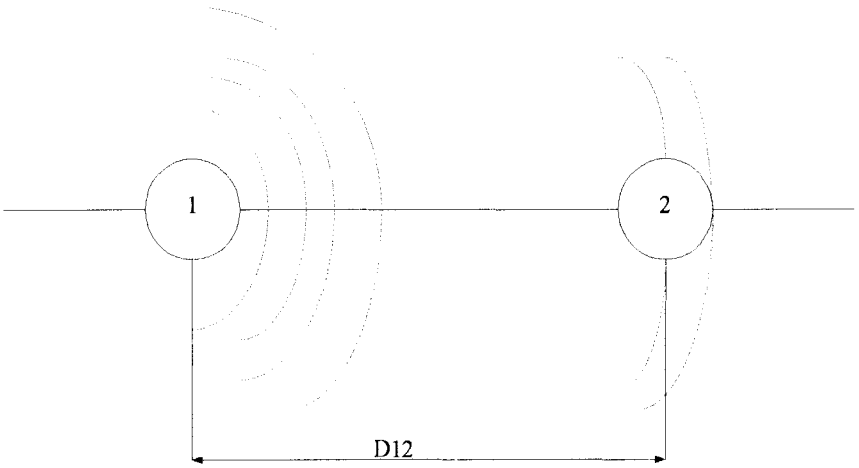

Figure B.3 : Two conductor line

For a solid, round conductors shown above, the inductive reactance formula for one conductor is;

$$X_{11} = X_{i1} + 0.0020223 \cdot f \cdot \ln(\frac{1}{r}) + 0.0020223 \cdot f \cdot \ln(\frac{D_{12}}{1}) \text{-----(2.22)} \quad \text{(ohm/mile)}$$

Xi1 = internal reactance of the conductor

0.0020223f.ln(1/r) = inductive reactance due to flux outside the conductor to a radius of one foot.

0.0020223flin(D12/1) is inductive reactance due to flux external from one foot radius to D12 feet.

D12 = distance between conductor 1 and 2.

Method of images (as mentioned in chapter (2)

Consider a point Q situated at height h above an infinite perfectly conducting plane as shown in figure. We can replace the infinite plane with an equal but negative charge -Q at a distance h below the previous location of the surface plane.

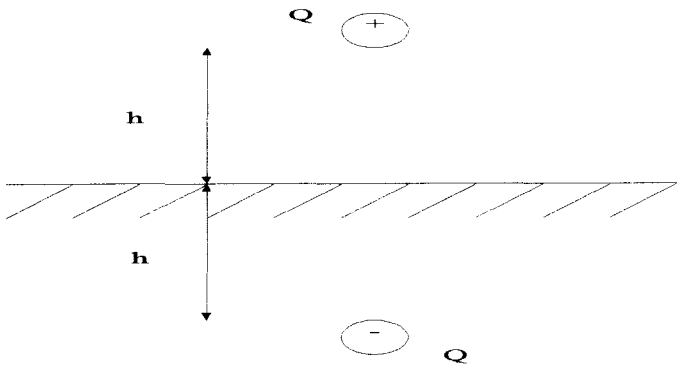

Figure B.4: -Q is the image of +Q. the same can be done for currents.

B.3 Derivation of transmission line equation form differential form of Maxwell's equations (Section 2.5)[6,7]

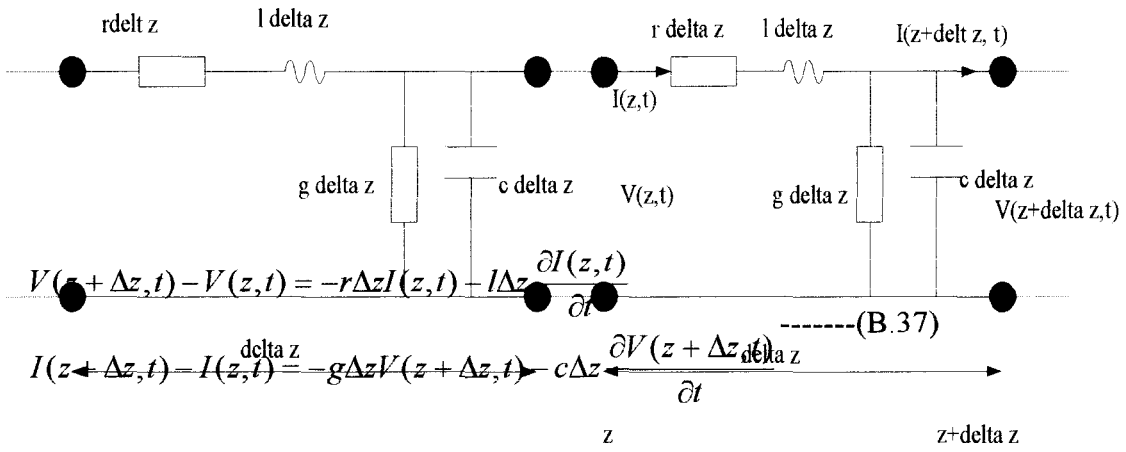

Figure B.5: The per-unit-length model for use in deriving the TL equations

Divide by delta z and taking the limit=0 gives;

$$\frac{I(z+\Delta z,t)-I(z,t)}{\Delta z}=-gV(z,t)-c\frac{\partial V(z,t)}{\partial t}+\Delta z[grI(z,t)+(gl+rc)\frac{\partial I(z,t)}{\partial t}+lc\frac{\partial^2(z,t)}{\partial t^2}]\text{-(B.38)}$$

Taking the limit as delta z=0 gives the second TL equation:

$$\frac{\partial I(z,t)}{\partial z}=igV(z,t)-c\frac{\partial V(z,t)}{\partial t}\text{-----(B.39)}$$

Ampere's law

$$\oint_c \vec{H}_t \cdot d\vec{l} = I$$

gives; ------(B.40)

$$H_t = \frac{I}{2\pi r}$$

Gusses's law

States that there are no (known) isolated sources of the magnetic field. Thus the total magnetic flux through a closed surface must be zero;

$$\psi_m = \oiint_s \vec{B}.d\vec{s} = 0$$

$$\psi_m = \oiint_{s1} \vec{B}.d\vec{s}$$

$$\psi_m = \Delta z \int_{R_1}^{R_2} \frac{\mu I}{2\pi r}\cdot dr \quad \text{------(B.42)}$$

$$\psi_m = \Delta z \frac{\mu I}{2\pi}\ln(\frac{R_2}{R_1})$$

Faraday's law

$$\nabla \times \vec{E} = -j\omega\mu\vec{H} \text{ ------(B.43)}$$

APPENDIX

C

C.1 List of publications

1. Abdulaziz I M and Gupta N K, "Electromagnetic Interference in Electric Railway Systems", International Power Engineering Conference (IPEC) Refereed Proceedings, Singapore, May 2001.
2. Abdulaziz I M, Gupta N K, "Induced Voltage Calculations in Electrified Railways using Mathematical Modelling", University Power Engineering Conference (UPEC) Refereed Proceedings, University of Wales, Swansea, September 2001.
3. Abdulaziz I M and Gupta N K, "Booster Transformers in Railways", UPEC Refereed Proceedings, University of Staffordshire, UK, September 2002.
4. Abdulaziz I M, and Gupta N K, "Power Supply in Electric Railways", Energize Power Journal, March 2003.
5. Abdulaziz I M and Gupta N K "EMC in Railways", Electronic Journal, Accepted "in print".
6. Abdulaziz I M and Gupta N K, "Rail Track Impedance Calculations using Carson's FE and FDTD Methods", IEE Proc. Elect. Power Applic., to be submitted.
7. Abdulaziz I M and Gupta N K, "FDTD Method in Calculating Induced Voltage in Railways", SAIEE Proceedings, Submitted "Under Review".
8. Abdulaziz I M and Gupta N K, "Compensated Systems in Electrified Railways: The Use of Booster Transformers", SAIEE Proceedings, Submitted "under review"

Missing pages are unavailable